Mass Spectrometry, Biological Screening and Informatics of Prenylated Natural Products

Dissertation

zur Erlangung des Doktorgrades der Naturwissenschaften

(Dr. rer. nat.)

der

Naturwissenschaftlichen Fakultät II

Chemie, Physik und Mathematik

der Martin-Luther-Universität

Halle-Wittenberg

vorgelegt von

Frau Ramona Heinke

geboren am 24. April 1985 in Potsdam

Gutachter: Prof. Dr. Ludger Wessjohann

Prof. Dr. Uwe Karst

Datum der Verteidigung: 22. April 2015

Contents

Abbreviations

AAC	Acetoacetyl-CoA
AACT	Acetoacetyl-CoA-thiolase (EC 2.3.1.9)
AcorA	Activity correlation analysis
ADP	Adenosine diphosphate
ATP	Adenosine triphosphate
BioMAP	Antibiotic mode of action profile
CDP-ME	4-Dihosphocytidyl-2-methyl-D-erythritol
CDP-MEP	4-Diphosphocytidyl-2-methyl-D-erythritol-2-phosphate
Co-A	Coenzyme-A
CYP	Cytochrome P450
DA	Discriminate analysis
DMAPP	Dimethylallyl diphosphate
DOXP	1-Deoxy-D-xylulose-5-phosphate
DXR	DOXP-reductoisomerase
DXS	DOXP-synthase
ESI	Electrospray ionisation
FTICR	Fourier transform ion cyclotron resonance
GAP	D-Glyceraldehyde-3-phosphate
GC	Gas chromatography
HCA	Hierarchical cluster analysis
HMBPP	(E)-4-Hydroxy-3-methyl-but-2-enyl-diposphate
HMG	3-(S)-Hydroxy-3-methyl-glutaryl
HMGR	HMG-CoA-reductase (EC 1.1.1.34)
HMGS	HMG-CoA-synthase (EC 4.1.3.5)
HR-MS	High resolution mass spectrometry
HTS	High-throughput screening
IC_{50}	Half maximal inhibitory concentration
IDI	IPP-DMAPP isomerase
IP	Isopentenyl phosphate
IPI	IPP-DMAPP-isomerase (EC 5.3.3.2)
IPP	Isopentenyl diphosphate
LC	Liquid chromatography
LC-MS	Liquid chromatography/mass spectrometry

MEcPP	2-Methyl-D-erythritol-2,4-cyclodiphosphate
MEP	2-Methyl-D-erythritol-4-phosphate
MS	Mass spectrometry
MS^n	Tandem mass spectrometry
MDA	Multivariate data analysis
MPD	MVAPP-decarboxylase (EC 4.1.1.33)
MVA	Mevalonic acid
MVAP	Mevalonic acid 5-phosphate
MVAPP	Mevalonic acid 5-diphosphate
MVK	MVA-kinase (EC 2.7.1.36)
m/z	Mass-to-charge ratio
NAD(P)	Nicotinamide adenine dinucleotide (phosphate)
NMR	Nuclear magnetic resonance
OPLS	Orthogonal partial least square
9-oxo-ODE	9-Oxo-10-(*E*),12-(*Z*)-octadecadienoic acid
PC	Principal component
PCA	Principal component analysis
PLS	Partial least square
PMK	MVAP-kinase (EC 2.7.4.2)
QCAR	Quantitative composition-activity relationship
QPAR	Quantitative pattern activity relationship
RNA	Ribonucleic acid
RT	Retention time
s.l.	sensu lato
9,10,13-11*E*-THOD	9,10,13-Trihydroxy-11-(*E*)-octadecenoic acid
TPP	Thiamine diphosphate
UHPLC	Ultra-high-performance liquid chromatography
UPLC	Ultra-performance liquid chromatography

1.   General introduction

1.1   Introduction and aim

The present thesis is focused on natural products containing a prenyl side chain. The prenylation of metabolites often enables or enhances a biological activity such as antimicrobial, antioxidative, anti-inflammatory or cytotoxic activity and affinity e.g., to a dopamine or vanilloid receptor. Moreover, prenylated compounds are widespread in different organisms and show a high structural variability. They can possess a different or higher activity than their non-prenylated parent compounds.

This thesis is aiming at the identification of known or new prenylated bioactive compounds in crude extracts obtained from macromycetes without the need of prior separation To set the basis for a direct identification, the mass spectral fragmentation behavior of several prenylated plant and fungal metabolites with different substitution pattern was analyzed in the positive and negative ion mode in combination with liquid chromatography/electrospray tandem mass spectrometry (LC/ESI-MS^n). The main focus of this project is to check the possibility to identify/characterize such compounds by using their MS fragmentation pattern under electrospray ionization conditions. LC/ESI tandem mass spectrometry represents a valuable tool for structural characterization and investigation of such compounds (Chapter 2 and Chapter 3).

The herein used methods provide a basis for detection and characterization of prenylated compounds from basidiomyceteous fruiting bodies such as *Albatrellus* and *Suillus* as well as cultures thereof. A combination of analytical techniques and multivariate data analysis (MDA) was used for analyzing the metabolites of crude extracts from different fungal species. In this connection, an extraction method was established which allowed the recording of prenylated metabolites (prenylom). In order to analyze the biological samples, the methods of choice were high resolution mass spectrometry (HR-MS) and LC/ESI-MS because of their high sensitivity and wide range of detection. On one hand, the metabolite profiles of various *Suillus* species were investigated and the possibility of a classification of such extracts via principal component analysis (PCA), hierarchical cluster analysis (HCA) and orthogonal partial least squares (OPLS) were tested (Chapter 4). On the other hand, a direct method for the identification of antibacterial prenylated metabolites in extracts was successfully applied. In this context, species of the genus *Albatrellus* were analyzed with regard to their antibacterial activity against the Gram-positive bacterium *Bacillus subtilis* and their metabolite profile determined by mass spectrometry (Chapter 5 and Chapter 6).

Therefore, a new method called 'reverse metabolomics' for a rapid identification of metabolites with an antibacterial activity from crude extracts was used without knowledge of the

structures of relevant compounds or the isolation of the active ones. As analytical techniques HR-MS, LC coupled with ESI-MS and ESI-MS^n were employed for this purpose. 'Reverse metabolomics' is based on the correlation (<u>a</u>ctivity-<u>cor</u>relation-<u>a</u>nalysis, AcorA) of chromatographic and spectroscopic profiles with biological or other activity data. The results are summarized in a hit list. An *ab initio* identification of the most selected top hit activity-relevant prenylated compounds was carried out using the fragmentation pattern. Disadvantages of traditional non-directed or bioassay-guided isolations of natural products are the time-consuming purification and structural elucidation procedure. Thus, 'reverse metabolomics' marks a new approach, enabling the direct detection of activity-relevant metabolite clusters in complex mixtures and the identification of metabolites. The concept of 'reverse metabolomics' has been developed in the Wessjohann group before. A proof of principle has been achieved. Now a realistic application-oriented system had to be studied as part of this project (Chapter 5 and Chapter 6).

Moreover, the activity against the Gram-negative bacterium *Aliivibrio fischeri* and cell proliferation inhibitory effects of *Albatrellus* extracts were investigated (Chapter 6) as well as the antibacterial activity of various *Suillus* extracts (see 11.2.6).

Figure 1 summarizes the workflow on which this thesis is based and gives an overview about the relation between analytical chemistry, biological testing, and chemoinformatic methods as well as its application in the field of natural product research. In the following sections each part of this project is explained in more detail.
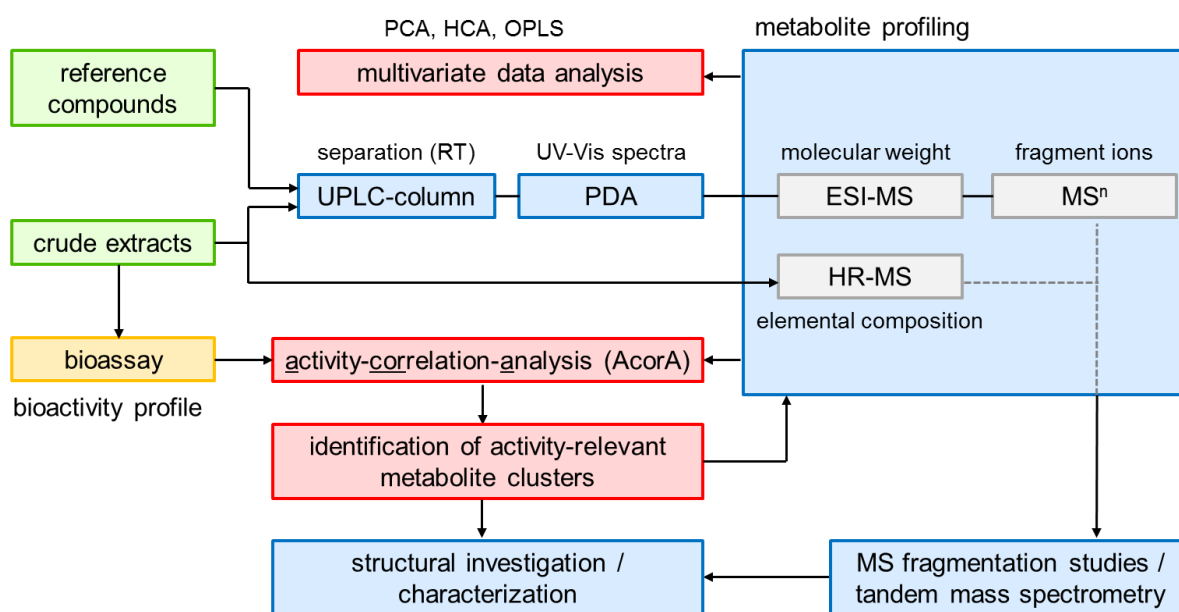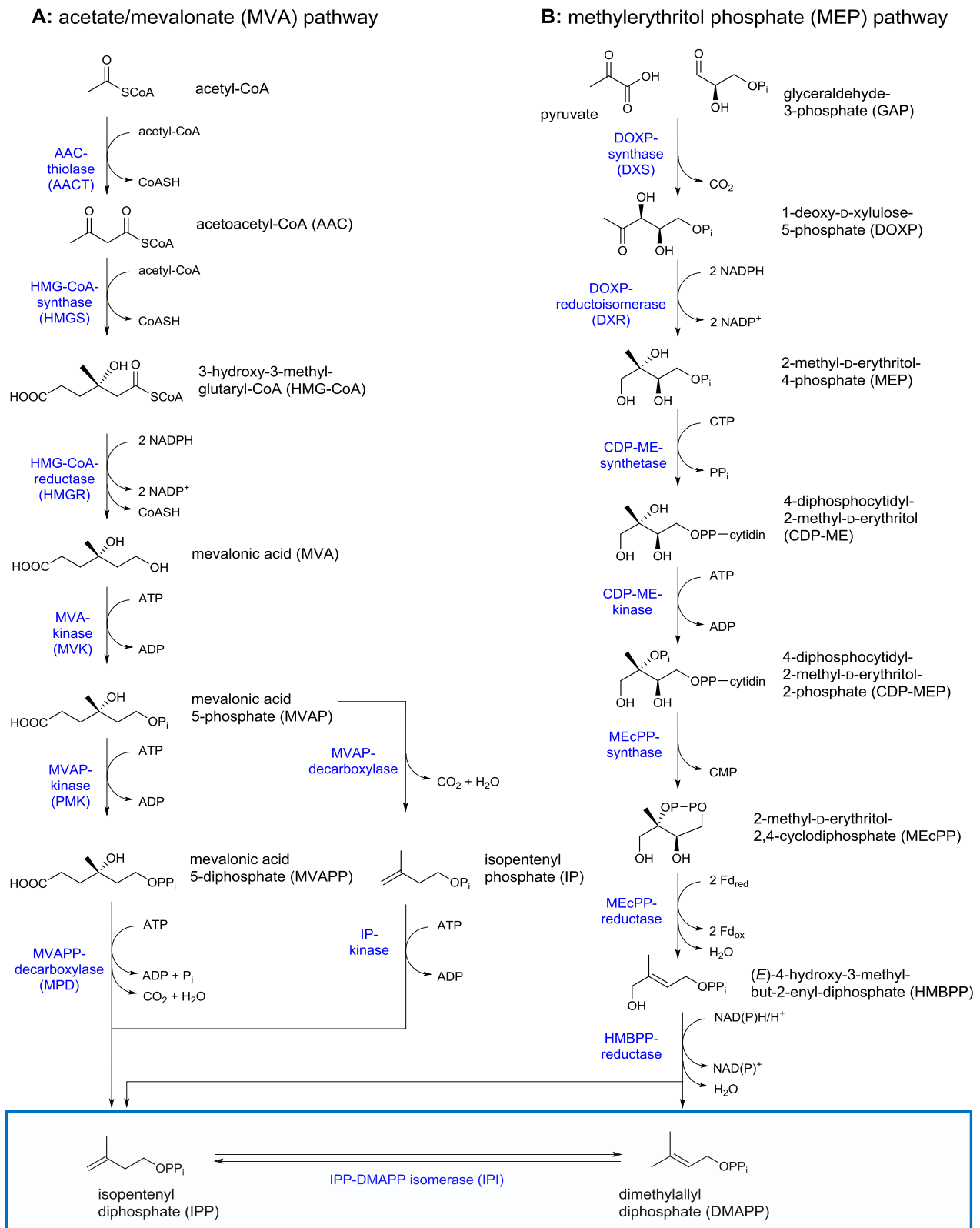

Figure 1. Overall workflow of the thesis linking analytical chemistry, biological screening and chemo- and bioinformatic methods in the field of natural product research.

1.2 Prenylation und prenylated natural products

Nature provides a huge variety of secondary metabolites. These compounds are recognized as low molecular weight organic substances of a high structural diversity and with various biological activities.[1] Since early history, natural products play an important role in drug discovery.[2–5] The large number of secondary metabolites in organisms (fungi, plants and microorganisms) is synthesized as a consequence of complex interactions with the environment. The structural multiplicity and complexity of bioactive metabolites as a consequence of evolution have a pivotal role in finding new lead compounds both for pharmaceutical purposes and synthetic organic chemistry. The success of natural products as basis for therapeutics can be attributed to their biochemical specificity resulting from evolutionary development.[6]

Prenylated natural products possess a broad spectrum of biological activities.[7–9] They are widely-distributed in nature and have been isolated from different organisms such as bacteria,[8] fungi,[9,10] marine sponges,[11,12] and plants.[13] Prenylation plays a major role in the structural diversification of natural products.[14] Prenylation represents a chemical or enzymatic addition of isoprene units to small-molecule natural products, peptides and proteins. The transfer of a prenyl moiety to aromatic molecules such as phenylpropanoids, flavonoids, and coumarins is catalyzed by prenyltransferases and is realized by an electrophilic or Friedel-Crafts alkylation of the aromatic system.[7,14] This biosynthetic reaction describes the crucial coupling process of an aromatic moiety derived from the shikimate or polyketide pathway and a prenyl unit from the isoprenoid pathway. While the acetate/mevalonate pathway (Figure 2.A) mainly is active in the cytosol and the endoplasmic reticulum, the 2-methyl-D-erythritol-4-phosphate (MEP) pathway (Figure 2.B) mainly operates in the plastids yielding isopentenyl diphosphate (IPP) and dimethylallyl diphosphate (DMAPP). Figure 2.A illustrates the acetate/mevalonate pathway. This pathway starts with a two-step condensation of three acetyl-CoA molecules forming 3-hydroxy-3-methyl-glutaryl-CoA (HMG-CoA). Mevalonic acid (MVA) is produced in a following reduction by HMG-CoA reductase in a two coupled reaction. Two ATP-dependent phosphorylations as well as an additional phosphorylation along with a decarboxylation yield IPP. An IPP-DMAPP isomerase (IDI) is responsible for the isomerization of IPP producing DMAPP.[15,16]

Grochowski *et al.* (2006) proposed a modified mevalonate pathway in archaea catalyzed by an enzyme identified in *Methanocaldococcus jannaschii*.[17] Instead of a second phosphorylation of mevalonic acid 5-phosphate (MVAP), they postulate a decarboxylation reaction to form isopentenyl phosphate (IP). A subsequent ATP-dependent phosphorylation by an IP kinase generates IPP.[17–20]

A: acetate/mevalonate (MVA) pathway   **B:** methylerythritol phosphate (MEP) pathway

Figure 2. Pathways for the biosynthesis of isopentenyl diphosphate (IPP) and dimethylallyl diphosphate (DMAPP), **A**: acetate/mevalonate pathway and **B**: methylerythritol phosphate (MEP) pathway.[15–18,21]

However, the proposed phosphomevalonate decarboxylase is still unknown so far. In comparison to the cytosolic pathway, the IPP and DMAPP biosynthetic pathway localized in the plastids starts with pyruvate and thiamine diphosphate (TPP). The resulting hydroxyethyl-TPP (not shown in Figure 2.B) condenses with glyceraldehyde-3-phosphate to form 1-deoxy-D-xylulose-5-phosphate (DOXP). Subsequently, a rearrangement and reduction is catalyzed by DOXP reductase yielding 2-methyl-D-erythritol.[15,16,21]
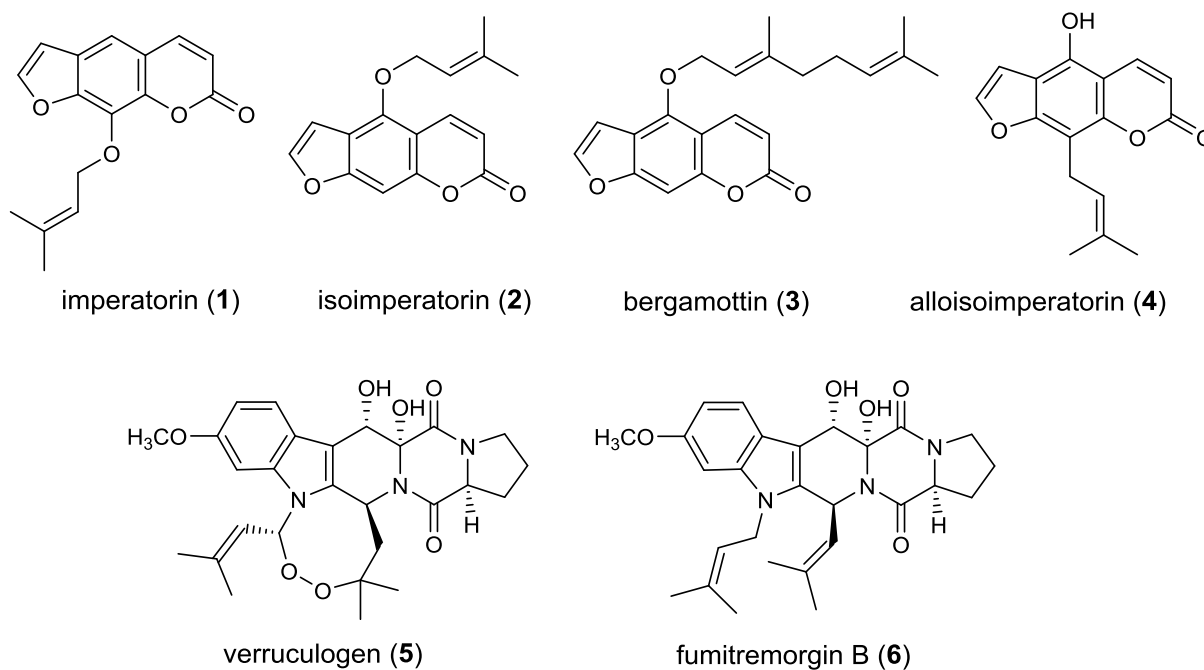
For hydrophobic modifications, an isopentenyl (C_5), geranyl (C_{10}) or a farnesyl (C_{15}) unit is attached to a skeleton. Generally, one can differentiate between *C*-, *O*-, *S*-, and *N*-prenylation.[21-23] From a pharmacological point of view, the addition of an isoprenoid side chain can lead to remarkable changes in the biological activity compared to the parent compound.[23-25] This can be attributed to an increased lipophilicity, conferring to the molecule a stronger affinity for biological membranes and consequently to an improved transport, or it can enhance the interaction with proteins.[26–28] The relationship between activity and the presence of an isoprenoid side chain at key positions at different alkaloids, flavonoids, and other polyphenols can be associated with biological activities like, e.g., antitumor and cytotoxic,[24,25,28-31] anti-inflammatory,[33] antioxidant,[34–36] antityrosinase,[37,38] estrogenic,[39] and antimicrobial properties[29,40,41] as well as the inhibitions of sulfotransferase[42] and phospholipase.[43]

More than 1000 prenylated polyphenols have been isolated[14] from a limited number of plant families such as Moraceae,[27,29,44] Leguminosae (Fabaceae),[27] Cannabaceae,[45] Guttiferae (Clusiaceae),[40,46] Umbelliferae (Apiaceae)[47] and Rutaceae[48]. In particular, the diversification of flavonoids strongly depends on prenylation. Different positions at the flavonoid skeleton, various lengths of the prenyl side chain as well as further modifications like cyclization and hydroxylation result in a large number of prenylated flavonoids in plants. These flavonoids are responsible for the biological activities of medicinal plants, such as antioxidative,[34,35,49,50] anti-inflammatory,[33,51] anti-cancer,[25] anti-leishmania, and anti-nitric oxide production or strong estrogenic activities.[52]

Species of the genus *Dorstenia* (Moraceae) represent rich sources of prenylated flavonoids,[52-55] but also a high number of prenylated furanocoumarins[57,58] (Figure 3) were isolated. Furanocoumarins are known as plant phototoxins and are responsible for photo-sensitization. Prenyloxyfuranocoumarins such as imperatorin (**1**) in addition to photo-sensitizing properties exhibit such as antiproliferative,[59] anti-inflammatory,[60] or calcium antagonistic activities.[61] In contrast to 5-prenyloxypsoralen (imperatorin, **1**), 8-prenyloxypsoralen (isoimperatorin, **2**) possesses anti-inflammatory and calcium antagonistic properties, and inhibits acetylcholinesterase.[60–62] Furthermore, furanocoumarins show inhibitiory effects on cytochrome P450 enzymes, especially CYP 3A4 which is important for drug metabolism.[63] Bergamottin (**3**) occurring in grapefruit juice, interacts with cytochrome P450 3A4, P450 3A5 and P450 2B6.[64,65]

However, *C*-prenylated furanocoumarins like alloisoimperatorin (**4**) shows an estrogenic effect and antioxidant properties.[66,67]

Next to *C*- and *O*-prenylation, also azoprenylated secondary metabolites can be found in nature such as *N*-prenylated alkaloids from bacteria, filamentous fungi, marine organisms and plants belonging to the Rutaceae family.[22] Also several fungi of the genera *Penicillium* and *Aspergillus* (Ascomycetes) contain prenylated indole alkaloids.[24,68] Such metabolites often exhibit quite different biological and pharmacological activities compared with the corresponding non-prenylated alkaloids. Verruculogen (**5**) and fumitremorgin B (**6**) possessing two isoprenoid moieties are mycotoxins (Figure 3).[68] In addition to verruculogen (**5**), further indole alkaloids with cytotoxic properties have been isolated from *Aspergillus fumigatus*.[68,69]

imperatorin (**1**)   isoimperatorin (**2**)   bergamottin (**3**)   alloisoimperatorin (**4**)

verruculogen (**5**)   fumitremorgin B (**6**)

Figure 3. Structures of some prenylated furanocoumarins and alkaloids.

1.3   Basidiomycetes and meroterpenoids

A series of prenylated metabolites could be detected in many genera of macromycetes (Basidiomycetes). Especially, prenylated phenols are of particular importance, because this class of secondary metabolites contains antimicrobial, antioxidant, anti-inflammatory and cytotoxic substances.[70] Fruiting bodies of the genera *Albatrellus*, *Suillus* (Figure 4) and *Gomphidius* are well-known natural sources of polyprenyl phenols und quinones.[71–75] These types of prenylated compounds are called 'meroterpenoids', natural products derived from different biosynthetic origin. Initially, Cornforth used the term meroterpenoid as '*compound containing terpenoid elements along with structures of different biosynthetic origin*'.[76] Thereinafter, Simpson confined meroterpenoids to a more limited class, '*compounds of mixed polyketide–terpenoid origins*'.[77] Meroterpenoids extracted from fruiting bodies and axenic cultures of Basidiomycetes can be classified into polyketide-terpenoids and non-polyketide-terpenoids.[71,75,78] Therefore, in this work the original definition of Cornforth is used.

Figure 4.   A: *Albatrellus ovinus* (fruiting bodies), **B**: *Suillus bovinus* and *Gomphidius roseus* (fruiting bodies). (Pictures by R. Heinke)

Fungal meroterpenoids possess a broad structural diversity with a wide range of biological activities as shown in Table 1.[75] Structurally related 2,5-dihydroxy-1,4-benzoquinones with prenyl side chains (Figure 5) such as boviquinone-3 (**7**) and boviquinone-4 (**8**) belong to the non-polyketide–terpenoids.[75] These fungal secondary metabolites have been isolated from different species belonging to the Boletales s.l. (Basidiomycetes).[71] Prenylated 1,4-benzoquinones mainly occur in the genera *Suillus*, *Chroogomphus* and *Gomphidius*. This type of compounds is produced both in fruiting bodies and cultures.[78] Beaumont and Edwards (1971) isolated dihydroxybenzoquinones bearing polyprenyl side chains in the fruiting bodies of *Suillus bovinus* and *Chroogomphus rutilus* being responsible for their purple color reaction with alkali.[79] Boviquinone-3 (**7**) with a farnesyl moiety represents the predominant pigment of *C. rutilus*. Its

occurrence is accompanied by 4-acetoxy-1,2-dihydroxy-6-farnesylbenzene (**9**), diboviquinones as methylenediboviquinone-3,3 (**10**) and methylenediboviquinone-3,4 (**11**).[71,79] So, the principal pigment which is responsible for the brown–orange color of *S. bovinus* was identified as boviquinone-4 (**8**), a geranylgeranyl substituted quinone.[71,80] Furthermore, meroterpenoids such as suillin (**12**), bolegrevilol (**13**), bovilactone-4,4 (**14**), diboviquinone-4,4 (**15**) and methylenediboviquinone-4,4 (**16**) were isolated from *S. bovinus.*[71,79]

Table 1.   Biological activities of meroterpenoids from *Suillus* and *Albatrellus* species.

Compound	Biological activities
suillin (**12**)	cytotoxic and tumor growth inhibitory effects[81] immunsupressive property[82]
bolegrevilol (**13**)	antimicrobial activity[81] lipid peroxidase inhibitory effects[83] anti-inflammatory, antirheumatic and antisclerotic activities[84]
diboviquinone-4,4 (**15**)	antioxidative effects[85]
6-geranylgeranyl-2,4-dihydroxy-1-methoxybenzene (**18**)	antimicrobial activity[81]
grifolin (**19**)	antibacterial activity[86–91] antifungal activity[91,92] antioxidative effects[93] cytotoxic and tumor growth inhibitory effects[90,94,95] tyrosinase-inhibiting activity[96]
neogrifolin (**20**)	antibacterial activity[90,91] cytotoxic effects[90,97] antioxidative effects[97] affinity to vanilloid and dopamine receptor[98–100] tyrosinase-inhibiting activity[96]
scutigeral (**21**)	antibacterial activity[91] affinity to vanilloid and dopamine receptor [98,99]
grifolic acid (**22**)	antibacterial activity [88,89,91] cytotoxic effects[88] antifungal activity[91] hemolytic property[88]
cristatic acid (**23**)	antibacterial activity[88] cytotoxic effects[88] hemolytic property[88]

boviquinone-3 (**7**)   boviquinone-4 (**8**)   tridentoquinone (**17**)

methylenediboviquinone-3,3 (**10**)   methylenediboviquinone-3,4 (**11**)

amitenone (methylenediboviquinone-4,4; **16**)

diboviquinone-4,4 (**15**)   bovilactone-4,4 (**14**)

4-acetoxy-1,2-dihydroxy-   suillin (**12**)   bolegrevilol (**13**)   6-geranylgeranyl-
6-farnesylbenzene (**9**)   2,4-dihydroxy-
                                                                                                              1-methoxybenzene (**18**)
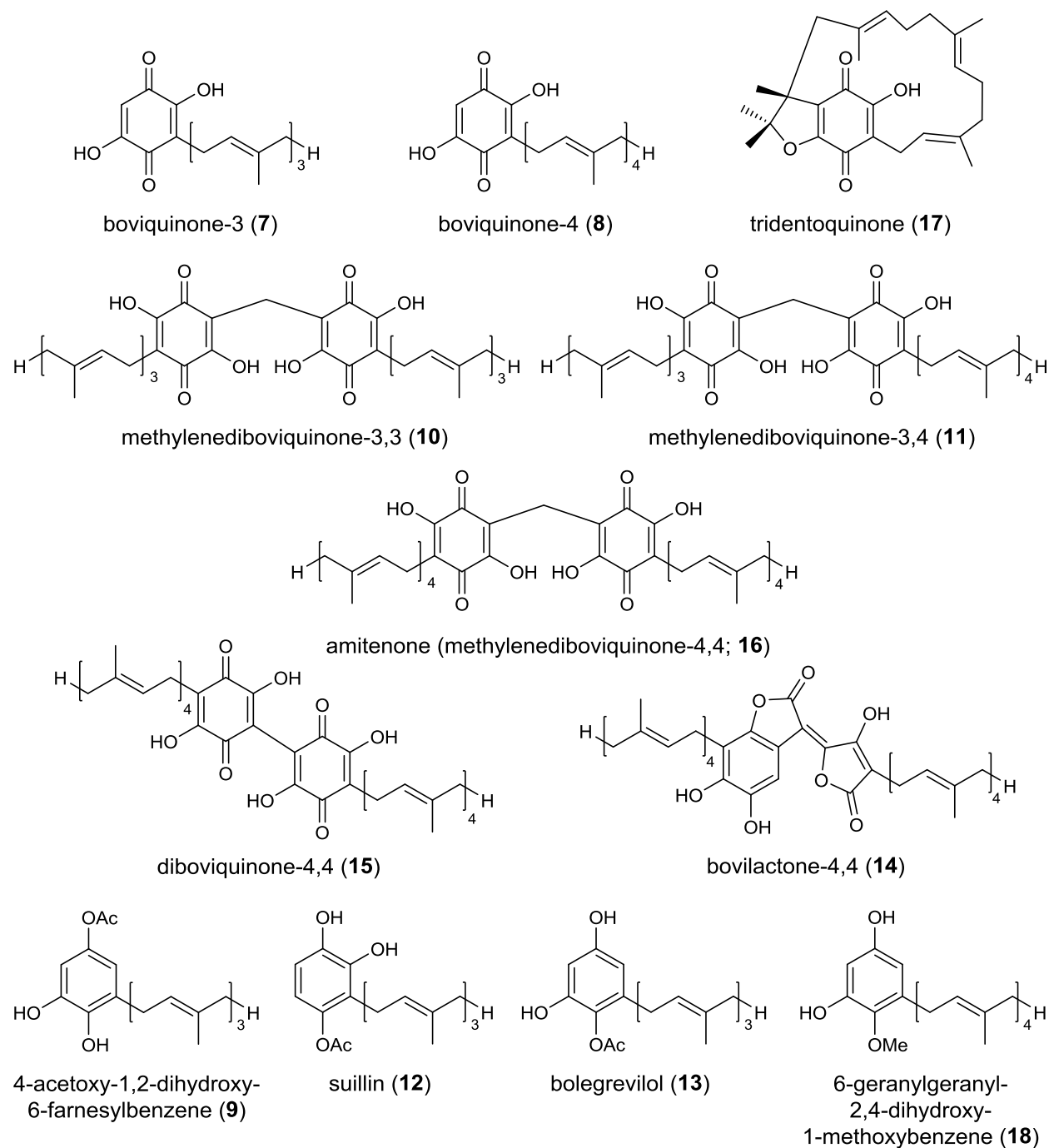
Figure 5. Occurrence of prenylated metabolites in *Suillus* species.

A

Proposed suillin pathway

● ^{13}C labelled

boviquinone-4 (**8**)

suillin (**12**)

bovilactone-4,4 (**14**)

B

Proposed bolegrevilol pathway

● ^{13}C labelled

bolegrevilol (**13**)

deoxytridentoquinone

tridentoquinone (**17**)
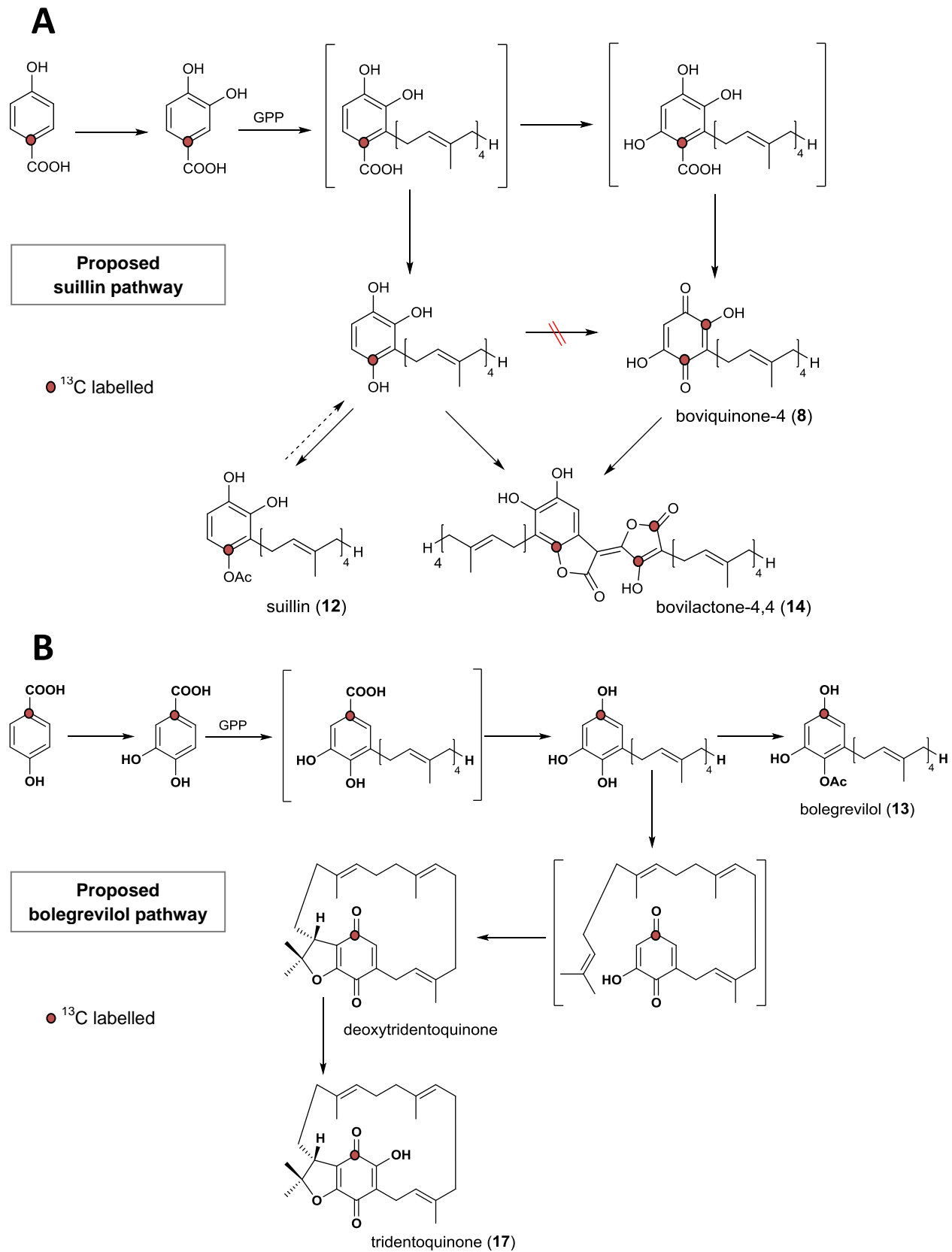
Figure 6.   A: Proposed suillin pathway, and **B:** proposed bolegrevilol pathway.[101,102]

The unique red tridentoquinone (**17**) represents the main pigment in the fruiting bodies of *S. tridentinus*.[103] It was described as the first native quinone with an ansastructure containing only carbon atoms.[103] Biosynthetic studies of tridentoquinone (**17**) and the structurally related linear boviquinone-4 (**8**) using labelled 4-hydroxy-[1-^{13}C]benzoic acid or 3,4-dihydroxy-[1-^{13}C]benzoic acid demonstrated the existence of two different pathways. While the primary step of the suillin pathway leading to boviquinone-4 (**8**), suillin (**12**) and bovilacton-4,4 (**14**) is based on the prenylation of 3,4-dihydroxybenzoic acid at position *C*-2, the meroterpenoids bolegrevilol (**13**) and tridentoquinone (**17**) are originated from a different route (bolegrevilol pathway) starting with a prenylation at position *C*-5 (Figure 6.A and B).[101,102]

The colorless tetraprenylphenols suillin (**12**) and bolegrevilol (**13**) are stabilized by acetylation of the hydroquinone system.[78,104] While suillin (**12**) exhibits tumor growth inhibiting, cytotoxic[81] and immunosuppressive properties,[82] bolegrevilol (**13**) shows lipid peroxidation inhibition,[83] anti-inflammatory, antirheumatic and antisclerotic activities.[84] In addition to suillin (**12**) and bolegrevilol (**13**), the fruiting bodies of *S. granulatus* contains 6-geranylgeranyl-2,4-dihydroxy-1-methoxybenzene (**18**) possessing antimicrobial activity against Gram-positive and Gram-negative microorganisms.[81]

Closely related meroterpenoids belonging to the group of polyketide–terpenoids were isolated from *Albatrellus* ssp. (Basidiomycetes).[86,105,106] So, farnesylphenols as grifolin (**19**), neogrifolin (**20**) and derived compounds such as scutigeral (**21**), grifolic acid (**22**) and cristatic acid (**23**) depict typical metabolites for fungi of the genus *Albatrellus*. Grifolin (**19**), isolated for the first time from *A. confluens*, and its derivatives possess a wide spectrum of bioactivities. Besides antimicrobial properties[86,88,89,106] also antioxidative,[93] tyrosinase-inhibiting,[96] plant growth inhibiting[107] and cytotoxic activities[73] as well as affinity to the vanilloid receptors[100] have been reported. Furthermore, grifolin (**19**) shows a slight antibacterial activity.[86,87]

grifolin (**19**)   neogrifolin (**20**)   scutigeral (**21**)

grifolic acid (**22**)   cristatic acid (**23**)
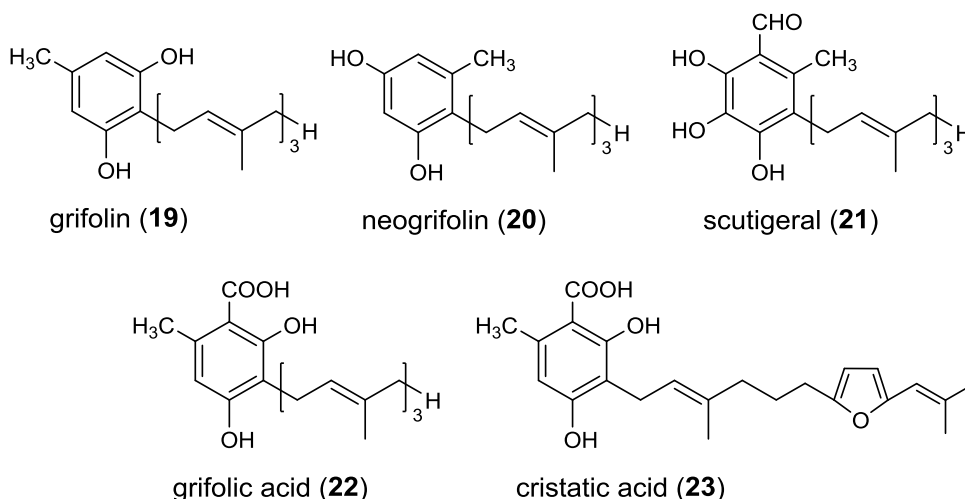
Figure 7. Structures of some meroterpenoids from *Albatrellus* species.

1.4   Natural product research and antibiotics

The chemical diversity of natural products and also derived drugs is much larger than that of synthetic compounds derived from chemistry.[108] Most of all, natural products are preselected for activity by evolution. Therefore, natural products or their (semi)synthetic derivatives are important in drug discovery, e.g. infection defense with antibiotics.[109] Since the discovery of penicillin over 80 years ago, natural products and their derivatives have served as sources for more than two-thirds of clinically used antibiotics in the treatment of infectious diseases. Most of the drugs are based on metabolites isolated from microorganisms. A majority of them originate from actinomycetes and fungi or represent semisynthetic derivatives.[3,4,110]

Over the past decades large numbers of resistance mechanisms surfaced. Faced with continuous new appearances of antibiotic resistance phenomena, sustained research efforts concerning new antibiotics and their development into drugs are necessary.[110,111] In several reviews the increasing problem of pathogen resistance to antibiotics and the need of novel antibacterial drugs as a consequence was discussed.[111–113]

The traditional ways of drug discovery such as classical non-directed isolation (Figure 8.A) or bioactivity-guided fractionation (Figure 8.B) and subsequently structural elucidation are highly sophisticated processes, because crude extracts of biological materials (plants, fungi, microorganisms) represent complex mixtures of hundreds or even thousands of compounds. Furthermore, the classical strategies for isolation and identification of bioactive metabolites are time-consuming and connected with a high risk of replication.
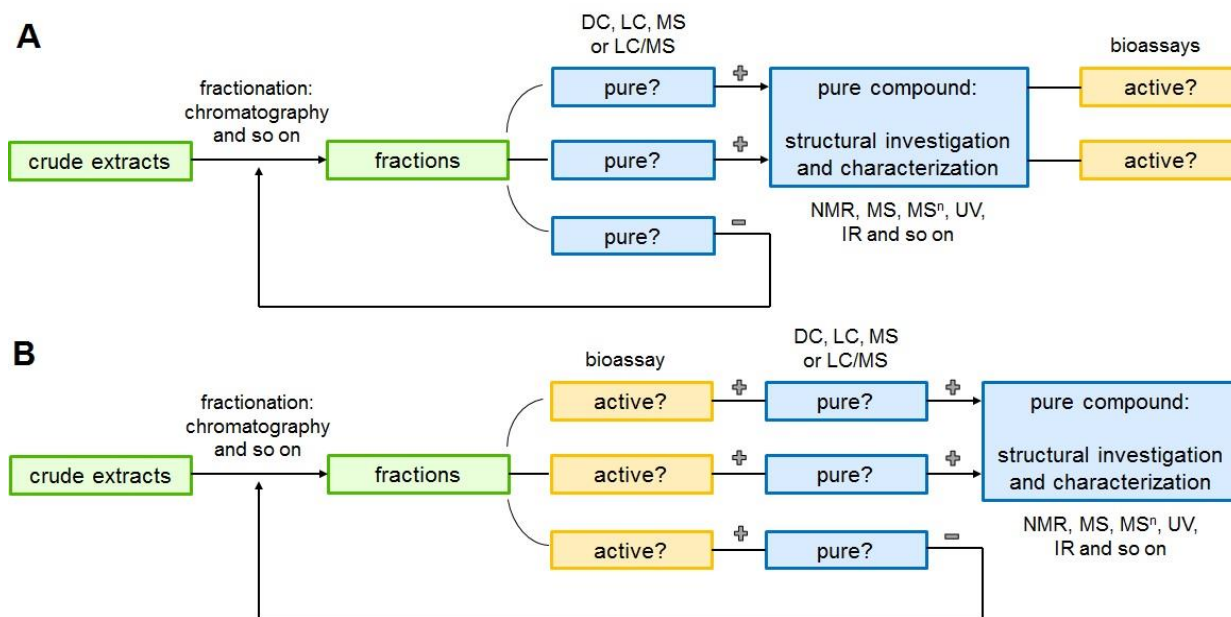

Figure 8.   A: Classical non-directed isolation of natural products, **B:** bioactivity-guided fractionation.[6]

The identification of the bioactive-relevant compounds represents an uncertain and costly screening process, irrespective of high-throughput screening (HTS) and combinatorial chemistry which have taken a more important role in natural product research.[114] In principle, three different strategies are applied in detecting bioactive compounds from natural sources 1) non-target-based, 2) target-based, and 3) structure-based drug discovery.[115] Advances in fractionation and analytical techniques improved both the isolation and structure determination for a faster screening process of compound mixtures.[116–120] Nevertheless, efforts are necessary to increase the efficiency and speed of the natural product-based drug discovery. During the past years, new technologies based on genomics, bioinformatics, structural biology and different HTS methods were developed.[121]

Especially in the field of antibiotic research different strategies are used and further technologies are developed for the identification of novel structures and molecular mechanisms of action. Many of the clinically used antibiotics were discovered via a classical biological approach in whole-cell or non-target-based screenings. Target-based high-throughput screening (HTS) is based on *in vitro* assays with isolated biochemical targets identified by genomic approaches. Identification of new potential targets in bacterial pathogens and genomic information becomes a powerful tool to discover selected pathway-specific genes. The concept of 'antisense RNA technology' is a rapid and general approach to identify essential genes in bacteria cells.[122,123] A target-based whole-cell strategy with antisense RNA technology led to novel fatty acid synthesis inhibitors[124] such as platensimycin (**24**) and platencin (**25**) as shown in Figure 9.[125–127] Another whole-cell HTS approach is premised on a spectroscopic assay of bacterial sugar fermentation.[128] The structurally new antibacterial compound mirandamycin (**26**) was identified as a broad-spectrum antibiotic against different bacteria including the methicillin-resistant *Staphylococcus aureus* and *Mycobacterium tuberculosis* (Figure 9).[128] Furthermore, the bacterial topoisomerase inhibitor kibdelomycin (**27**) was discovered using 'chemical-genetic profiling' (Figure 9).[129] Other screening concepts to identify antibacterially active natural products in extracts are 'differential smart screens'[130] or direct chromatography affinity selection-mass spectrometry assay.[131] The structure-based drug discovery as third strategy includes the *in silico* methods comprising virtual high-throughput screening and fragment-based drug discovery. Alternative virtual screening approaches of complex compound mixtures are developed as prediction models for the identification of bioactive substances like the quantitative composition-activity relationship (QCAR)[132,133] and quantitative pattern-activity relationship (QPAR).[134] These two modeling approaches use several multivariate analysis methods.
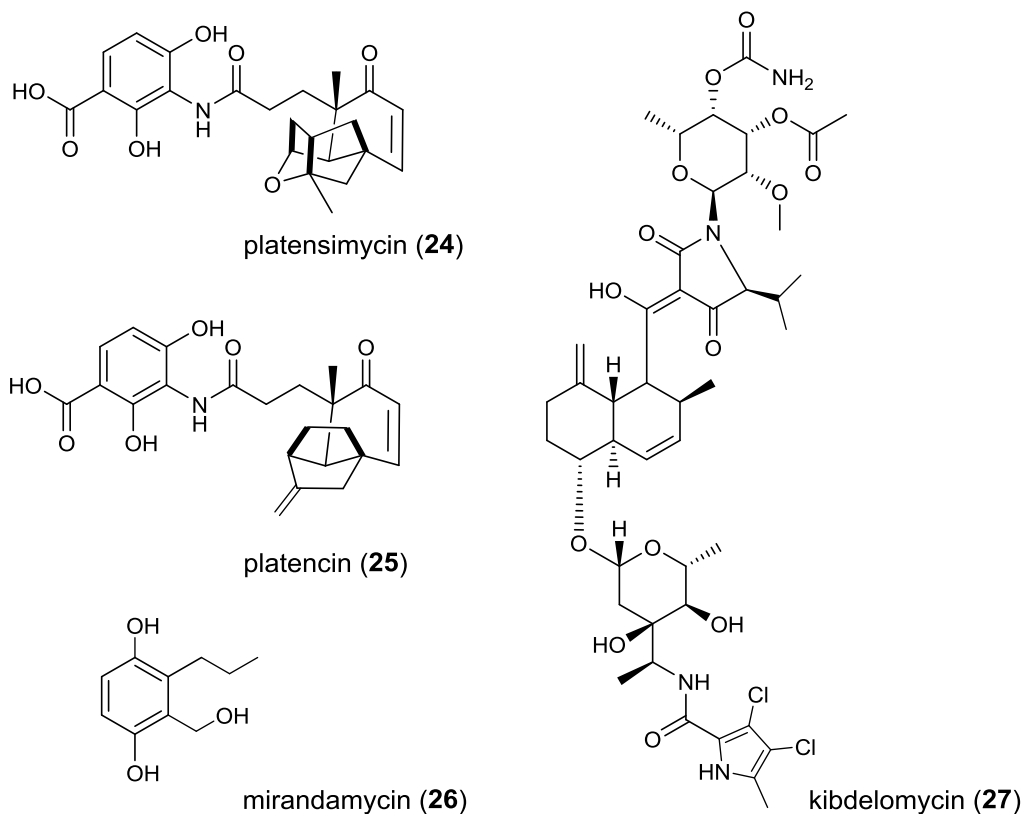
Figure 9.   Antibacterial compounds platensimycin (**24**), platencin (**25**), mirandamycin (**26**) and kibdelomycin (**27**).[125–129]

Another approach in the course of the development of antibiotics is the antibiotic mode of action profile (BioMAP) screening platform. This screening method provides a target-independent mechanism for classifying natural products as compound classes directly from complex mixtures and offers new opportunities for the discovery of natural-based antibiotics.[135,136]

1.5   Mass spectrometry, metabolomics and multivariate data analysis

Metabolomics is a '*comprehensive analysis of the whole metabolome under a given set of conditions*'.[137] For the analysis of the complete set of metabolites in biological samples it is necessary to use a combination of analytical techniques and multivariate data analysis (MDA).[138] In most of the cases well-known analytical tools like chromatography, mass spectrometry (MS) and nuclear magnetic resonance (NMR) spectroscopy are applied to create the 'omics' data set.[139] The sensitive and selective analytical techniques provide important information for the structure identification.

Mass spectrometry has become the method of choice in most of metabolomics studies, especially LC-MS and high resolution MS (HR-MS) because of its high sensitivity and wide range of detectable metabolites. The sample obtained from an extraction process can be used both for direct infusion experiments and chromatographic separation. MS represents an effective tool to analyze both a large number of metabolites and a special substance class. Therefore, mass spectrometry is extensively used for metabolic fingerprinting and metabolite profiling. Liquid chromatography combined with tandem mass spectrometric methods leads to important structural information of a compound, such as molecular weight, molecular formula, fragmentation pattern, isotopic pattern as well as its retention time. LC-MS are important especially in the field of natural products. An overview of the role, the capabilities and the application areas of mass spectrometry in natural product research is given in the review articles of Jarmusch and Cooks (2014)[140] and Carter (2014).[141]

MS-based metabolomic approaches generate large data sets.[142] When extracting information from those data sets with multiple variables, different kinds of MDA can be used. By using all variables simultaneously MDA simplifies and visualizes compositional differences between samples.[143] In this context principal component analysis (PCA),[143,144] partial least squares to latent structures (PLS)[143] and orthogonal PLS (OPLS)[145] are important tools to analyze and interpret complex mixtures.

1.5.1   Mass spectrometry based characterization of prenylated compounds

The use of the combination of liquid chromatography with positive ion electrospray ionization tandem mass spectrometry (LC/ESI-MS^n) for the identification of prenylflavonoids is described by Simons *et al.* (2009).[146] This method is based on a neutral loss screening of 42 Da and 56 Da in the positive-ion mode MS^2 and MS^3 spectra. An important criterium to distinguish between a prenyl side chain and a cyclized prenyl unit forming a pyrane ring system is the ratio of the relative abundance of the fragment ions after loss of C_3H_6 or C_4H_8.[146] It should be noted, that not each neutral loss of 42 Da or 56 Da hints at the occurrence of an isoprene unit. Such losses are also detectable, when C_2H_2O (42 Da)[147] or two CO molecules (56 Da)[148] are lost during the mass spectral fragmentation. Kang *et al.* (2008) could also show that the identification of oxyprenyl substituents in furanocoumarins is feasible by their characteristic fragmentation pattern (Figure 10).[149] The mono-oxyprenylated furanocoumarins imperatorin (**1**) and isoimperatorin (**2**) produce a fragment ion at *m/z* 203 [M+H-C$_5$H$_8$]$^+$ in their MS^2. This fragmentation behavior with an initial C_5H_8 loss followed by the sequential losses of CO in compounds **1** and **2** was also described by Concannon *et al.* (2000).[150] These results are comparable to those obtained under EI conditions.[151,152] Further fragmentation of the ion at *m/z* 203 gives information about the position of the isopentenoxy group. In case of imperatorin (**1**) with an oxyprenylation at *C*-8 and no substitution at *C*-5, the relative abundance of the CO loss from the ion at *m/z* 203 (*m/z* 175) is higher than the relative abundance of the CO$_2$ loss (*m/z* 159). If only an isopentenoxy group is located at *C*-8, as in isoimperatorin (**2**), the relative abundance of *m/z* 159 ([203-CO$_2$]$^+$) is higher than that of *m/z* 175 (203-CO]$^+$). Kang *et al.* (2008) discussed these observations under the aspect of formation of a π-π-conjugation after such a neutral loss and justified thus abundance differences of the corresponding key ions.[149]

Furthermore, the fragmentation pattern of isopimpinellin (**28**, [M+H]$^+$ ion at *m/z* 247, Figure 11) with methoxy groups at *C*-5 and *C*-8 was characterized. Successive elimination of methyl radicals (CH$_3$·) and further losses of CO leads to the fragment ions at *m/z* 232, *m/z* 217, *m/z* 189, and *m/z* 161, whereas no CO$_2$ loss is observable. Because of the formed homo-quinone conjugation (see Figure 10.A, shown in red) next to the π-π–conjugation, the losses of CO units are preferred.[149] The fragmentation behavior of *C*-prenylated or furanocoumarins with *C*- and *O*-prenylation is not known in detail. Only a few MS^n investigations of *C*-prenylated compounds can be found in the literature. Rutamarin (**29**, Figure 11) displaying losses of C_3H_6 and C_4H_8 in the MS^2 spectrum is an example with a reverse prenyl side chain. Concannon *et al.* (2000) suggested in case of the C_3H_6 loss a cyclization mechanism. However, the loss of C_4H_8

was not commented.[150] First investigations to the fragmentation behavior of *C*-prenylated and furanocoumarins with *C*- and *O*-prenylation were discussed in the diploma thesis of R. Heinke.[153]
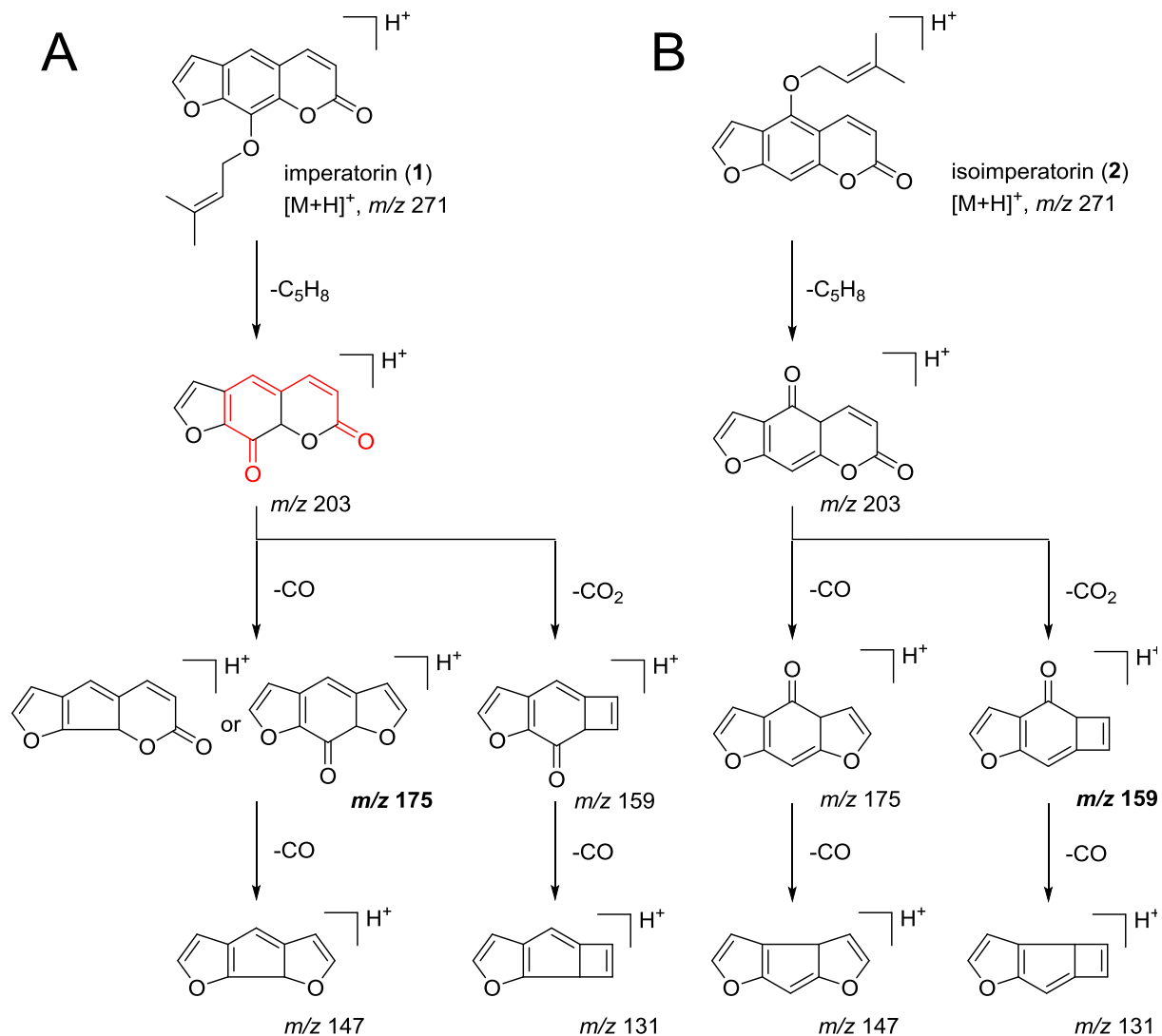
Figure 10. Mass spectral fragmentation pattern with putative structures of fragment ions of **A**: imperatorin (**1**) and **B**: isoimperatorin (**2**).[149]

isopimpinellin (**28**)   rutamarin (**29**)
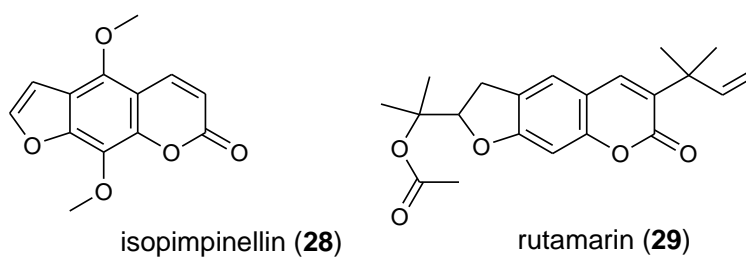
Figure 11. Structures of some furanocoumarins.

1.5.2   Metabolomics, metabolite profiling and metabolite fingerprinting

Metabolomics represents the third major pillar of the functional genomics besides mRNA profiling (transcriptomics) and proteomics.[150] The aim of the metabolomics approach is the identification and quantification of a complete set of metabolites (metabolome) in biological objects (cell, biofluid, tissue) or organisms.[154] Compared with the other 'omics' analyses, metabolomics shows some important differences. The first characteristic is caused by the high diversity of the structural and chemical properties of the metabolites (typically small molecules with a molecular weight lower than 1000 Da). The second feature is related to the high variability of the metabolite concentration of different chemical classes.[139,155] Thus, Fiehn defines several approaches used in metabolomics studies: 1) targeted analysis, 2) metabolite profiling and 3) metabolic fingerprinting.[156]

1) The metabolite target analysis is restricted to qualitative and quantitative analysis of predefined metabolites or compound classes related to a particular enzyme system or pathway.[142,156–159] In contrast to the targeted analysis, the unbiased approaches metabolite profiling and fingerprinting are focused on the detection of as many metabolites as possible without necessity of specific knowledge of these metabolites.[160]

2) Metabolite profiling is used for the identification and quantification of a specific group of metabolites belonging to the same classes of chemical compounds or associated with a certain biochemical pathway.[155,157] This approach is used for searching biomarkers of different diseases, diagnostics, and target search of new drugs or investigations of a special compound class. Metabolite profiling was applied to secondary metabolites of plants such as various *Arabidopsis* mutants,[161] tomato (*Lycopersicon esculentum*)[162] or hop (*Humulus lupulus*)[163] and also of filamentous fungi and yeast.[164] Furthermore, metabolite profiling plays an important role in chemotaxonomy, e.g. of filamentous fungi[165,166] as well as in the classification and identification of extracts.[167,168]

3) Metabolite fingerprinting represents a global and rapid analysis of biological samples for classification based on characteristic metabolite patterns. This approach serves as tool for the differentiation between samples from various biological origins or status (e.g. wild type/mutant; disease/healthy; stressed/non-stressed).[155–158,169,170] Metabolite fingerprinting was preferably used as diagnostic tool[169] for the determination of biomarkers,[142,171] differentiation of wild type and transgenic plants[172] and also the distinction of developmental stages of organisms[173] and not compulsory for the structural identification of metabolites.[142]

Several MS techniques[161,163,174–178] and NMR spectroscopy[162,163,179] are the most frequently used analytical methods in metabolomics research.[159,180,181] High sensitivity detection and

quantification of low molecular weight metabolites at concentrations below the nanogram per milliliter range,[182] the determination of a large number of different chemical classes of metabolites and its accessibility and versatility are valuable advantages of modern MS technologies. Consequently, mass spectrometry plays an important role in the analysis of small molecules and in many metabolomics studies. Several reviews and articles deal with MS and LC/MS-based metabolomics methods.[155,159,175,183,184] Different mass spectral methods like FT-MS,[176,177,185,186] liquid chromatography coupled with mass spectrometry (LC-MS)[161,175,187] and gas chromatography-mass spectrometry (GC-MS)[137,174,188,189] allow the analysis of a wide variety of compound classes. High resolution MS leading to accurate mass measurements and structural information obtained from tandem mass spectrometry often additionally allow structural identification.[163] Combined with separation techniques the capability of the analysis of highly complex mixtures is remarkably expanded. Furthermore, the analysis time could be reduced significantly by introducing ultra-performance liquid chromatography (UPLC).[190,191]

Within the past decades, almost all available mass spectrometry platforms have been applied to target analysis and more recently to metabolic profiling and fingerprinting. Furthermore, the introduction of LC/MS-based data analysis including peak detection and mass spectral deconvolution is an important improvement in the metabolomics field. Open source freeware like XCMS contains novel algorithms allowing a LC/MS metabolite data processing (peak-picking and alignment).[192] Data matrices are generally described by *m/z* values and their corresponding intensities of the detected ions. Additionally, in case of a preceding separation step, retention times can be also used to index metabolites.[193] In summary, matrices containing *m/z* values, ion abundances and retention times represent a valuable input for further multivariate data analysis such as PCA,[143,144] PLS[143] or OPLS.[145]

1.5.3   Principal component analysis (PCA)

The principal component analysis (PCA) represents the basis and starting point for all multivariate data analysis (MDA).[143] It is an unsupervised clustering method for data visualization and simplification. Data tables containing observations (e.g. spectra of crude extracts) are described by several dependent variables (spectral information such as RT, *m/z*).[194] PCA does not require any detailed knowledge of the data sets and uses mathematical projection principles to reduce the dimensionality of multivariate data while preserving most of the variances within to lower dimensionality.[143,194,195] The projection points out the dominating characteristics and important information of the given multivariate data set.[143,194] This procedure allows a first look into the structure of the data and helps to detect outliers and recognize trends, groups or other patterns.[143]

1.5.4   Orthogonal partial least squares (OPLS)

The partial least squares to latent structures (PLS) analysis represents an amplified PCA model, where the data matrices are divided into two or more groups of variables.[143] The orthogonal partial least squares (OPLS) is a multivariate equivalent modification of PLS developed by Trygg and Wold (2002).[145] In comparison to PLS the projection is rotated in that way, that the first component PC1 shows the between class difference.[196] The model is focused on the effect of interest and separates data into predictive and uncorrelated information.[197] In contrast to PCA, the OPLS method is a supervised prediction and regression model, in which information about the data sets are compulsory. The variables contain information (measured or known) about the samples which can be distinguished between continuous (time, concentration) or discrete (control or treated; male or female; species 1 or species 2) values.[198] In case of OPLS-discriminate analysis (DA) discrete variables are used. This model is guided by the known class information and shows differences between groups as a whole. Therefore, OPLS-DA is useful for the classification and is easy to interpret with two classes. The two class model exhibit which variables are responsible for class discrimination. Furthermore, potential biomarkers can be extracted using a S-plot visualizing the OPLS-DA loadings. Combining the S-plot with the loading plot containing jack-knifed confidence intervals statistically significant but not necessarily biochemically significant biomarkers can be identified. OPLS-DA can be also extended to more than two classes, but the interpretation is difficult.[198]

1.5.5   'Reverse metabolomics' and activity correlation analysis (AcorA)

A new approach for a direct identification of unknown bioactive compounds in complex mixture, called 'reverse metabolomics", combines the metabolite profiling with biological screening methods and mathematical informatics deconvolution (Figure 12). Combination of modern metabolomics techniques and traditional natural product isolation form the concept of this novel approach. On the one hand, 'reverse metabolomics' describes an untargeted metabolome analysis measured with different chromatographic and/or spectroscopic methods like mass spectrometry (MS) with and without coupling liquid chromatography (LC-MS) or nuclear magnetic resonance (NMR) spectroscopy. On the other hand, crude extracts were screened with respect to their biological activities. Based on an activity correlation analysis (AcorA) chromatographic and spectroscopic metabolite profiles were correlated with activity profiles of the extracts. The AcorA results yield a hit list, which shows the statistically significant correlations of MS signals to a specific biological activity. Therefore, 'reverse metabolomics' pursues a holistic metabolomics strategy in which almost all simultaneously measurable metabolites are recorded. Using statistical data analysis, preferentially compounds responsible for the activity of interest are identified. This method was developed by L. Wessjohann and coworkers at the Leibniz Institute of Plant Biochemistry (IPB), Halle (Germany).[199]

One of the first application of the 'reverse metabolomics' approach was used for the correlation of sensorial attributes with GC-MS, LC-MS and NMR data of culinary beef stocks.[200]
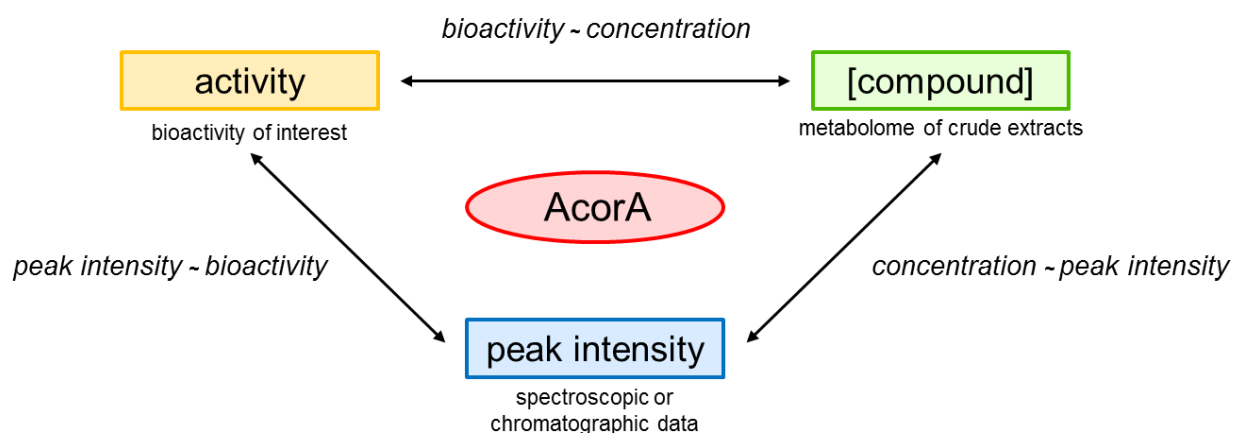
Figure 12. Concept of the 'reverse metabolomics' approach with the assumed correlation of the activity-correlation analysis (AcorA).[199]

1.6   References

1.   Williams, D. H., Stone, M. J., Hauck, P. R. & Rahman, S. K. (1989) Why are secondary metabolites (natural products) biosynthesized? *J. Nat. Prod.* **52**, 1189–1208.

2.   Harvey, A. L. (2008) Natural products in drug discovery. *Drug Dis. Today* **13**, 894–901.

3.   Newman, D. J. & Cragg, G. M. (2007) Natural products as sources of new drugs over the last 25 years. *J. Nat. Prod.* **70**, 461–477.

4.   Newman, D. J. & Cragg, G. M. (2012) Natural products as sources of new drugs over the 30 years from 1981 to 2010. *J. Nat. Prod.* **75**, 311–335.

5.   Clark, A. M. (1996) Natural Products as a Resource for New Drugs. *Pharm. Res.* **13**, 1133–1141.

6.   Koehn, F. E. & Carter, G. T. (2005) The evolving role of natural products in drug discovery. *Nat. Rev. Drug Discov.* **4**, 206–220.

7.   Saleh, O., Haagen, Y., Seeger, K. & Heide, L. (2009) Prenyl transfer to aromatic substrates in the biosynthesis of aminocoumarins, meroterpenoids and phenazines: The ABBA prenyltransferase family. *Phytochemistry* **70**, 1728–1738.

8.   Ansaldi, M., Marolt, D., Stebe, T., Mandic-Mulec, I. & Dubnau, D. (2002) Specific activation of the *Bacillus* quorum-sensing systems by isoprenylated pheromone variants. *Mol. Microbiol.* **44**, 1561–1573.

9.   Scherlach, K., Schuemann, J., Dahse, H.-M. & Hertweck, C. (2010) Aspernidine A and B, prenylated isoindolinone alkaloids from the model fungus *Aspergillus nidulans*. *J. Antibiot.* **63**, 375–377.

10.   Li, S.-M. (2010) Prenylated indole derivatives from fungi: structure diversity, biological activities, biosynthesis and chemoenzymatic synthesis. *Nat. Prod. Rep.* **27**, 57–78.

11.   Buchanan, M. S., Carroll, A. R., Fechner, G. A., Boyle, A., Simpson, M., Addepalli, R., Avery, V. M.,Hooper, J. N. A., Cheung, T., Chen, H & Quinn, R. J. (2008) Aplysamine 6, an alkaloidal inhibitor of isoprenylcysteine carboxyl methyltransferase from the sponge *Pseudoceratina* sp. *J. Nat. Prod.* **71**, 1066–1067.

12.   Sunassee, S. N. & Davies-Coleman, M. T. (2012) Cytotoxic and antioxidant marine prenylated quinones and hydroquinones. *Nat. Prod. Rep.* **29**, 513–535.

13.   Mukne, A. P., Viswanathan, V. & Phadatare, A. G. (2011) Structure pre-requisites for isoflavones as effective antibacterial agents. *Pharmacog. Rev.* **5**, 13–18.

14.   Yazaki, K., Sasaki, K. & Tsurumaru, Y. (2009) Prenylation of aromatic compounds, a key diversification of plant secondary metabolites. *Phytochemistry* **70**, 1739–1745.

15.   Zhao, L., Chang, W.-C., Xiao, Y., Liu, H.-W. & Liu, P. (2013) Methylerythritol phosphate pathway of isoprenoid biosynthesis. *Annu. Rev. Biochem.* **82**, 497–530.

16.   Boucher, Y. & Doolittle, W. F. (2000) The role of lateral gene transfer in the evolution of isoprenoid biosynthesis pathways. *Mol. Microbiol.* **37**, 703–716.

17. Grochowski, L. L., Xu, H. & White, R. H. (2006) *Methanocaldococcus jannaschii* uses a modified mevalonate pathway for biosynthesis of isopentenyl diphosphate. *J. Bacteriol.* **188**, 3192–3198.

18. Mabanglo, M. F., Schubert, H. L., Chen, M., Hill, C. P. & Poulter, C. D. (2010) X-ray structures of isopentenyl phosphate kinase. *ACS Chem. Biol.* **5**, 517–527.

19. Dellas, N. & Noel, J. P. (2010) Mutation of archaeal isopentenyl phosphate kinase highlights mechanism and guides phosphorylation of additional isoprenoid monophosphates. *ACS Chem. Biol.* **5**, 589–601.

20. Chen, M. & Poulter, C. D. (2010) Characterization of thermophilic archaeal isopentenyl phosphate kinases. *Biochemistry* **49**, 207–217.

21. Hunter, W. N. (2007) The non-mevalonate pathway of isoprenoid precursor biosynthesis. *J. Biol. Chem.* **282**, 21573–21577.

22. Genovese, S., Curini, M. & Epifano, F. (2009) Chemistry and biological activity of azoprenylated secondary metabolites. *Phytochemistry* **70**, 1082–1091.

23. Majmudar, J. D. & Gibbs, R. A. (2011) Pericyclic prenylation: Peptide modification through a claisen rearrangement. *Chem. Bio. Chem.* **12**, 2723–2726.

24. Epifano, F., Genovese, S., Menghini, L. & Curini, M. (2007) Chemistry and pharmacology of oxyprenylated secondary plant metabolites. *Phytochemistry* **68**, 939–953.

25. Comte, G., Daskiewicz, J.-B., Bayet, C., Conseil, G., Viornery-Vanier, A., Dumontet, C., Di Pietro, A. & Barron, D. (2001) C-Isoprenylation of flavonoids enhances binding affinity toward P-glycoprotein and modulation of cancer cell chemoresistance. *J. Med. Chem.* **44**, 763–768.

26. Botta, B., Monache, G. D., Menendez, P. & Boffi, A. (2005) Novel prenyltransferase enzymes as a tool for flavonoid prenylation. *Trends Pharmacol. Sci.* **26**, 606–608.

27. Botta, B., Vitali, A., Menendez, P., Misiti, D. & Monache, G. D. (2005) Prenylated flavonoids: Pharmacology and biotechnology. *Curr. Med. Chem.* **12**, 713–739.

28. Barron, D. & Ibrahim, R. K. (1996) Isoprenylated flavonoids - a survey. *Phytochemistry* **43**, 921–982.

29. Sohn, H.-Y., Son, K. H., Kwon, C.-S., Kwon, G.-S. & Kang, S. S. (2004) Antimicrobial and cytotoxic activity of 18 prenylated flavonoids isolated from medicinal plants: *Morus alba* L., *Morus mongolica* Schneider, *Broussnetia papyrifera* (L.) Vent, *Sophora flavescens* Ait and *Echinosophora koreensis* Nakai. *Phytomedicine* **11**, 666–672.

30. Castanheiro, R. A. P., Castanheiro, R. A.P., Pinto, M. M.M., Silva, A. M. S., Cravo, S. M. M., Gales, L., Damas, A. M., Nazareth, N., Nascimento, M. S. J. & Eaton, G. (2007) Dihydroxyxanthones prenylated derivatives: synthesis, structure elucidation, and growth inhibitory activity on human tumor cell lines with improvement of selectivity for MCF-7. *Bioorg. Med. Chem.* **15**, 6080–6088.

31. Daskiewicz, J. B., Comte, G., Barron, D., Di Pietro, A. & Thomasson, F. (1999) Organolithium mediated synthesis of prenylchalcones as potential inhibitors of chemoresistance. *Tetrahedron Lett.* **40**, 7095–7098.

32. Tchamo, D. N., Dijoux-Franca, M.-G., Mariotte, A.-M., Tsamo, E., Daskiewicz, J. B., Bayet, C., Barron, D., Conseil, G.& Di Pietro, A. (2000) Prenylated xanthones as potential P-glycoprotein modulators. *Bioorg. Med. Chem. Lett.* **10**, 1343–1345.

33. Chi, Y. S., Jong, H. G., Son, K. H., Chang, H. W., Kang, S. S. & Kim, H. P. (2001) Effects of naturally occurring prenylated flavonoids on enzymes metabolizing arachidonic acid: cyclooxygenases and lipoxygenases. *Biochem. Pharmacol.* **62**, 1185–1191.

34. Kumazawa, S., Ueda, R., Hamasaka, T., Fukumoto, S., Fujimoto, T. & Nakayama, T. (2007) Antioxidant prenylated flavonoids from propolis collected in Okinawa, Japan. *J. Agric. Food Chem.* **55**, 7722–7725.

35. Miranda, C. L., Stevens, J. F., Ivanov, V., Mccall, M., Frei, B., Deinzer, M. L. & Buhler, D. R. (2000) Antioxidant and prooxidant actions of prenylated and nonprenylated chalcones and flavanones in vitro. *J. Agric. Food Chem.* **48**, 3876–3884.

36. Lee, J. H., Lee, B. W., Kim, J. H., Seo, W. D., Jang, K. C. & Park, K. H. (2005) Antioxidant effects of isoflavones from the stem bark of *Cudrania tricuspidata*. *Agric. Chem. Biotechnol.* **48**, 193–197.

37. Du, J., He, Z.-D., Jiang, R.-W., Ye, W.-C., Xu, H.-X. & But, P. P.-H. (2003) Antiviral flavonoids from the root bark of *Morus alba* L. *Phytochemistry* **62**, 1235–1238.

38. Kim, S. J., Son, K. H., Chang, H. W., Kang, S. S. & Kim, H. P. (2003) Tyrosinase inhibitory prenylated flavonoids from *Sophora flavescens*. *Biol. Pharm. Bull.* **26**, 1348–1350.

39. Dong, X., Fan, Y., Yu, L. & Hu, Y. (2007) Synthesis of four natural prenylflavonoids and their estrogen-like activities. *Arch. Pharm. Chem. Life Sci.* **340**, 372–376.

40. Wabo, H. K., Kouam, S. F., Krohn, K., Hussain, H., Tala, M. F., Tane, P., Van Ree, T., Hu, Q. & Schulz, B. (2007) Prenylated anthraquinones and other constituents from the seeds of *Vismia laurentii*. *Chem. Pharm. Bull.* **55**, 1640–1642.

41. Appendino, G., Gibbons, S., Giana, A., Pagani, A., Grassi, G., Stavri, M., Smith, E. & Rahman, M. M. (2008) Antibacterial cannabinoids from *Cannabis sativa*: A structure−activity study. *J. Nat. Prod.* **71**, 1427–1430.

42. Mesía-Vela, S., Sańchez, R. I., Estrada-Muñiz, E., Alavez-Solano, D., Torres-Sosa, C., Jiménez-Estrada, M., Reyes-Chilpa, R. & Kauffman, F. C. (2001) Natural products isolated from Mexican medicinal plants: Novel inhibitors of sulfotransferases, SULT1A1 and SULT2A1. *Phytomedicine* **8**, 481–488.

43. Oh, W. K., Kim, B. Y., Oh, H., Kim, B. S. & Ahn, J. S. (2005) Phospholipase Cγ1 inhibitory activities of prenylated flavonoids isolated from *Erythrina senegalensis*. *Planta Med.* **71**, 780–782.

44. Park, K. M., You, J. S., Lee, H. Y., Baek, N. I. & Hwang, J. K. (2003) Kuwanon G: An antibacterial agent from the root bark of *Morus alba* against oral pathogens. *J. Ethnopharmacol.* **84**, 181–185.

45. Stevens, J. F., Taylor, A. W., Nickerson, G. B., Ivancic, M., Henning, J., Haunold, A. & Deinzer, M. L. (2000) Prenylflavonoid variation in *Humulus lupulus*: Distribution and taxonomic significance of xanthogalenol and 4′-O-methylxanthohumol. *Phytochemistry* **53**, 759–775.

46. Wu, Q. L., Wang, S. P., Du, L. J., Yang, J. S. & Xiao, P. G. (1998) Xanthones from *Hypericum japonicum* and *H. henryi*. *Phytochemistry* **49**, 1395–1402.

47. Aoki, N., Muko, M., Ohta, E. & Ohta, S. (2008) C-geranylated chalcones from the stems of *Angelica keiskei* with superoxide-scavenging activity. *J. Nat. Prod.* **71**, 1308–1310.

48. Ribeiro, A. B., Abdelnur, P. V., Garcia, C. F., Belini, A., Severino, V. G. P., Da Silva, M. F. D. G. F., Fernandes, J. B., Vieira, P. C., De Carvalho, S. A., De Souza, A. & Machado, M. A. (2008) Chemical characterization of *Citrus sinensis* grafted on *C. limonia* and the effect of some isolated compounds on the growth of *Xylella fastidiosa*. *J. Agric. Food Chem.* **56**, 7815–7822.

49. Abegaz, B. M., Ngadjui, B. T., Dongo, E., Ngameni, B., Nindi, M. N. & Bezabih, M. (2002) Chalcones and other constituents of *Dorstenia prorepens* and *Dorstenia zenkeri*. *Phytochemistry* **59**, 877–883.

50. Dufall, K. G., Ngadjui, B. T., Simeon, K. F., Abegaz, B. M. & Croft, K. D. (2003) Antioxidant activity of prenylated flavonoids from the West African medicinal plant *Dorstenia mannii*. *J. Ethnopharmacol.* **87**, 67–72.

51. Jang, D. S., Cuendet, M., Hawthorne, M. E., Kardono, L. B. S., Kawanishi, K., Fong, H. H. S., Mehta, R. G., Pezzuto, J. M. & Kinghorn, A. D. (2002) Prenylated flavonoids of the leaves of *Macaranga conifera* with inhibitory activity against cyclooxygenase-2. *Phytochemistry* **61**, 867–872.

52. Kretzschmar, G., Zierau, O., Wober, J., Tischer, S., Metz, P. & Vollmer, G. (2010) Prenylation has a compound specific effect on the estrogenicity of naringenin and genistein. *J. Steroid Biochem.* **118**, 1–6.

53. Ngadjui, B. T., Dongo, E., Tamboue, H., Fogue, K. & Abegaz, B. M. (1999) Prenylated favanones from the twigs of *Dorstenia mannii*. *Phytochemistry* **50**, 1401–1406.

54. Abegaz, B. M., Ngadjui, B. T., Dongo, E. & Tamboue, H. (1998) Prenylated chalcones and flavones from the leaves of *Dorstenia kameruniana*. *Phytochemistry* **49**, 1147–1150.

55. Ngadjui, B. T., Ngameni, B., Dongo, E., Kouam, S. F. & Abegaz, B. M. (2002) Prenylated and geranylated chalcones and flavones from the aerial parts of *Dorstenia ciliata*. *Bull. Chem. Soc. Ethiop.* **16**, 157–163.

56. Abegaz, B., Ngadjui, B. & Folefoc, G. (2004) Prenylated flavonoids, monoterpenoid furanocoumarins and other constituents from the twigs of *Dorstenia elliptica* (Moraceae). *Phytochemistry* **65**, 221–226.

57. Franke, K., Porzel, A., Masaoud, M., Adam, G. & Schmidt, J. (2001) Furanocoumarins from *Dorstenia gigas*. *Phytochemistry* **56**, 611–621.

58. Heinke, R., Franke, K., Porzel, A., Wessjohann, L. A., Awadh Ali, N. A. & Schmidt, J. (2011) Furanocoumarins from *Dorstenia foetida*. *Phytochemistry* **72**, 929–934.

59. Ekiert, H., Chołoniewska, M. & Gom, E. (2001) Accumulation of furanocoumarins in *Ruta graveolens* L. shoot culture. *Biotechnol. Lett.* **23**, 543–545.

60. Ban, H. S., Lim, S. S., Suzuki, K., Jung, S. H., Lee, S., Lee, Y. S., Shin, K. H. & Ohuchi, K. (2003) Inhibitory effects of furanocoumarins isolated from the roots of *Angelica dahurica* on prostaglandin E2 production. *Planta Med.* **69**, 408–412.

61. Härmälä, P., Vuorela, H., Hiltunen, R., Nyiredy, Sz., Sticher, O., Törnquist, K. & Kaltia, S. (1992) Strategy for the isolation and identification of coumarins with calcium antagonistic properties from the roots of *Angelica archangelica*. *Phytochem. Anal.* **3**, 42–48.

62. Kang, S. Y., Lee, K. Y., Sung, S. H., Park, M. J. & Kim, Y. C. (2001) Coumarins isolated from *Angelica gigas* inhibit acetylcholinesterase: Structure-activity relationships. *J. Nat. Prod.* **64**, 683–685.

63. Guo, L.-Q. & Yamazoe, Y. (2004) Inhibition of cytochrome P450 by furanocoumarins in grapefruit juice and herbal medicines. *Acta Pharmacol. Sin.* **25**, 129–136.

64. He, K., Iyer, K. R., Hayes, R. N., Sinz, M. W., Woolf, T. F. & Hollenberg, P. (1998) Inactivation of cytochrome P450 3A4 by bergamottin, a component of grapefruit juice. *Chem. Res. Toxicol.* **11**, 252–259.

65. Kent, U. M., Lin, H., Noon, K. R., Harris, D. L. & Hollenberg, P. F. (2006) Metabolism of bergamottin by cytochromes P450 2B6 and 3A5. *J. Pharmacol. Exp. Ther.* **318**, 992-1005.

66. Piao, X. L., Park, I. H., Baek, S. H., Kim, H. Y., Park, M. K. & Park, J. H. (2004) Antioxidative activity of furanocoumarins isolated from *Angelicae dahuricae*. *J. Ethnopharmacol.* **93**, 243–246.

67. Piao, X. L., Yoo, H. H., Kim, H. Y., Kang, T. L., Hwang, G. S.& Park, J. H. (2006) Estrogenic activity of furanocoumarins isolated from *Angelica dahurica*. *Arch. Pharm. Res.* **29**, 741–745.

68. Li, S.-M. (2009) Applications of dimethylallyltryptophan synthases and other indole prenyltransferases for structural modification of natural products. *Appl. Microbiol. Biotechnol.* **84**, 631–639.

69. Wang, F., Fang, Y., Zhu, T., Zhang, M., Lin, A., Gu, Q. & Zhu, W. (2008) Seven new prenylated indole diketopiperazine alkaloids from holothurian-derived fungus *Aspergillus fumigatus*. *Tetrahedron* **64**, 7986–7991.

70. Geraci, C., Piattelli, M., Tringali, C., Verbist, J.-F. & Roussakis, C. (1992) Cytotoxic activity of tetraprenylphenols related to suillin, an antitumor principle from *Suillus granulatus*. *J. Nat. Prod.* **55**, 1772–1775.

71. Gill, M. & Steglich, W. (1987) Pigments of fungi (Macromycetes) in Zechmeister, L., Herz, W., Grisebach, H., Kirby, G. W. & Tamm, C. H. (eds.) *Progess in the chemistry of organic natural products*, vol. 51 Springer Vienna. ISBN: 978-3-7091-7456-2.

72. Liu, L.-Y., Li, Z.-H., Wang, G.-Q., Wei, K., Dong, Z.-J., Feng, T., Li, G.-T., Li, Y. & Liu, J.-K. (2014) Nine new farnesylphenols from the Basidiomycete *Albatrellus caeruleoporus*. *Nat. Products Bioprospect.* **4**, 119–128.

73. Yang, X.-L., Qin, C., Wang, F., Dong, Z.-J. & Ji-Kai, L. (2008) A new meroterpenoid pigment from the Basidiomycete *Albatrellus confluens*. *Chem. Biodivers.* **5**, 484–489.

74. Liu, L.-Y., Li, Z.-H., Ding, Z.-H., Dong, Z.-J., Li, G.-T., Li, Y. & Liu, J.-K. (2013) Meroterpenoid pigments from the Basidiomycete Albatrellus ovinus. *J. Nat. Prod.* **76**, 79-84.

75. Geris, R. & Simpson, T. J. (2009) Meroterpenoids produced by fungi. *Nat. Prod. Rep.* **26**, 1063–1094.

76. Cornforth, J. W. (1968) Terpenoid biosynthesis. *Chem. Ber.* **4**, 102–106.

77. Simpson, T. J. (1987) Applications of multinuclear NMR to structural and biosynthetic studies of polyketide microbial metabolites. *Chem. Soc. Rev.* **16**, 123–160.

78. Besl, H. & Bresinsky, (1997) A. Chemosystematics of Suillaceae and Gomphidiaceae (suborder Suillineae). *Pl. Syst. Evol.* **206**, 223–242.

79. Beaumont, P. C. & Edwards, R. L. (1971) Constituents of the higher fungi. Part XI. Boviquinone-3, (2,5-dihydroxy-3-farnesyl-1,4- benzoquinone), diboviquinone-3,4, methylenediboviquinone-3,3, and xerocomic acid from *Gomphidius rutilus* Fr. and diboviquinone-4,4 from *Boletus* (*Suillus*) *bovinus* (Linn ex Fr.) Kuntze. *J. Chem. Soc.* **14**, 2582–2585.

80. Beaumont, P. C. & Edwards, R. L. (1969) Constituents of the higher fungi. Part IX. Bovinone, 2,5-dihydroxy-3-geranylgeranyl-1,4-benzoquinone from *Boletus* (*Suillus*) *bovinus* (Linn. ex Fr.) Kuntze. *J. Chem. Soc.* **18**, 2398–2403.

81. Tringali, C., Piattelli, M., Geraci, C. & Nicolosi, G. (1989) Antimicrobial tetraprenylpenols from *Suillus granulatus*. *J. Nat. Prod.* **52**, 941–947.

82. Shirata, K., Kato, T. & Niwano, M. (1995) Selective suppression of the mitogenic response of murine lymphocytes by suillin from *Suillus bovinus*. *Mycologia* **87**, 360–361.

83. Hayashi, T., Kanetoshi, A., Ikura, M. & Shirahama, H. (1989) Bolegrevilol, a new lipid peroxidation inhibitor from the edible mushroom *Suillus grevillei*. *Chem. Pharm. Bull.* **37**, 1424–1425.

84. Kukovinets, O. S., Zainullin, R. A. & Kislitsyn, M. I. (2006) Natural arylterpenes and their biological activity. *Chem. Nat. Comp.* **42**, 1–15.

85. Kasuga, A., Aoyagi, Y. & Sugahara, T. (1995) Antioxidant activity of fungus *Suillus bovinus* (L: Fr.) 0. Kuntze. *J. Food Sci.* **60**, 1113–1115.

86. Hirata, Y. & Nakanishi, K. (1950) Grifolin, an antibiotic from a Basidiomycete. *J. Biol. Chem.* **184**, 135–143.

87. Goto, T., Kakisawa, H. & Hirata, Y. (1963) The structure of grifolin, an antibiotic from a basidiomycete. *Tetrahedron* **19**, 2079–2083.

88. Zechlin, L., Wolf, M., Steglich, W. & Anke, T. (1981) Cristatsäure, ein modifiziertes Farnesylphenol aus Fruchtkörpern von *Albatrellus cristatus*. *Liebigs Ann. Chem.* **12**, 2099-2105.

89. Hashimoto, T., Quang, D. N., Nukada, M. & Asakawa, Y. (2005) Isolation, synthesis and biological activity of grifolic acid derivatives from the inedible mushroom *Albatrellus dispansus*. *Heterocycles* **65**, 2431–2439.

90. Liu, X., Winkler, A. L., Schwan, W. R., Volk, T. J., Rott, M. A. & Monte, A. (2010) Antibacterial compounds from mushrooms I: A lanostane-type triterpene and prenylphenol derivatives from *Jahnoporus hirtus* and *Albatrellus flettii* and their activities against *Bacillus cereus* and *Enterococcus faecalis*. *Planta Med.* **76**, 182–185.

91. Tokuyama, S., Horikawa, M., Morita, T., Hashimoto, T., Quang, D. N., Asakawa, Y. & Kawagishi, H. (2007) Anti-MRSA and antifungal compounds from the mushroom *Albatrellus dispansus* (Lloyd) Canf. et Gilb. (Aphyllophoromycetideae). *Int. J. Med. Mushrooms* **9**, 159–161.

92. Luo, D.-Q., Shao, H.-J., Zhu, H.-J. & Liu, J.-K. (2005) Activity in vitro and in vivo against plant pathogenic fungi of grifolin isolated from the basidiomycete *Albatrellus dispansus*. *Z. Naturforsch. C.* **60**, 50–6.

93. Nukata, M., Hashimoto, T., Yamamoto, I., Iwasaki, N., Tanakab, M. & Asakawa, Y. (2002) Neogrifolin derivatives possessing anti-oxidative activity from the mushroom *Albatrellus ovinus*. *Phytochemistry* **59**, 731–737.

94. Ye, M., Liu, J., Lu, Z., Zhao, Y., Liu, S., Li, L., Tan, M., Weng, X., Li, W. & Cao, Y. (2005) Grifolin, a potential antitumor natural product from the mushroom *Albatrellus confluens*, inhibits tumor cell growth by inducing apoptosis in vitro. *FEBS Lett.* **579**, 3437–3443.

95. Ye, M., Luo, X., Li, L., Shi, Y., Tan, M., Weng, X., Li, W., Liu, J. & Cao, Y. (2007) Grifolin, a potential antitumor natural product from the mushroom *Albatrellus confluens*, induces cell-cycle arrest in G1 phase via the ERK1/2 pathway. *Cancer Lett.* **258**, 199–207.

96. Misasa, H., Matsui, Y., Uehara, H., Tanaka, H., Ishihara, M. & Shibata, H. (1992) Tyrosinase inhibitors from *Albatrellus confluens*. *Biosci. Biotech. Biochem.* **56**, 1660–1661.

97. Song, J., Manir, M. & Moon, S. S. (2009) Cytotoxic grifolin derivatives isolated from the wild mushroom *Boletus pseudocalopus* (Basidiomycetes). *Chem. Biodivers.* **6**, 1435–1442.

98. Szallasi, A., Bíró, T., Szabó, T., Modarres, S., Petersen, M., Klusch, A., Blumberg, P. M., Krause, J. E. & Sterner, O. (1999) A non-pungent triprenyl phenol of fungal origin, scutigeral, stimulates rat dorsal root ganglion neurons via interaction at vanilloid receptors. *Brit. J. Pharmacol.* **126**, 1351–1358.

99. Dekermendjian, K., Shan, R., Nielsen, M., Stadler, M., Sterner, O. & Witt, M. R. (1997) The affinity to the brain dopamine D1 receptor in vitro of triphenyl phenols isolated from the fruit bodies of *Albatrellus ovinus. Eur. J. Med. Chem.* **32**, 351-356.

100. Hellwig, V., Nopper, R., Mauler, F., Freitag, J., Ji-Kai, L., Zhi-Hui, D. & Stadler, M. (2003) Activities of prenylphenol derivatives from fruitbodies of *Albatrellus* spp. on the human and rat vanilloid receptor 1 (VR1) and characterisation of the novel natural product, confluentin. *Arch. Pharm. Pharm. Med. Chem.* **2**, 119–126.

101. Lang, M., Mühlbauer, A., Gräf, C., Beyer, J., Lang-Fugmann, S., Polborn, K. & Steglich, W. (2008) Studies on the structure and biosynthesis of tridentoquinone and related meroterpenoids from the mushroom *Suillus tridentinus* (Boletales). *Eur. J. Org. Chem.* **2008**, 816–825.

102. Lang, M., Jägers, E., Polborn, K. & Steglich, W. (2009) Structure and absolute configuration of the fungal ansabenzoquinone rhizopogone. *J. Nat. Prod.* **72**, 214–217.

103. Besl, H., Hecht, H.-J., Vinayagar, P. & Steglich, W. (1975) Tridentochinon, ein [13](3,6)Benzofuranophan aus *Suillus tridentinus* (Boletales). *Chem. Ber.* **108**, 3675–3691.

104. Jägers, E., Pasupathy, V., Hovenbitzer, A. & Steglich, W. (1986) Suillin, ein charakteristischer Inhaltsstoff von Röhrlingen der Gattung *Suillus* (*Boletales*). *Z. Naturforsch. b* **41**, 645–648.

105. Besl, H., Höfle, G., Jendrny, B., Jägers, E. & Steglich, W. (1977) Pilzpigmente, XXXI. Farnesylphenole aus *Albatrellus* Arten (Basidiomycetes). *Chem. Ber.* **110**, 3770–3776.

106. Vrkoč, J., Buděšinsky, M. & Dolejš, L. (1977) Phenolic meroterpenoids from the Basidiomycete *Albatrellus ovinus. Phytochemistry* **16**, 1409–1411.

107. Ikeda, M., Kanou, H. & Nukina, M. (1989) Plant growth inhibitors from fruit bodies of *Polyporus confluens. Bull. Yamagata Univ. Agric. Sci.* **10**, 849–852.

108. Feher, M. & Schmidt, J. M. (2003) Property distributions: Differences between drugs, natural products, and molecules from combinatorial chemistry. *J. Chem. Inf. Comput. Sci.* **43**, 218–227.

109. Donadio, S., Maffioli, S. & Monciardini, P. (2010) Antibiotic discovery in the twenty-first century: Current trends and future perspectives. *J. Antibiot.* **63**, 423–430.

110. Peláez, F. (2006) The historical delivery of antibiotics from microbial natural products--can history repeat? *Biochem. Pharmacol.* **71**, 981–990.

111. Wright, G. D. (2012) Antibiotics: A new hope. *Chem. Biol.* **19**, 3–10.

112. Walsh, C. (2003) Where will new antibiotics come from? *Nat. Rev. Microbiol.* **1**, 65–70.

113. Fischbach, M. A. & Walsh, C. T. (2009) Antibiotics for emerging pathogens. *Science* **325**, 1089–1093.

114. Henkel, T., Brunne, R. M., Müller, H. & Reichel, F. (1999) Statistical investigation into the structural complementarity of natural products and synthetic compounds. *Angew. Chem. Int. Ed.* **38**, 643–647.

115. Chopra, I. (2013) The 2012 Garrod Lecture: Discovery of antibacterial drugs in the 21st century. *J. Antimicrob. Chemother.* **68**, 496–505.

116. Wu, S., Yang, L., Gao, Y., Liu, X. & Liu, F. (2008) Multi-channel counter-current chromatography for high-throughput fractionation of natural products for drug discovery. *J. Chromatogr. A* **1180**, 99–107.

117. Singh, S. & Barrett, J. (2006) Empirical antibacterial drug discovery - foundation in natural products. *Biochem. Pharmacol.* **71**, 1006–1015.

118. Tu, Y., Jeffries, C., Ruan, H., Nelson, C., Smithson, D., Shelat, A. A., Brown, K. M., Li, X.-C., Hester, J. P., Smillie, T., Khan, I. A., Walker, L., Guy, K. & Yan, B. (2010) Automated high-throughput system to fractionate plant natural products for drug discovery. *J. Nat. Prod.* **73**, 751–754.

119. Cremin, P. A. & Zeng, L. (2002) High-throughput analysis of natural product compound libraries by parallel LC-MS evaporative light scattering detection. *Anal. Chem.* **74**, 5492–5500.

120. Eldridge, G. R., Vervoort, H. C., Lee, C. M., Cremin, P. A., Williams, C. T., Hart, S. M., Goering, M. G., O'Neil-Johnson, M. & Zeng, L. (2002) High-throughput method for the production and analysis of large natural product libraries for drug discovery. *Anal. Chem.* **74**, 3963–3971.

121. Silver, L. L. (2011) Challenges of antibacterial discovery. *Clin. Microbiol. Rev.* **24**, 71–109.

122. Ji, Y., Zhang, B., Van Horn, S. F., Warren, P., Woodnutt, G., Burnham, M. K. R. & Rosenberg, M (2001) Identification of critical staphylococcal genes using conditional phenotypes generated by antisense RNA. *Science* **293**, 2266–2269.

123. Forsyth, R. A., Haselbeck, R. J., Ohlsen, K. L., Yamamoto, R. T., Xu, H., Trawick, J. D., Wall, D., Wang, L., Brown-driver, V., Froelich, J. M., Kedar, G. C., King, P., Mccarthy, M., Malone, C., Misiner, B., Robbins, D., Tan, Z., Zhu, Z.-Y., Carr, G., Mosca, D. A., Zamudio, C., Foulkes, J. G. & Zyskind, J. W. (2002) A genome-wide strategy for the identification of essential genes in Staphylococcus aureus. *Mol. Microbiol.* **43**, 1387–1400.

124. Young, K., Jayasuriya, H., Ondeyka, J. G., Herath, K., Zhang, C., Kodali, S., Galgoci, A., Painter, R., Brown-Driver, V., Yamamoto, R., Silver, L. L., Zheng, Y., Ventura, J. I., Sigmund, J., Ha, S., Basilio, A., Vicente, F., Tormo, J. R., Pelaez, F., Youngman, P., Cully, D., Barrett, J. F., Schmatz, D., Singh, S. B. & Wang, J. (2006) Discovery of FabH/FabF inhibitors from natural products. *Antimicrob. Agents Chemother.* **50**, 519–526.

125. Wang, J., Soisson, Stephen M., Young, K., Shoop, W., Kodali, S., Galgoci, A., Painter, R., Parthasarathy, G., Tang, Y. S., Cummings, R., Ha, S., Dorso, K., Motyl, M., Jayasuriya, H., Ondeyka, J., Herath, K., Zhang, C., Hernandez, L., Allocco, J., Basilio, A., Tormo, J. R., Genilloud, O., Vicente, F., Pelaez, F., Colwell, L., Lee, S. H., Michael, B., Felcetto, T., Gill, C., Silver, L. L., Hermes, J. D., Bartizal, K., Barrett, J., Schmatz, D., Becker, J. W., Cully, D. & Singh, S. B. (2006) Platensimycin is a selective FabF inhibitor with potent antibiotic properties. *Nature* **441**, 358–361.

126. Singh, S. B., Jayasuriya, H., Ondeyka, J. G., Herath, K. B., Zhang, C., Zink, D. L., Tsou, N. N., Ball, R. G., Basilio, A., Genilloud, O., Diez, Maria T., Vicente, F., Pelaez, F., Young, K. & Wang, J. (2006) Isolation, structure, and absolute stereochemistry of platensimycin, a broad spectrum antibiotic discovered using an antisense differential sensitivity strategy. *J. Am. Chem. Soc.* **128**, 11916–11920.

127. Wang, J., Kodali, S., Lee, S. H., Galgoci, A., Painter, R., Dorso, K., Racine, F., Motyl, M., Hernandez, L., Tinney, E., Colletti, S. L., Herath, K., Cummings, R., Salazar, O., González, I., Basilio, A., Vicente, F., Genilloud, O., Pelaez, F., Jayasuriya, H., Young, K., Cully, D. F. & Singh, S. B. (2007) Discovery of platencin, a dual FabF and FabH inhibitor with in vivo antibiotic properties. *Proc. Natl. Acad. Sci. USA* **104**, 7612–7616.

128. Ymele-Leki, P. Cao, S., Sharp, J., Lambert, K. G., McAdam, A. J., Husson, R. N., Tamayo, G., Clardy, J. & Watnick, P. I. (2012) A high-throughput screen identifies a new natural product with broad-spectrum antibacterial activity. *PLoS One* **7**, e31307.

129. Phillips, J. W., Goetz, M. A., Smith, S. K., Zink, D. L., Polishook, J., Onishi, R., Salowe, S., Wiltsie, J., Allocco, J., Sigmund, J., Dorso, K., Lee, S., Skwish, S., De la Cruz, M., Martín, J., Vicente, F., Genilloud, O., Lu, J., Painter, R. E., Young, K., Overbye, K., Donald, R. G. K. & Singh, S. B. (2011) Discovery of kibdelomycin, a potent new class of bacterial type II topoisomerase inhibitor by chemical-genetic profiling in Staphylococcus aureus. *Chem. Biol.* **18**, 955–965.

130. Littleton, J., Rogers, T. & Falcone, D. (2005) Novel approaches to plant drug discovery based on high throughput pharmacological screening and genetic manipulation. *Life Sci.* **78**, 467–475.

131. Schug, K. A., Wang, E., Shen, S., Rao, S., Smith, S. M., Hunt, L. & Mydlarz, L. D. (2012) Direct affinity screening chromatography-mass spectrometry assay for identification of antibacterial agents from natural product sources. *Anal. Chim. Acta* **713**, 103–110.

132. Cheng, Y., Wang, Y. & Wang, X. (2006) A causal relationship discovery-based approach to identifying active components of herbal medicine. *Comput. Biol. Chem.* **30**, 148–154.

133. Wang, Y., Wang, X. & Cheng, Y. (2006) A computational approach to botanical drug design by modeling quantitative composition-activity relationship. *Chem. Biol. Drug Des.* **68**, 166–172.

134. Chau, F.-T., Chan, H.-Y., Cheung, C.-Y., Xu, C.-J., Liang, Y. & Kvalheim, O. M. (2009) Recipe for uncovering the bioactive components in herbal medicine. *Anal. Chem.* **81**, 7217–7225.

135. Wong, W. R., Oliver, A. G. & Linington, R. G. (2012) Antibiotic mode of action profiling (Biomap) as a platform for the discovery of novel natural product antibiotics. *Planta Med. Kongressbericht* **78** – CL72.

136. Wong, W. R., Oliver, A. G. & Linington, R. G. (2012) Development of antibiotic. Activity profile screening for the classification and discovery of natural product antibiotics. *Chem. Biol.* **19**, 1483–1495.

137. Fiehn, O., Kopka, J., Dörmann, P. Altmann, T., Trethewey, R. N., Willmitzer, L. (2000) Metabolite profiling for plant functional genomics. *Nat. Biotechnol.* **18**, 1157–1161.

138. Werner, E., Heilier, J.-F., Ducruix, C., Ezan, E., Junot, C. & Tabet, J.-C. (2008) Mass spectrometry for the identification of the discriminating signals from metabolomics: Current status and future trends. *J. Chromatogr. B* **871**, 143–163.

139. Joyce, A. R. & Palsson, B. Ø. (2006) The model organism as a system: integrating "omics" data sets. *Nat. Rev. Mol. Cell Bio.* **7**, 198–210.

140. Jarmusch, A. K. & Cooks, R. G. (2014) Emerging capabilities of mass spectrometry for natural products. *Nat. Prod. Rep.* **31**, 730-738.

141. Carter, G. T. (2014) NP/MS since 1970: from the basement to the bench top. *Nat. Prod. Rep.* **31**, 711-717.

142. Shulaev, V. (2006) Metabolomics technology and bioinformatics. *Brief. Bioinform.* **7**, 128-139.

143. Wold, S., Esbensen, K. & Geladi, P. (1987) Principal Component Analysis. *Chemom. Intell. Lab.* **2**, 37–52.

144. Jolliffe, I. T. (2002) Principal component analysis. *Encycl. Stat. Behav. Sci.*, Springer New York. IBSN: 978-0-387-95442-4.

145. Trygg, J. & Wold, S. (2002) Orthogonal projections to latent structures (O-PLS). *J. Chemom.* **16**, 119–128.

146. Simons, R., Vincken, J.-P., Bakx, E. J., Verbruggen, M. A. & Gruppen, H. (2009) A rapid screening method for prenylated flavonoids with ultra-high-performance liquid chromatography/electrospray ionisation mass spectrometry in licorice root extracts. *Rapid Commun. Mass Spectrom.* **23**, 3083–3093.

147. Ma, Y. L., Li, Q. M., Van den Heuvel, H. & Claeys, M. (1997) Characterization of flavone and flavonol aglycones by collision-induced dissociation tandem mass Spectrometry. *Rapid Commun. Mass Spectrom.* **11**, 1357–1364.

148. Kuhn, F., Oehme, M., Romero, F., Abou-Mansour, E. & Tabacchi, R. (2003) Differentiation of isomeric flavone/isoflavone aglycones by MS^2 ion trap mass spectrometry and a double neutral loss of CO. *Rapid Commun. Mass Spectrom.* **17**, 1941–1949.

149. Kang, J., Zhou, L., Sun, J., Han, J. & Guo, D.-A. (2008) Chromatographic fingerprint analysis and characterization of furocoumarins in the roots of *Angelica dahurica* by HPLC/DAD/ESI-MS^n technique. *J. Pharm. Biomed. Anal.* **47**, 778–785.

150. Concannon, S., Ramachandran, V. N. & Smyth, W. F. (2000) A study of the electrospray ionisation and ion trap fragmentation of hemiterpenoid and dimeric coumarin derivatives. *Rapid Commun. Mass Spectrom.* **14**, 2260–2270.

151. Games, D. E., Jackson, A. H., Millington, D. S. & Rossiter, M. (1974) The field ionization spectra of some natural coumarins. *Biomed. Mass Spectrom.* **1**, 5–9.

152. Kutney, J. P., Engendorf, G., Inaba, T. & Dreyer, D. L. (1971) Mass spectral fragmentation studies in monomeric and dimeric coumarins. *Org. Mass Spectrom.* **5**, 249–263.

153. Heinke, R. (2009) Phytochemische Untersuchungen von Furanocumarinen aus jemenitischen Dorstenia- Arten. Diploma thesis Martin-Luther University Halle-Wittenberg.

154. Fiehn, O. (2001) Combining genomics, metabolome analysis, and biochemical modelling to understand metabolic networks. *Comp. Funct. Genomics* **2,** 155–168.

155. Lokhov, P. G. & Archakov, A. I. (2009) Mass spectrometry methods in metabolomics. *Biochem. Suppl. Ser. B Biomed. Chem.* **3**, 1–9.

156. Fiehn, O. (2002) Metabolomics–the link between genotypes and phenotypes. *Plant Mol. Biol.* **48**, 155–171.

157. Hollywood, K., Brison, D. R. & Goodacre, R. (2006) Metabolomics: Current technologies and future trends. *Proteomics* **6**, 4716–4723.

158. Dunn, W. B. & Ellis, D. I. (2005) Metabolomics: Current analytical platforms and methodologies. *Trends Anal. Chem.* **24**, 285–294.

159. Villas-Bôas, S. G., Mas, S., Akesson, M., Smedsgaard, J. & Nielsen, J. (2005) Mass spectrometry in metabolome analysis. *Mass Spectrom. Rev.* **24**, 613–646.

160. Schwudke, D., Hannich, J. T., Surendranath, V., Grimard, V., Moehring, T., Burton, L., Kurzchalia, T. & Shevchenko, A. (2007) Top-down lipidomic screens by multivariate analysis of high-resolution survey mass spectra. *Anal. Chem.* **79**, 4083–4093.

161. Von Roepenack-Lahaye, E., Degenkolb, T., Zerjeski, M., Franz, M., Roth, U., Wessjohann, L., Schmidt, J., Scheel, D. & Clemens, S. (2004) Profiling of *Arabidopsis* secondary metabolites by capillary liquid chromatography coupled to electrospray ionization quadrupole time-of-flight mass spectrometry. *Plant Physiol.* **134**, 548–559.

162. Le Gall, G., Colquhoun, I. J., Davis, A. L., Collins, G. J. & Verhoeyen, M. E. (2003) Metabolite profiling of tomato (*Lycopersicon esculentum*) using ^{1}H NMR spectroscopy as a

tool to detect potential unintended effects following a genetic modification. *J. Agric. Food Chem.* **51**, 2447–2456.

163. Farag, M. A., Porzel, A., Schmidt, J. & Wessjohann, L. A. (2012) Metabolite profiling and fingerprinting of commercial cultivars of *Humulus lupulus* L. (hop): A comparison of MS and NMR methods in metabolomics. *Metabolomics* **8**, 492–507.

164. Smedsgaard, J. & Nielsen, J. (2005) Metabolite profiling of fungi and yeast: from phenotype to metabolome by MS and informatics. *J. Exp. Bot.* **56**, 273–286.

165. Larsen, T. O., Smedsgaard, J., Nielsen, K. F., Hansen, M. E. & Frisad, J. C. (2005) Phenotypic taxonomy and metabolite profiling in microbial drug discovery. *Nat. Prod. Rep.* **22**, 672–695.

166. Frisvad, J. C., Andersen, B. & Thrane, U. (2008) The use of secondary metabolite profiling in chemotaxonomy of filamentous fungi. *Mycol. Res.* **112**, 231–240.

167. Koulman, A., Tapper, B. A., Fraser, K., Cao, M., Lane, G., A. & Rasmussen, S. (2007) High-throughput direct-infusion ion trap mass spectrometry: a new method for metabolomics. *Rapid Commun. Mass Spectrom.* **21**, 421–428.

168. Koulman, A., Woffendin, G., Narayana, V. K., Welchman, H., Crone, C. & Volmer, D. A. (2009) High resolution extracted ion chromatography, a new tool for metabolomics and lipidomics using a second generation orbitrap mass spectrometer. *Rapid Commun. Mass Spectrom.* **23**, 1411–1418.

169. Ellis, D. I., Dunn, W. B., Griffin, J. L., Allwood, J. W. & Goodacre, R. (2007) Metabolic fingerprinting as a diagnostic tool. *Pharmacogenomics* **8**, 1243–1266.

170. Grata, E., Boccard, J., Glauser, G., Carrupt, P.-A., Farmer, E. E., Wolfender, J.-L. & Rudaz, S. (2007) Development of a two-step screening ESI-TOF-MS method for rapid determination of significant stress-induced metabolome modifications in plant leaf extracts: The wound response in *Arabidopsis thaliana* as a case study. *J. Sep. Sci.* **30**, 2268–78.

171. Zhen, Y., Krausz, K. W., Chen, C., Idle, J. R. & Gonzalez, F. J. (2007) Metabolomic and genetic analysis of biomarkers for peroxisome proliferator-activated receptor alpha expression and activation. *Mol. Endocrinol.* **21**, 2136–2151.

172. Choi, H.-K., Choi, Y. H., Verberne, M., Lefeber, A. W. M., Erkelens, C. & Verpoorte, R. (2004) Metabolic fingerprinting of wild type and transgenic tobacco plants by ^{1}H NMR and multivariate analysis technique. *Phytochemistry* **65**, 857–64.

173. Ma, C., Wang, H., Lu, X., Xu, G. & Liu, B. (2008) Metabolic fingerprinting investigation of Artemisia annua L. in different stages of development by gas chromatography and gas chromatography-mass spectrometry. *J. Chromatogr. A* **1186**, 412–419.

174. De Vos, R. C. H., Moco, S., Lommen, A., Keurentjes, J. J. B., Bino, R. J. & Hall, R. D. (2007) Untargeted large-scale plant metabolomics using liquid chromatography coupled to mass spectrometry. *Nat. Protoc.* **2**, 778–791.

175. Allwood, J. W. & Goodacre, R. (2010) An introduction to liquid chromatography-mass spectrometry instrumentation applied in plant metabolomic analyses. *Phytochem. Anal.* **21**, 33–47.

176. Han, J., Danell, R. M., Patel, J. R., Gumerov, D. R., Scarlett, C. O., Speir, J. P., Parker, C. E., Rusyn, I., Zeisel, S. & Borchers, C. H. (2008) Towards high-throughput metabolomics using ultrahigh-field Fourier transform ion cyclotron resonance mass spectrometry. *Metabolomics* **4**, 128–140.

177. Ohta, D., Shibata, D. & Kanaya, S. (2007) Metabolic profiling using Fourier-transform ion-cyclotron-resonance mass spectrometry. *Anal. Bioanal. Chem.* **389**, 1469–1475.

178. Aharoni, A., De Vos, R. C. H., Verhoeven, H. A., Maliepaard, C. A., Kruppa, G., Bino, R. & Goodenowe, D. B. (2002) Nontargeted metabolome analysis by use of Fourier Transform Ion Cyclotron Mass Spectrometry. *Omics* **6**, 217–234.

179. Krishnan, P., Kruger, N. J. & Ratcliffe, R. G. (2005) Metabolite fingerprinting and profiling in plants using NMR. *J. Exp. Bot.* **56**, 255–265.

180. Mehl, F., Marti, G., Boccard, J., Debrus, B., Merle, P., Delort, E., Baroux, L., Raymo, V., Velazco, M. I., Sommer, H., Wolfender, J.-L. & Rudaz, S. (2014) Differentiation of lemon essential oil based on volatile and non-volatile fractions with various analytical techniques: A metabolomic approach. *Food Chem.* **143**, 325–35.

181. Glauser, G., Veyrat, N., Rochat, B., Wolfender, J.-L. & Turlings, T. C. J. (2013) Ultra-high pressure liquid chromatography – mass spectrometry for plant metabolomics: A systematic comparison of high-resolution quadrupole-time-of-flight and single stage Orbitrap mass spectrometers. *J. Chromatogr. A* **1292**, 151–159.

182. Seger, C. & Sturm, S. (2007) Analytical aspects of plant metabolite profiling platforms: current standings and future aims. *J. Proteome Res.* **6**, 480–497.

183. Theodoridis, G., Gika, H. G. & Wilson, I. D. (2008) LC-MS-based methodology for global metabolite profiling in metabonomics/metabolomics. *Trends Anal. Chem.* **27**, 251–260.

184. Sawada, Y., Akiyama, K., Sakata, A., Kuwahara, A., Otsuki, H., Sakurai, T., Saito, K. & Hirai, M. Y. (2009) Widely targeted metabolomics based on large-scale MS/MS data for elucidating metabolite accumulation patterns in plants. *Plant Cell Physiol.* **50**, 37–47.

185. Nakamura, Y., Kimura, A., Saga, H., Oikawa, A., Shinbo, Y., Kai, K., Sakurai, N., Suzuki, H., Kitayama, M., Shibata, D., Kanaya, S. & Ohta, D. (2007) Differential metabolomics unraveling light/dark regulation of metabolic activities in *Arabidopsis* cell culture. *Planta* **227**, 57–66.

186. Aharoni, A., Giri, A. P., Deuerlein, S., Griepink, F., De Kogel, W.-J., Verstappen, F. W. A., Verhoeven, H. A., Jongsma, M. A., Schwab, W. & Bouwmeester, H J. (2003) Terpenoid metabolism in wild-type and transgenic *Arabidopsis* plants. *Plant Cell* **15**, 2866–2884.

187. Tolstikov, V. V. & Fiehn, O. (2002) Analysis of highly polar compounds of plant origin: Combination of hydrophilic interaction chromatography and electrospray ion trap mass spectrometry. *Anal. Biochem.* **301**, 298–307.

188. Lisec, J., Schauer, N., Kopka, J., Willmitzer, L. & Fernie, A. R. (2006) Gas chromatography mass spectrometry-based metabolite profiling in plants. *Nat. Protoc.* **1**, 387–396.

189. Hirai, M. Y., Yano, M., Goodenowe, D. B., Kanaya, S., Kimura, T., Awazuhara, M., Arita, M., Fujiwara, T. & Saito, K. (2004) Integration of transcriptomics and metabolomics for understanding of global responses to nutritional stresses in Arabidopsis thaliana. *Proc. Natl. Acad. Sci. USA* **101**, 10205–10210.

190. Yang, F. Q., Guan, J. & Li, S. P. (2007) Fast simultaneous determination of 14 nucleosides and nucleobases in cultured Cordyceps using ultra-performance liquid chromatography. *Talanta* **73**, 269–273.

191. Liu, M., Li, Y., Chou, G., Cheng, X., Zhang, M. & Wang, Z. (2007) Extraction and ultra-performance liquid chromatography of hydrophilic and lipophilic bioactive components in a Chinese herb radix *Salviae miltiorrhizae. J. Chromatogr. A* **1157**, 51–55.

192. Smith, C. A., Want, E. J., O'Maille, G., Abagyan, R. & Siuzdak, G. (2006) XCMS: Processing mass spectrometry data for metabolite profiling using nonlinear peak alignment, matching, and identification. *Anal. Chem.* **78**, 779–787.

193. Dettmer, K., Aronov, P. A. & Hammock, B. D. (2007) Mass spectrometry-based metabolomics. *Mass Spectrom. Rev.* **26**, 51–78.

194. Abdi, H. & Williams, L. (2010) J. Principal component analysis. *Comput. Stat.* **2**, 433–459.

195. Goodacre, R., Shann, B., Gilbert, R. J., Timmins, E. M., McGovern, A. C., Alsberg, B. K., Kell, D. B. & Logan, N. A. (2000) Detection of the dipicolinic acid biomarker in *Bacillus* spores using Curie-point pyrolysis mass spectrometry and Fourier transform infrared spectroscopy. *Anal. Chem.* **72**, 119–127.

196. Kvalheim, O. M. & Karstang, T. V. (1989) Interpretation of latent-variable regression models. *Chemom. Intell. Lab.* **7**, 39–51.

197. Bylesjö, M., Rantalainen, M., Cloarec, O., Nicholson, J. K., Holmes, E. & Trygg, J. (2006) OPLS discriminant analysis : Combining the strengths of PLS-DA and SIMCA classification. *J. Chemom.* **20**, 341–351.

198. Wiklund, S., Johansson, E., Sjöström, L., Mellerowicz, E. J., Edlund, U., Shockcor, J. P., Gottfries, J., Moritz, T. & Trygg, J. (2008) Visualization of GC/TOF-MS-based metabolomics data for identification of biochemically interesting compounds using OPLS class models. *Anal. Chem.* **80**, 115–122.

199. Michels, K. (2011) Entwicklung einer LC-MS basierten Methode zur Identifizierung von aktivitätsrelevanten Metaboliten in komplexen Mischungen. Dissertation, Martin-Luther University Halle-Wittenberg.

200. Degenhardt, A., Wittlake, R., Seilwind, S., Liebig, M., Runge, C., Hilmer, J.-M., Kramer, G., Gohr, A., Wessjohann, L. (2013) Quantification of important flavor compounds in beef stocks and correlation to sensory results by "reverse metabolomics". Ferreira, V., & Lopez, R. (eds.). *Flavour Science: Proceedings from XIII Weurman Flavour Research Symposium.* Page 16–19. Academic Press. ISBN: 978-0-12-398549-1.

2.   Analysis of furanocoumarins from Yemenite *Dorstenia* species by liquid chromatography/electrospray tandem mass spectrometry

Abstract

A series of prevailing prenylated furanocoumarins from leaves of *Dorstenia gigas* and *Dorstenia foetida* (Moraceae), were investigated by liquid chromatography/electrospray tandem mass spectrometry (LC-ESI-MS/MS). The mass spectral behavior of the furanocoumarins under positive ion electrospray conditions is discussed using both an ion trap and a triple quadrupole system. It is demonstrated, that both methods represent valuable tools not only for the rapid classification of this type of compounds, but also with respect to their substitution pattern.

Keywords

positive ion electrospray tandem mass spectrometry; ion trap; triple quadrupole; furanocoumarins; *Dorstenia* species; Moraceae

3. Negative ion electrospray tandem mass spectrometry of prenylated fungal metabolites and their derivatives

R. Heinke, N. Arnold, L. Wessjohann, J. Schmidt (2013).

Anal. Bioanal. Chem. **405**, 177-189.

Abstract

Liquid chromatography negative ion electrospray ionization tandem mass spectrometry has been used for characterization of naturally occurring prenylated fungal metabolites and synthetic derivatives. The fragmentation studies allow an elucidation of the decomposition pathways for these compounds. It could be shown, that the prenyl side chain is degraded by successive radical losses of C_5-units. Both the benzoquinones and the phenolic derivatives display significant key ions comprising the aromatic ring. In some cases the formation of significant oxygen-free key ions could be evidenced by high-resolution MS/MS measurements. Furthermore, the different types of basic skeletons, benzoquinones and phenol-type as well as cyclic prenylated compounds, can be differentiated by their MS/MS behavior.

Keyword

Meroterpenoids; prenylated fungel metabolites; boviquinones; fungi; Basidiomycetes; negative ion ESI-MS/MS

4. Metabolite profiling and fingerprinting of *Suillus* species (Basidiomycetes) by electrospray mass spectrometry

Abstract

The genus *Suillus* is known for the occurrence of a series of prenylated phenols and boviquinones. The extracts of four different *Suillus* species (*S. bovinus, S. granulatus, S. tridentinus* and *S. variegatus*) were investigated by using rapid ultra-performance liquid chromatography/electrospray ionization mass spectrometry (UPLC/ESI-MS) and direct infusion electrospray ionization Fourier transform ion cyclotron resonance mass spectrometry (ESI-FTICR-MS). While the direct infusion ESI-FTICR mass spectra give a fast overview concerning the elemental compositions of the compounds and therefore hints to the main metabolites, UPLC/electrospray tandem mass spectrometry is shown to be an useful tool for their identification. A principal component analysis (PCA) and hierarchical cluster analysis (HCA) based on the UPLC/ESI-MS showed clearly that the metabolite profiles can be used not only for the identification and classification of such fungi but also as a sophisticated and powerful tool for the chemotaxonomy of fungi. Furthermore, a clear discrimination of various types of biological samples (fruiting bodies *versus* mycelial cultures) is also possible. While, orthogonal partial least squares (OPLS) two class models of both UPLC/ESI-MS and ESI-FTICR-MS possess a clear differentiation of two compared *Suillus* species representing the between class variation and the within class variation. Based on generated S-plots and loading plots statistically significant metabolites could be identified as potential biomarker for one species.

Keywords

Electrospray mass spectrometry; UPLC/MS; FT-ICR; *Suillus*; Basidiomycetes; PCA; HCA; OPLS; visualization; classification

5. Reverse metabolomics – a correlation approach for the direct identification of active compounds in complex mixture

L. Wessjohann, K. Michels, A. Gohr, M. Haid, R. Heinke, N. Arnold, J. Schmidt,
Unpublished

Abstract

The identification of new bioactive compounds, especially of lead structures for drug development of new antibiotics, is a time-consuming and challenging process. A new technique termed 'reverse metabolomics' based on the correlation of bioactivities to mass spectral data combines modern metabolomics approaches (metabolite profiling) and traditional natural product research (screening methods) with the aid of mathematic informatics deconvolution. This approach enables the direct identification of known and unknown activity-relevant metabolite cluster in complex mixtures. The untargeted 'reverse metabolomics' using a deconvolution method named activity correlation analysis (AcorA) correlates chromatographic and spectroscopic properties, especially metabolite profiles, with bioactivity profiles of extracts. The AcorA results represent a hit list displaying a statistically significant correlation of the mass spectral signals (m/z values) with their biological activities. In a proof of concept study, inactive fungal extracts were spiked with three different antibiotics. After biological testing and liquid chromatography/electrospray ionization mass spectrometry (LC/ESI-MS) measurements, the raw data were analysed by using AcorA. 3% of the peaks correlated significantly with the antibacterial bioactivity at which 2/3 of the peaks can be assigned to the antibiotics. Comparable results received using direct infusion electrospray ionization Fourier transform ion cyclotron resonance mass spectrometry (ESI-FTICR-MS). Furthermore, the procedure was applied to crude fungal extracts of *Albatrellus* and *Hygrophorus* species (Basidiomycetes) and the obtained results demonstrate the ability of AcorA to identify the activity-relevant peaks prior to purification. The *ab initio* identification enables a directed isolation of active metabolites towards retention time and m/z values with minimization of replication.

Keywords

Reverse metabolomics – a correlation approach for the direct identification of active compounds in complex mixtures

Katharina Michels[1], Mark Haid[1,2], André Gohr[1,3], Ramona Heinke[1],
Jürgen Schmidt[1], Norbert Arnold[1], Ludger Wessjohann[1*]

[1]Leibniz Institute of Plant Biochemistry, Department of Bioorganic Chemistry, Weinberg 3, 06120 Halle/Saale, Germany, Tel: +49 (0) 345-55821301, Fax: +49 (0) 345-55821309

[2]Helmholtz Zentrum Munich, Institute of Experimental Genetics, Ingolstädter Landstraße 1, 85764 Neuherberg, Germany

[3]Institute of Computer Science, Martin-Luther University Halle-Wittenberg, 06099 Halle/Saale, Germany

*corresponding author: wessjohann@ipb-halle.de

unpublished

ABSTRACT

The identification of new bioactive compounds, especially of lead structures for drug development of new antibiotics, is a time-consuming and challenging process. A new technique termed 'reverse metabolomics' based on the correlation of bioactivities to mass spectral data combines modern metabolomics approaches (metabolite profiling) and traditional natural product research (screening methods) with the aid of mathematical informatics deconvolution. This approach allows for the direct identification of known and unknown activity-relevant peak clusters in complex mixtures. The untargeted 'reverse metabolomics' using a deconvolution method named activity correlation analysis (AcorA) correlates chromatographic and spectroscopic properties, especially metabolite profiles, and bioactivity profiles of crude extracts. AcorA results in hit lists of chromatographic and spectroscopic signals which significantly correlate with the biological activities of the crude extracts. In a proof of concept study, inactive fungal extracts were spiked with three different antibiotics. After biological testing and liquid chromatography/electrospray ionization mass spectrometry (LC/ESI-MS) measurements, the raw data were analyzed with AcorA. AcorA hit lists comprise 3 % of all m/z-signals and 2/3 of them are caused by the antibiotics. Similar results were received using direct infusion electrospray ionization Fourier transform ion cyclotron resonance mass spectrometry (ESI-FTICR-MS). Furthermore, the procedure was applied to crude fungal extracts of *Albatrellus* and *Hygrophorus* species (Basidiomycetes) and the results demonstrate the ability of AcorA to identify the activity-relevant peaks prior to purification. The *ab initio* identification allows a directed isolation of active metabolites towards retention time and m/z signals with minimization of replication.

KEYWORDS

Metabolomics, activity correlation analysis (AcorA), natural product research, mass spectrometry, antibacterial activity, Basidiomycetes

INTRODUCTION

Nature provides a huge number of several hundred thousands of low molecular weight compounds in different organisms (mushrooms, plants and microorganisms). This large number of secondary metabolites is synthesized as a consequence of the complex interactions between the organism and its environment that lead to a vast structural variety of bioactive compounds.[1] Nowadays, natural products play a very important role in drug discovery for the treatment of human diseases.[2] Natural products might have diverse

activities because of their high chemical diversity and biochemical specificity. Thus, the finding of potential lead compounds from natural products for the development of new drugs is a challenge both for the pharmaceutical industry and the synthetic organic chemistry.[1,3] More than two-third of clinically used antibiotics are based on natural products isolated from microorganisms, especially from actinomycetes and fungi, or are semisynthetic derivatives of natural products.[2,4,5] Regarding the constant appearance of the rising problem of drug-resistant pathogenic bacteria and the deficit of novel antibiotics, there are no doubts that sustained research efforts in new antibiotics are necessary.[5–8]

The traditional process of drug discovery is time-consuming and tedious because crude extracts of biological materials represent complex mixtures of hundreds or thousands of compounds with different chemical properties. As a result, the identification of the relevant active compounds remains a laborious screening process, regardless whether using high-throughput screening (HTS) or classical bioactivity-guided fractionation. Some sophisticated approaches like on-line liquid-chromatography-biochemical detection (LC-BCD),[9–11] and frontal affinity chromatography mass spectrometry (FAC-MS) are based on direct identification of active compounds.[12,13] However, these approaches are incapable of identifying additive or synergistic effects. Therefore, they can be used only in case of known specific targets.

In recent years, the alternative route of computational approaches for analyzing the chemical composition and predicting the activity of complex mixtures has been started to be increasingly used for the identification of active compounds. Specifically, multivariate analysis methods such as principal component analysis (PCA), principal component regression (PCR), and partial least square (PLS) analysis for identification of active compounds of complex mixtures are of increasing importance.[14–16] Those methods were used for the prediction of the antioxidant capacity of green tea from chromatographic fingerprints.[14] However, is has been shown that techniques like PCA and PCR are relatively inappropriate for the identification of active compounds.[16] These multivariate methods aim at transforming the original variables into a set of uncorrelated variables called 'principal components' (PC) where the first PC has the largest variance and all successive PCs exhibit an decreasing degree of variance but the size of the variance is often not properly related to the activity of the analyzed samples.

More suitable results could be obtained by partial least square (PLS) and in particular orthogonal PLS (OPLS).[14,17] Both algorithms maximize the principal components not only with respect to the variance, but also with regard to the covariance between the spectral data and the target variable (in that case the activity). Similar to the OPLS is the 'target projection' (TP) approach developed by Kvalheim *et al.* (1989; 1990).[18,19] However, both methods offer similar problems as in some cases a substance with a high concentration but a low correlation to the biological activity is preferred over a substance with a low concentration and a high correlation value. To avoid this problem, the so called 'selectivity ratio plot' (SR-plot) was established yielding a dimension of significance for the obtained correlation.[20,21] The combination of the TP and SR-plot for the identification of active compounds was introduced under the term 'quantitative pattern activity relationship' (QPAR) which was successfully applied to the prediction of antioxidant compounds from a mixture of herbal medicine radix *Puerariae lobatae*.[22] All these methods require that the users have the necessary skills and sufficient knowledge in the field of multivariate statistics to process the data and to implement these computational techniques.

The present paper deals with the development of an un-targeted technique termed 'reverse metabolomics' for the identification of new bioactive natural products. This approach combines metabolome analyses using mass spectrometry (MS), liquid chromatography (LC), LC-MS or nuclear magnetic resonance (NMR) spectroscopy and LC-NMR with high-throughput screening to determine the activities of the complex mixtures. In contrast to classical metabolomics studies involving the analysis of the complete set of metabolites (metabolome) of biological objects,[23,24] 'reverse metabolomics' represents an approach leading to the direct identification of bioactive compounds or compound clusters in complex mixtures. In contrast to classical or bioassay-guided isolation of bioactive natural products the analysis of the relevant metabolites is carried out at the beginning of the process. Furthermore, the determination of the bioactivity is necessary only once and allows a HTS of the samples in various assays. These new 'reverse metabolomics' approach takes advantage of the native biodiversity of organisms which has an influence on the activity and metabolite profiles.

2

For the application of activity correlation analysis (AcorA) variances in the data sets resulting in different metabolite profiles and activity values are mandatory. Next to the natural biodiversity also artificial modification of the samples can be used in that approach. The AcorA method ascertains the correlation between metabolite and activity profiles of mixtures resulting in a hit list with potential metabolite clusters which could be responsible for the bioactivity. Thereby, the multivariate data sets have been analyzed that especially those signals were determined which correspond to the activity relevant compounds.

Here, we apply 'reverse metabolomics' and AcorA to correlate the metabolite profiles obtained by liquid chromatography/electrospray ionization mass spectrometry (LC/ESI-MS) and direct infusion electrospray ionization Fourier transform ion cyclotron resonance mass spectrometry (ESI-FTICR-MS) with antibacterial activity data. The *ab initio* identification allows a directed determination of active metabolites with respect to their retention times (RT) and *m/z* values accompanied by a minimization of replication. The AcorA method was not only investigated with inactive extracts spiked with known antibiotics, but the functionality was also shown with fungal extracts from different species belonging to the genera *Albatrellus* and *Hygrophorus* (Basidiomycetes) of hitherto unknown activity. Therefore, both natural and artificial biodiversity of the fungal extracts were used. Furthermore, the AcorA approach is compared with two other methods, using complex metabolomics approaches as PCA (principal component analysis)[25,26] and QPAR (quantitative pattern activity relationship)[22] to find bioactive natural products.

THEORY

Basic principle. The activity correlation analysis (AcorA) aims at analyzing high-throughput metabolomics measurements of active crude natural extracts in combination with measured activity profiles of the investigated extracts with the goal to predict signals which are potentially caused by the active compounds of the extracts. AcorA is applicable to a variety of types of high-throughput metabolomics data (e.g., HPLC, MS, LC-MS, NMR, LC-NMR) and to different kinds of activity (e.g., antibacterial, antifungal, growth inhibition).Knowing the predicted signals allows the identification of the active compounds prior to isolation in order to prevent replication, i.e., the isolation of already known compounds, and the signal-guided isolation of the active compounds only. To this end, AcorA exploits the following fundamental relationship: the intensity of a peak caused by an active compound across the high-throughput measurements of the investigated extracts (samples) is directly proportional to the activity of these samples. This relationship results from the two assumptions: i) the activity of an active compound is directly proportional to its concentration, and ii) its concentration is directly proportional to the intensity of peaks caused by this active compound (see Figure 1). To predict signals which are caused by the active compounds, AcorA measures how well their intensities across the samples are directly proportional to the activities of the samples. To this end, AcorA determines the Spearman rank correlation coefficient between signal intensities and the activities. Peaks whose intensities indeed are direct proportional to the activity are returned as potential candidate peaks which potentially might be caused by the active compounds.
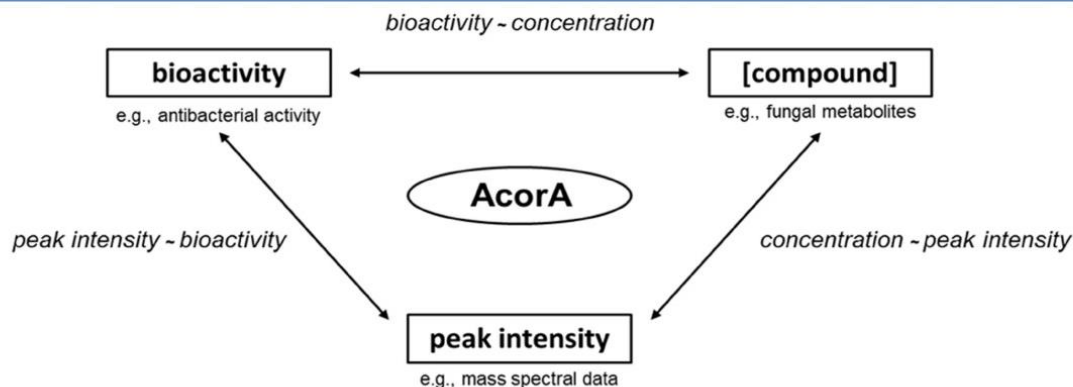
Figure 1. AcorA exploits the direct relationship between peak intensities and activities.

Activity correlation analysis (AcorA). AcorA is described for N samples which have been analyzed by any chosen metabolomics high-throughput technique. After peak-picking and peak-alignment where M peaks have been found and aligned across all N samples, these data are represented by the following M x N matrix

$$x = \left(x_{ij}\right)_{1 \leq i \leq M, 1 \leq j \leq N}$$

whose rows and columns correspond to the M aligned peaks and N samples, respectively. The m-th row contains the measured intensities of the m-th aligned peak across all N samples. The following vector contains the determined activities for each of the N samples

$$\vec{b} = (b_{1 \leq n \leq N}).$$

In order to identify peaks which are potentially caused by some active compound in the samples, AcorA exploits the assumption that the intensity of such signals is directly proportional to the activity across the N samples. This assumption allows for a straight-forward approach for predicting peaks which are potentially caused by active compounds, i.e., identifying those peaks whose intensity across the N samples well agrees with this assumption. AcorA measures this agreement by the coefficient for the Spearman rank correlation between each of the M columns (peaks) of the data matrix x and the activity vector $\vec{b}$, i.e., for $1 \leq m \leq M$

$$\rho_{m=} \frac{6 \sum (d_{mn})^2}{m \cdot (m^2 - 1)}$$

with

$$d_{mn} = \text{rank}(x_{mn}) - \text{rank}(b_n)$$

where the function rank() returns the rank of its argument with respect to the increasing ordering of the values of the entire row of the matrix x or the activity vector $\vec{b}$. Sorting the M peaks according to decreasing Spearman rank correlation coefficients gives a ranking of all peaks according to the degree to which their intensities are directly proportional to the activity across the N samples.

In comparison to the Pearson correlation coefficient the Spearman rank correlation coefficient has three advantages: i) the relation between the peak intensity and the activity could be of any direct proportional type whereas the Pearson correlation assumes a linear relationship, ii) through the representation of the data points by their ranks, the Spearman rank correlation is robust and insensible with respect to outliers, and iii) the distribution of the data might be of any (even unknown) kind whereas

the Pearson correlation coefficient assumes the data to be Normal distributed.

Significance test. In order to identify those top-ranked peaks whose intensity significantly correlates with the activity, AcorA uses a permutation strategy for approximating the cumulative distribution function $F(y)$ of Spearman rank correlation coefficients under the null hypothesis of absent correlations between peak intensities and the activity. Knowing $F(y)$ allows to determine an upper significance threshold for the Spearman rank correlation coefficient according to an error probability of $\alpha = 5\,\%$, i.e., t_u with $F(t_u) = 0.975$. All peaks with a Spearman rank correlation coefficient higher than this upper threshold are assumed to significantly correlate to the activity and so are returned.

As a two-sided significance test is applied, which considers significant positively and negatively correlating peaks, the error probability splits up to equal parts for the upper and lower significance threshold. The lower significance threshold might be applied in order to determine significant anti-correlations between the peak intensity and the measured activity allowing for the determination of active compounds with negative (inversely correlated) effect on the activity. Since our focus lay on active compounds which affect the activity in a positive way, the lower significance threshold is neglected in the rest of this manuscript. After determining the upper significance threshold t_u, AcorA returns the top-ranked L peaks (identified by their indices m) whose peak intensity across all N samples show a Spearman rank correlation higher than t_u, i.e.,

$$m_1, \dots, m_L \quad \text{with} \quad \forall\, 1 \leq i, j \leq L, i \leq j\, :\, \rho_{m_i} \geq t_u,$$
$$\rho_{m_j} \geq t_u, \quad \rho_{m_i} \geq \rho_{m_j}.$$

Permutation strategy for the determination of significant correlations. The permutation strategy is implemented as follows. In order to fulfill the constraint of absent correlations (null hypothesis) all entries along each row of the matrix x are permuted resulting in the destruction of all existing correlations between rows of the data matrix and the activity vector. This permutation is repeated J times, each time resulting in a permuted matrix $\hat{x}$ for which the Spearman correlation coefficients between its rows and the activity vector $\vec{b}$ are computed. These correlation coefficients obtained under the null hypothesis are stored and, afterward, used to calculate the upper significance threshold t_u as summarized by Algorithm 1.

4

```
r⃗ := empty vector
for all j in 1 … J do
    x̂ := permute entries in each column of matrix x
    for all m in 1 … M do
        p̂ := Spearman rank correlation coefficient between x̂_m and b⃗
        append (r⃗, p̂)
    end for
end for
s⃗ := sort (r⃗)
t_u := s⃗ [⌊N · J · 0.975⌋]
```

Algorithm 1. Permutation approach for determining significance thresholds.

Modifications of the samples increase necessary variation in the data. For a successful application in reverse metabolomics, AcorA relies on a sufficient variation in the activities of the samples and the intensities of the peaks. A sufficient variation might be naturally present, e.g., due to different sources (different species, organs or parts of an investigated organism) of the samples. If only one sample is available or if the variation is insufficient, the variation in the activities and in the peak intensities might be enhanced by splitting the samples into several sub-samples each of which might be modified chemically (e.g., by treatment with acids, bases or other reactive chemicals) or physically (e.g., by heating at different temperatures or by separation with diverse chromatographic column materials). Such treatments might increase the variation of the activity across the samples and might alter the signal intensities in each sample. By increasing these variations, these treatments support the analysis with AcorA.

EXPERIMENTAL

Fungal material. An overview of specimens used in the different studies is given in the supporting information in Tables S-1 and S-2. Fresh fruiting bodies of different *Albatrellus* and *Hygrophorus* species were collected and directly extracted or after collection stored at -20°C, freeze-dried, or air dried. Voucher specimens are deposited at the Leibniz Institute of Plant Biochemistry Halle, Germany (IPB).

Chemicals and reagents. The antibiotics erythromycin, rifampicin and amoxicillin were provided by Fluka Analytical. Acetonitrile (ultra gradient HPLC grade), formic acid and acetic acid (LCMS/HPLC grade) were from J.T. Baker (Netherlands), milliQ water was used for the HPLC and UPLC analysis. Authentic compound **1** was kindly provided by Prof. Dr. Dr. h.c. Wolfgang Steglich (Ludwig-Maximilians-University, Munich).

Stock solutions were prepared in methanol (1 mg/ml).

Extraction procedure and sample preparation. Frozen and freeze-dried fruiting bodies of *Hygrophorus* spp. were extracted with different extraction solvents (Table S-1). Fresh fruiting bodies of *Albatrellus* ssp. were extracted three times under ultrasonication with methanol; ethyl acetate or hydrochloric acetone. After evaporation to dryness *in vacuo* the extracts were dissolved in methanol and processed with Chromabond® C18 cartridge (Macherey-Nagel) using methanol as eluent for the antibacterial testing and MS measurements.

Sample preparation for the proof of concept experiments. *Experiment 1.* After the extract preparation with Chromabond® C18 cartridge (Macherey-Nagel) the resulting methanolic extracts of the five different *Hygrophorus* ssp. were spiked partially with antibiotics. Therefore, 16 different compositions of three antibiotics (erythromycin, rifampicin and amoxicillin) in four different concentrations were mixed with an extract aliquot, randomly chosen from the *Hygrophorus* extracts one to five (Table S-3).

Experiment 2. Extract No. 2 of *H. chrysodon* (Batsch.: Fr.) Fr. containing erythromycin and rifampicin (each in a concentration of 10 µM) was modified with different methods (Table S-4).

Antibacterial bioassay. The antibacterial activity against *Bacillus subtilis* was determined with a quantitative fluorescence-based antibacterial growth inhibition assay.[27] The fluorescence was measured on a microtiter plate reader GENios Pro (Fa. Tecan, excitation, 510 nm; emission, 535 nm). The *B. subtilis* strain 168 (PAbrB-IYFP) was maintained on TY (tryptone-yeast extract) medium supplemented with 1 % Bacto-tryptone, 0.5 % Bactoyeast extract, 1 % NaCl and chloramphenicol (5 µg/ml).[28]

LC/ESI-IT-MS. The ESI ion trap (IT) mass spectra were recorded on a LCQ Deca XP MAX (Thermo Scientific) spray voltage 4.0 kV; sheath gas: nitrogen; capillary temperature: 275°C, capillary voltage: 30 V, coupled with system 1 (*Hygrophorus* ssp.): Surveyor micro-HPLC system (RP18-column 5 µm, 1.0 x 150 mm, Hypersil GOLD, Thermo Scientific) and a photodiode array detector (λ = 200 – 800 nm) or system 2 (*Albatrellus* ssp.): Waters ACQUITY UPLC system (BEH C8 1.7 µm, 1.0 x 100 mm) and equipped with a photodiode array detector (Waters). For HPLC (system 1) a gradient system was used starting from

water/acetonitrile (each containing 0.2 % acetic acid) 80:20 to 0:100 within 30/40 min followed by a 10/15 min isocratic period; flow rate 70 µl/min. On the ACQUITY UPLC (system 2) the chromatographic separation was performed by gradient elution using water/acetonitrile (each containing 0.2 % acetic acid) 90:10 for 0.2 min to 0:100 within 16.3 min followed by a 2.5 min isocratic period; flow rate 150 µl/min. The column was maintained at 40°C.

ESI-IT-MS spectra were acquired in negative and positive ion electrospray ionization mode by scanning over the *m/z* range 100-1000. Data dependent MS[2] and MS[3] experiments were performed by selection of the ions of the highest intensity, whereas the intensity had to be larger than 10^5 a.i., and using a normalized collision energy of 35 % or 45 % in negative ion mode and 35 % in the positive ion mode (activation Q: 0.250; activation time: 30.0 msec). Isolation width was set to +/- 2 Da. The mass spectra were evaluated using the software Xcalibur 2.0 and 2.0.7 (Thermo Scientific).

ESI-FTICR-MS. The high-resolution ESI mass spectra were obtained from a Bruker Apex III FTICR mass spectrometer (Bruker Daltonics, Billerica, USA) equipped with an Infinity™ cell, a 7.0-T superconducting magnet (Bruker, Karlsruhe, Germany), a radio frequency-only hexapole ion guide and an external APOLLO electrospray ion source (Agilent, off axis spray, negative ion mode: voltages: endplate, 3700 V; capillary, 4200 V; capillary exit, -100 V; skimmer 1, -15.0 V; skimmer 2, -10.0 V or -12.0 V; positive ion mode - 3700 V; capillary, -4.200 V; capillary exit, 100 V; skimmer 1, 15.0 V; skimmer 2, 10.0 V or 12.0 V). Nitrogen was used as drying gas at 150°C. The sample solutions were introduced continuously via a syringe pump with a flow rate of 120 µl/h. The mass spectra were evaluated using the Bruker software XMASS 7.0.8.

LC/ESI-QTOF-MS. The high-resolution ESI MS[2] spectra were recorded on a microTOF-Q II (Bruker Daltonics) spray voltage 4.0 kV; sheath gas: nitrogen; capillary temperature: 190°C, coupled with Waters ACQUITY UPLC system (HSS T3 1.8 µm, 1.0 x 100 mm, Waters). The chromatographic separation was performed by gradient elution using water/acetonitrile (each containing 0.1 % formic acid) 95:5 for 1 min to 5:95 within 16 min followed by a 2 min isocratic period; flow rate 150 µl/min. The collision-induced dissociation (CID) mass spectra were acquired in negative ion electrospray ionization mode using collision energies of 10 to 30 eV

(collision gas: nitrogen). The mass spectra were evaluated using the Bruker software Data Analysis 4.0.

MS data pre-processing. Using ProteoWizard the LC/ESI-IT-MS data of *Albatrellus* and *Hygrophorus* extracts were converted to mzXML file format whereas the ESI-FTICR-MS files were converted to mzdata file format. Peak-picking and peak-alignment were done with the R package XCMS and the following parameter settings for 1.) UPLC/ESI-IT-MS:
method='centWave', mzdiff=0.3, peakwidth=c(5,12), snthr=5, verbose.columns=F, prefilter=c(2,500), minsamp=2, bw=7, mzwid=1; and for
2.) ESI-FTICR-MS:
method='MSV', SNR.method='data.mean', winSize.noise=500, peakThr=80000, snthresh=3, amp.Th=0.005, scales=c(1,seq(7,9,3)); minsamp=2, mzppm=7. The output is a data matrix with peak intensities whose rows / columns correspond to the MS signals which have been aligned across all samples / the samples, respectively.

RESULTS AND DISCUSSION

Proof of concept. With help of this proof of concept study we investigated how well the activity correlation analysis (AcorA), which is described in detail in the theory section, is suited for predicting those peaks of spectroscopic or chromatographic measurements of complex crude natural extracts that are caused by active compounds. For the generation of the metabolite profiles data dependent liquid chromatography/electrospray ionization ion trap tandem mass spectrometry (LC/ESI-IT-MS[3]) and direct infusion electrospray ionization Fourier transform ion cyclotron resonance mass spectrometry (ESI-FTICR-MS) were applied as analytical tools. A quantitative antibacterial growth inhibition assay (*Bacillus subtilis*) was used for the determination of the bioactivities of the fungal extracts. Methanolic extracts of five different *Hygrophorus* ssp. without or with only a slight antibacterial activity were partially spiked with various compositions of three antibiotics (erythromycin, rifampicin and amoxicillin) in four different concentrations (Table S-3). After biological testing and mass spectral measurements in triplicates of all samples, the raw data were converted and pre-processed (peak-picking and alignment) using the R package XCMS.[29]

The given set of aligned peaks could be used to identify the elemental composition based on ESI-FTICR-MS measurements or in case of LC/ESI-IT-

MS the nominal mass-to-charge ratio (m/z) and retention time (RT). The Spearman rank correlation coefficient was calculated for the determination of the relation between the bioactivities and the intensities of each mass signal in all samples. A peak list was obtained containing those peaks that possess a positive correlation coefficient exceeding a given significance threshold. The significance threshold was determined by a statistical permutation test for each data set. The result of the complete analysis is a hit list of significant positively correlating peaks described by their m/z value, signal intensity and retention time (RT). As a result of the 'reverse metabolomics' approach the activity correlation analysis (AcorA) allows an m/z-guided fractionation instead of a laborious bioactivity-guided fractionation, or classical total separation with testing of individual compounds.

As a result of the first proof of concept study, two of the bioactivity-relevant antibiotics dominated the hit list regardless whether LC/ESI-IT-MS or ESI-FTICR-MS was used. Moreover, a few specific retention times and clusters of m/z values were repeated several times within these hit lists caused by the fact that the antibiotics are represented by both the [M+H]$^+$ signals as well as their isotopic peaks, fragments and/or adduct ions. Furthermore, we detected correlations to some derivatives and impurities of the antibiotics, e.g., rifampicin and its dehydrated derivative or erythromycin after a loss of a sugar moiety and so on.[30,31] Amoxicillin did not appear in the hit list due to lack of inhibitory effect on bacterial growth at the applied concentration.

In case of the positive ion ESI-FTICR-MS correlation analysis, 50 peaks out of 1666 aligned peaks (in 21 x 3 samples) correlated significantly to the bioactivity (Figure 2a). Around two-thirds of the correlating peaks correspond to antibiotic substances active in the assay and could be assigned to rifampicin and erythromycin. Moreover, we detected correlations to some impurities of the antibiotic mixtures (~20 %). The remaining peaks could not be annotated and were probably due to random correlations, because these peaks did appear as single peaks instead of clusters. Thus, we propose that peak clusters and retention time repetitions can improve the identification of a true correlation.

After pre-processing and activity correlation analysis of the LC/ESI-IT-MS data, 182 peaks out of 5890 aligned peaks revealed a significant correlation to the activity (Figure 2a). 40 % of the positively

correlating peaks corresponded to the antibiotics. Most of the remaining peaks eluted in the first two minutes are ranked at the end of the hit list and interfered with the injection peak. Furthermore, using LC/ESI-IT-MS data, altogether 82 peaks of the antibiotics erythromycin and rifampicin are contained in the aligned peak matrix. It was possible to identify around 80 % (68/82) of the calculated peaks using the AcorA procedure. Only 14 of the 82 signals could not be determined as significantly correlating peaks. In most cases, these peaks were isotopic signals of low abundance. Using the ESI-FTICR-MS analysis, it was even possible to identify around 95 % of the aligned antibiotics peaks (34/36).

In the second basic experiment, some variations are generated using different modification methods (Table S-4). For this case study, a only slightly biologically active methanolic extract of *Hygrophorus chrysodon* (Batsch.: Fr.) Fr. (1838) spiked with erythromycin and rifampicin (c = 10 µM) was selected for the experiment to simulate a strong native bioactivity. The required variation of bioactivity and metabolite profiles was realized by applying different modifications to aliquots of this extract (Table S-4). Thereby the concentration of each contained compound is relatively enhanced or reduced in comparison to other compounds resulting in an altered bioactivity.

In order to modify aliquots, the following modification methods were applied: autoclaving, heating, boiling in methanol, treatment with different amounts of charcoal, ion exchanger (anion and cation, respectively) and different polymeric resins. In summary, we obtained 18 modified extract aliquots. MS measurements, the bioassay and the resulting AcorA procedure were carried out in the same way as described above. In this way, it was possible to identify the activity-relevant peaks by using both analytical tools. The positive correlating antibiotic peaks are ranked at the beginning of the hit list but they did not dominate the hit list. The reason for this phenomenon is probably, that other biologically active compounds present in the extracts also exhibit a significant positive correlation. It is already known from *Hygrophorus* species that fungi of this genus contain cyclopentenone derivatives (hygrophorones) possessing a strong antibacterial activity.[32] At the time of study, it was not known, if *H. chrysodon* contains hygrophorones, but two antifungal acylcyclopentenediones are known.[33]

7
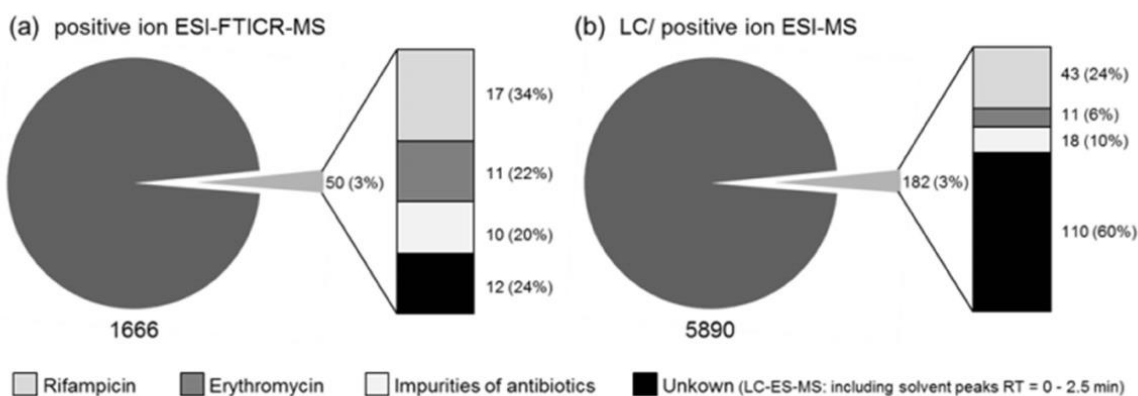
Figure 2. Summary of the results of (a) ESI-FTICR-MS (the 50 top-ranked peaks are significant, 1666 peaks in total) and (b) of LC/ESI-IT-MS (the 182 top-ranked peaks are significant, 5890 peaks in total) of the first proof of concept experiment (positive electrospray ionization mode).

These findings demonstrate the capability of AcorA to identify the activity-relevant peaks prior to purification. Furthermore, it was possible to demonstrate that the application of different modification procedures also reflects the relation of the required variation between metabolite profile and bioactivity.

Comparison of AcorA with PCA and QPAR. The principle component analysis (PCA) is often used to analyze metabolomics data,[25] e.g., as obtained from MS or NMR measurements. The obtained data of diverse mass spectrometers or NMRs result in different PCA score plots.[34,35] Whereas comparable techniques, e.g., high resolution MS gave similar patterns along the first PC of control and wounded sample.[36] Each measurement of a sample is represented by a high-dimensional data point (M-dimensional vector) whose components correspond to M signals like m/z bins or peaks while their entries of which represent the intensities of these signals in the measurements. Primarily, PCA provides an overview of such high-dimensional data points by projecting them onto a low dimensional sub-space. This procedure allows, for instance, the identification of outliers (data points being relatively far away from almost all other data points). In contrast, the aim of AcorA is the identification of signals whose intensities across all samples correlate well with the biological activity of the samples. Although PCA is not directly capable to determine signals well correlating with the activity, the following heuristic based in PCA can be used for ranking signals according to their correlation with the activity. We applied PCA to the N aligned and pre-processed ESI-FTICR-MS and LC/ESI-IT-MS

measurements. N principle components (PC) (as $N \ll M$) were obtained, each of which captures a certain fraction of the variation of the high-dimensional data. All N high-dimensional data points were projected onto each of the PCs resulting in N scalar values (scores) for each of the N measurements for each projection. Next, we selected that PC for which these scores show the highest Spearman rank correlation to the measured activity of the N measurements. Last, all peaks were ranked by their decreasing loadings according to the selected principle component. The rationale of this ranking is that the larger the loading of a signal for a given PC is the more this signal contributes to the variation captured by the PC and this variation may correlate well to the measured activity. Besides PCA, quantitative pattern activity relationship (QPAR) was applied to our data for this comparison. In contrast to PCA, QPAR is able to identify signals directly from metabolomics data corresponding to bioactive compounds of the analyzed metabolomics samples.[22]

We applied all three methods, AcorA, PCA and QPAR, to our proof of concept data (ESI-FTICR-MS and LC/ESI-IT-MS, both in positive ion mode, $N = 21$, $M = 1666/5890$). For AcorA, a significance threshold of $\alpha = 5\%$ was used for determining a threshold on the Spearman correlation coefficient by a permutation test with 500 repeats. All peaks whose Spearman correlation coefficient was greater than this threshold were predicted as peaks whose intensity positively correlates to the activity. For the QPAR analysis the data has been centralized (mean equal to zero) firstly. Within QPAR, data vectors were target projected onto the first six partial least square (PLS) components. The selection of the PLS

components was done following the example described by Chau *et al.*[22] Again, a permutation test was used for determining the cut off threshold ($\alpha = 5\,\%$) to predict peaks whose intensity correlates well to the bioactivity. For PCA, the data were centralized and scaled (mean equal to zero, variance equal to one). As described, one PC was selected and all peaks were ranked according to their loadings corresponding to the chosen PC. The suggested heuristic PCA-approach does not allow any permutation test. In case of the ESI-FTICR-MS data, AcorA predicted 53 positively correlating peaks, while QPAR predicted 25. For the sake of comparison, the QPAR ranking was extended to the top 53 peaks and we took the 53 top-PCA-ranked peaks. For the LC/ESI-IT-MS data, AcorA identified 182 peaks (QPAR: 79). Again, the QPAR and PCA rankings were extended to the top 182 peaks for this comparison.

When inspecting the Venn-diagram of the results obtained from the ESI-FTICR-MS data (Figure 3a), it is obvious that AcorA and QPAR prognosticate almost the same peaks. In detail, they share 46 peaks (86 %) and differ only by 8 peaks (14 %). PCA predicted many peaks which have not been predicted neither by AcorA nor by QPAR. Only 6 peaks predicted by PCA were also found by AcorA or QPAR. These rankings were compared in more detail by depicting the number of true positive peaks among the L top-ranked peaks with L ranging from 1 to 53 (Figure 3b). The rankings obtained by AcorA and QPAR yield comparable results, the solid and dashed lines are mostly on top of each other. For L between 20 and 30, the solid line is above the dashed line indicating that among the 20 up to 30 top-ranked peaks, AcorA predicted slightly more true positives. For $L > 46$, the dashed line is above the solid line indicating that among the top-53 ranked peaks QPAR found two true positives more than AcorA. In comparison, the dotted line is clearly below the both other ones indicating that PCA yields a considerably worse prediction than AcorA and QPAR. These findings suggest that the top-53 peaks as predicted by AcorA and QPAR contain a high fraction of almost similar true positives, i.e., peaks which indeed belong to the added active antibiotics.

A reason for the worse prediction of PCA might be that PCA aims not directly at ranking peaks according to their correlation of their intensities to the activity across the analyzed samples. Inspecting the Venn-diagram (Figure 4a) for the LC/ESI-IT-MS data, it becomes evident that the predictions of AcorA and QPAR have 39 peaks in common (about

64 %) and that the top-50 peaks predicted by PCA do not overlap at all with those obtained by AcorA and QPAR. A detailed comparison of the three rankings shows that the fraction of true positives among the top-ranked ten peaks is similar good for AcorA and QPAR, while it is clearly worse for PCA (Figure 4b). Considering the 20 to 150 top-ranked peaks, the dashed line is above the solid line indicating that QPAR accumulates slightly more true positives. For instance, among the top-36 peaks, QPAR identifies 36 true positives, whereas AcorA finds 29. Contrary to this, the fraction of true positives becomes equal again if the approx. 160 top-ranked peaks are considered. Considering even more top-ranked peaks, AcorA predicts slightly more true positives compared to QPAR as indicated by the fact that the solid line is above the dashed line. These findings indicate that AcorA and QPAR are equally well suited for the prediction of peaks of active compounds with respect to the fraction of true positives.
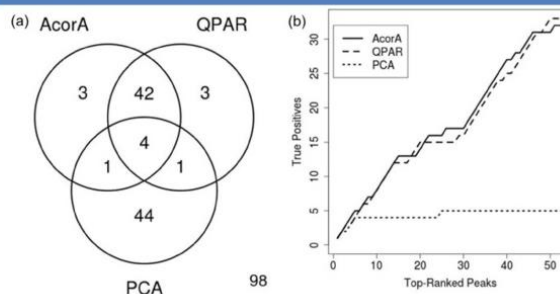
Figure 3. (a) Venn-diagram of 50 top-ranked peaks (ESI-FTICR-MS) and (b) number of true positives among the top-ranked peaks (ESI-FTICR-MS data). X-axis: the number of the considered top-ranked peaks is varied from 1 to 53.
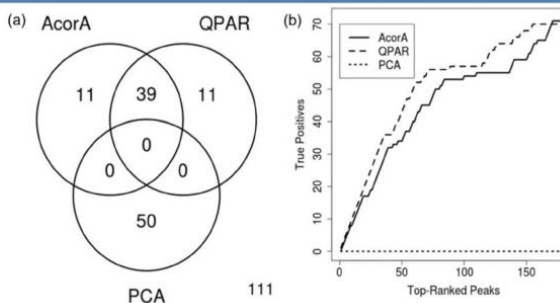
Figure 4. (a) Venn-diagram of 50 top-ranked peaks (LC/ESI-IT-MS) and (b) number of true positives among the top-ranked peaks (LC/ESI-IT-MS data). X-axis: the number of the considered top-ranked peaks is varied from 1 to 182.

9

In summary, in the case of the analyzed LC-MS data, the top-10 peaks ranked by AcorA and QPAR are of comparable quality. Both AcorA and QPAR give equally good predictions. For the studied case, QPAR gives a slightly better ranking considering the top-20 to top-150 ranked peaks, AcorA yields more true positives if all significantly predicted top-182 peaks are considered. In contrast, the rankings obtained by PCA are significantly worse indicating that PCA is not suited for the identification of peaks of active compounds in natural extracts.

Application in natural product research. Based on the results of the discussed 'reverse metabolomics' approach the AcorA methodology was used to identify metabolites with antibacterial activity from fungi of the genera *Albatrellus* and *Hygrophorus* (Basidiomycetes). As described in the proof of concept experiments two different approaches were used. Firstly, the similarity and native biodiversity of the metabolite profiles of different species belonging to one genus were used for the correlation analysis. Therefore, the mass spectral profiles of both UPLC/ESI-MS and ESI-FTICR-MS (positive and negative ion mode) as well as the activity profiles of three *Albatrellus* species derived from three different extraction solvents were computed with AcorA. Secondly, the modification method based on one single extract of *Hygrophorus latitabundus* was utilized for the identification of bioactive compounds.

Identification of antibacterial metabolites of Albatrellus species. For the identification of bioactive metabolites from unspiked extracts, fruitingbodies of the species from the genus *Albatrellus* were analyzed with the 'reverse metabolomics' approach.

Therefore, fresh fungal material species from different collections of three were separately extracted with ethyl acetate, methanol and hydrochloric acetone. The antibacterial activity against *Bacillus subtilis* was determined with a fluorescence-based bioassay. The results of the antibacterial assay are given in Figure S-1. In general, all extracts show a concentration-dependent activity, whereas the methanolic extracts exhibit lower activities than the ethyl acetate or hydrochloric acetone ones. The extracts exhibit activities between 37 % and 77 % ($c_{extract}$ = 10 µg/mL MeOH) and 60 % and 100 % growth inhibition of *B. subtilis* ($c_{extract}$ = 50 µg/mL MeOH).

The metabolite profiles of the extracts measured in triplicate with UPLC/ESI-MS and ESI-FTICR-MS in the positive and negative ion mode were used for the 'reverse metabolomics' approach. After pre-processing the MS data were correlated with the bioactivities for the concentrations $c_{extract}$ = 10 µg/mL MeOH and $c_{extract}$ = 50 µg/mL MeOH of the crude extracts. Based on this, a number of activity relevant peak clusters could be identified using AcorA.

The hit list of the positive ion ESI-FTICR-MS data contains 50 and 49 out of 879 aligned peaks exhibiting a positive correlation with the bioactivity profiles for $c_{extract}$ = 10 µg/mL and $c_{extract}$ = 50 µg/mL, respectively. In both cases clusters could be identified among the top-11 ranked peaks which belong to prenylated compounds (Table 1).

A further prenylated metabolite at *m/z* 379.2244 ($[M+H]^+$, calcd. *m/z* 379.2244 for $C_{23}H_{32}O_3Na^+$) correlates on rank 21 of the hit list with a correlation coefficient of 0.55. In agreement with the positive ion ESI-FTICR-MS data, the negative ion ones show a correlation of the $[M-H]^-$ ions at *m/z* 355.2279 (calcd. *m/z* 355.2279 for $C_{23}H_{31}O_3^-$) and *m/z* 343.2276 (calcd. *m/z* 343.2279 for $C_{22}H_{31}O_3^-$). These two compounds probably correspond to an aromatic aldehyde and a hydroxylated neogrifolin/grifolin, respectively. The hit lists resulting from the UPLC/ESI-MS data contain all *m/z* values of the prenylated metabolites (Spearman correlation coefficient > 0.45) which are also present in the hit list of the positive ion ESI-FTICR-MS. Table S-5 shows the retention times (RT), MS² data and correlation coefficient of a few potential prenylated compounds which could be active metabolites with the exception of compound **2**. All listed metabolites exhibit losses of C_5-units in the negative ion mode under electrospray ionization conditions. This fragmentation is typical for prenylated compounds as described previously.[37] The mass spectral fragmentation of the $[M-H]^-$ ions shows a consecutive loss of two isoprene units and an additional loss of an C_4-unit forming a benzyl anion. This fragmentation pattern is in accordance with metabolites that possess a farnesyl side chain. Furthermore, a differentiation of the aromatic moieties is possible.

Both scutigeral (**1**) and grifolic acid (**2**) show a $[M-H]^-$ ion at *m/z* 371 contain a farnesyl side chain, but differ in their aromatic moiety (Figure 5). In the extracted ion chromatograms of the *Albatrellus* extracts several peaks could be found for *m/z* 371 (Figure 6a and b).

10

Table 1. Hit list of the top-11 ranked peaks based on positive ion ESI-FTICR-MS data correlated with the antibacterial bioactivity profiles of the *Albatrellus* extracts ($c_{extract}$ = 50 µg/mL).

Rank	Spearman correlation coefficient	[M+Na/H]$^+$ (*m/z*)	Elemental composition	Error (ppm)	Possible compound
1	0.82	395.2196	$C_{23}H_{32}O_4Na^+$	0.8	Scutigeral/Grifolic acid
2	0.81	368.2280			Isotope peak of *m/z* 367.2246
3	0.80	367.2246	$C_{22}H_{32}O_3Na^+$	0.6	Hydroxyneogrifolin
4	0.78	351.2297	$C_{22}H_{32}O_2Na^+$	0.7	Grifolin/Neogrifolin
5	0.78	396.2227			Isotope peak of *m/z* 395.2196
6	0.75	365.2089	$C_{22}H_{30}O_3Na^+$	0.7	Not determined
7	0.69	443.2405	$C_{24}H_{36}O_6Na^+$	0.2	Not determined
8	0.67	401.2300	$C_{22}H_{34}O_5Na^+$	0.4	Not determined
9	0.65	739.4553			Not determined
10	0.64	707.4288	$C_{44}H_{60}O_6Na^+$	0.8	Albatrellin A
11	0.64	708.4331			Isotope peak of *m/z* 707.4288
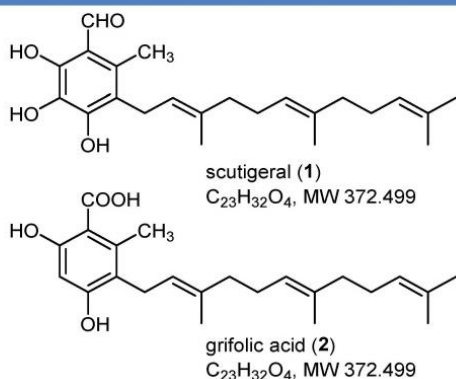
Figure 5. Structures, elemental compositions and molecular weights of scutigeral (**1**) and grifolic acid (**2**).

The fragmentation pattern of these compounds at RT = 6.4 min (Figure 6c) and RT = 7.0 min (spectrum not shown) are quite different. Moreover, the metabolite at RT = 7.0 min exhibits a positive correlation to the antibacterial activity with a Spearman correlation coefficient of 0.69. This metabolite was clearly identified as scutigeral (**1**) by an UPLC/ESI-MS/MS comparison with an authentic reference compound (Figure 6d).

The IC_{50} value of scutigeral (**1**) is 2 µg/mL. In comparison to the metabolites at *m/z* 343 [M-H]$^-$ (RT = 6.6 min) and at *m/z* 355 [M-H]$^-$ (RT = 7.3 min), scutigeral (**1**) possess one formyl moiety and one hydroxyl group more at the aromatic skeleton, respectively. Therefore an antibacterial activity can

be also assumed for such compounds. Moreover, compound **2** are described as bioactive metabolite against *B. subtilis* (14 mm diameters of inhibitory zone obtained by the disk diffusion test [c = 100 µg]).[38]

Identification of antibacterial metabolites from Hygrophorus latitabundus. Furthermore, for the identification of antibacterial metabolites, the modification method as described above in the proof of concept experiments was used. Therefore, a methanolic extract of *H. latitabundus* was modified to alter aliquots (Table S-6). The selected crude extract exhibited a strong native activity (87 +/- 6 % growth inhibition $c_{extract}$ = 100 µg/mL MeOH, 46 +/- 2 % $c_{extract}$ = 10 µg/mL MeOH) against *B. subtilis*, which is enhanced or reduced after modification (Figure S-2).
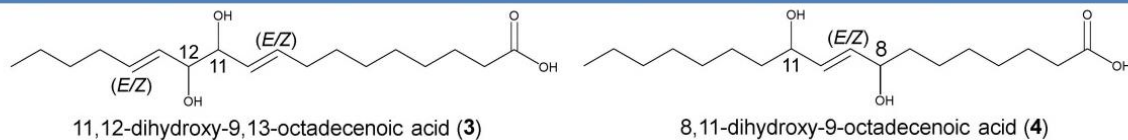
Using AcorA the activity-relevant metabolites are identified. In case of LC/ negative ion ESI-IT-MS 238 out of 2185 aligned peaks and in case of ESI-FTICR-MS 36/497 exhibited a positive correlation to the bioactivity. On rank two and three of the hit list, obtained from LC/ negative ion ESI-IT-MS data, appeared a peak cluster which corresponds to metabolite **3** at *m/z* 311 [M-H]$^-$ (RT ~ 22 min) and its first isotopic peak at *m/z* 312. Previous experiments demonstrated that repetition of peaks (isotopes, fragments etc.) indicate a true correlation of the metabolite. A further evaluation of the hit list based on sorting according to RT values, pointed out another peak cluster of a compound (**4**) with a

11

m/z 313 [M-H]$^-$ (RT ~ 24 min) and a m/z 314 for the first isotopic peak. Negative ion ESI-FTICR-MS data yielded the molecular formulas as $C_{18}H_{32}O_4$ and $C_{18}H_{34}O_4$ ([M-H]$^-$ ions at m/z 311.2226, calcd. m/z 311.2228 for $C_{18}H_{31}O_4^-$ and m/z 313.2384, calcd. m/z 313.2384 for $C_{18}H_{33}O_4^-$), respectively.
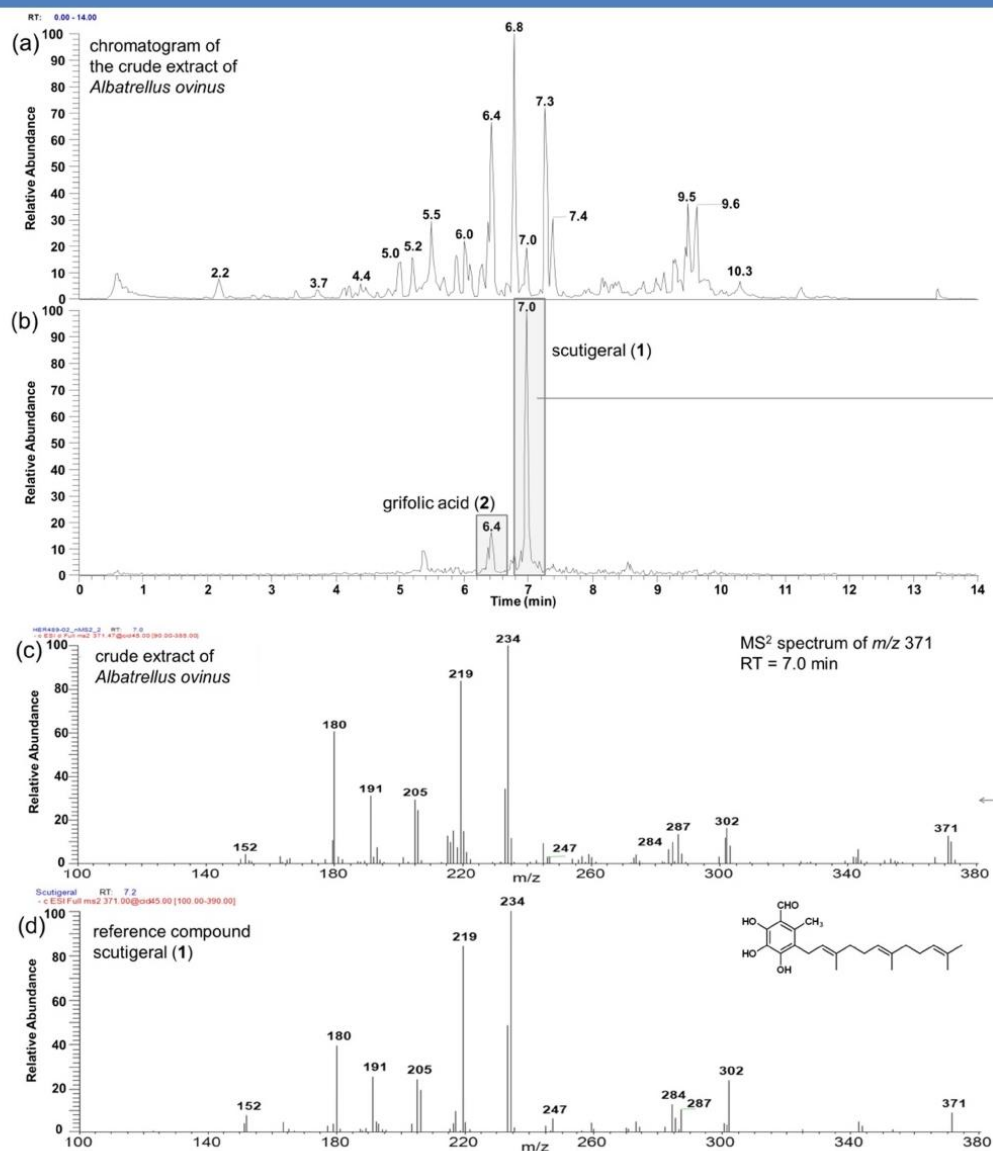
Figure 6. Total ion chromatogram (a) and the selected base peak chromatogram for the [M-H]$^-$ ion at m/z 371 (b) and the MS^2 spectra of the [M-H]$^-$ ion at m/z 371 (RT = 7.0 min, c) of the metanolic extract of *Albatrellus ovinus* and of the reference compound scutigeral (**1**, d).

11,12-dihydroxy-9,13-octadecenoic acid (**3**)   8,11-dihydroxy-9-octadecenoic acid (**4**)

Figure 7. Structures of 11,12-dihydroxy-12,13-dienoic acid (**3**) and 8,11-dihydroxy-9-octadecenoic acid (**4**). (positive electrospray ionization mode).

12

In both cases, these metabolites belong to the group of oxidized fatty acids according to their fragmentation behavior. Based on high-resolution UPLC/ESI-QTOF-MS[2] fragmentation experiments we propose their structures as 11,12-dihydroxy-12,13-dienoic acid (**3**) and 8,11-dihydroxy-9-octadecenoic acid (**4**) (Figure 7, Table S-7).[39–42] Moreover, we were able to confirm the activity for both compounds. Both oxidized fatty acids show comparable activities. Compound **3** inhibit the bacterial growth with 34 +/- 4 % (c = 10 µg/mL) and 69 +/- 3 % (c = 100 µg/mL) and compound **4** exhibit 29 +/- 6 % (c = 10 µg/mL) and 71 +/- 8 % (c = 100 µg/mL) growth inhibition of *B. subtilis*.[27]

CONCLUSIONS

For the isolation and identification of new bioactive natural products we introduced a technique termed 'reverse metabolomics' which exploits variation with respect to the chemical composition of active crude natural extracts and their variable activity to identify some of the active compounds. The necessary variation might be naturally given by different sources of the biological extracts, e.g. different species, or might be artificially generated by chemical or physical modifications of the extracts.

'Reverse metabolomics' involves a multivariational analysis method called activity correlation analysis (AcorA) which is applied to high-throughput measurements like HPLC, MS, and NMR of the crude extracts and which predicts peaks that are potentially caused by the active compounds. Knowing these peaks brings several advantages for the isolation of the active compounds: i) the identification of already known active compounds prior to isolation in order to prevent replication, ii) a proberty (spectroscopy or chromatography) guided isolation towards the identified peaks which is less laborious compared to the traditional activity-guided isolation for which an activity assay has to be run after each isolation step, iii) the activity of the initial extracts has to be measured only once with an initial activity assay, iv) as the isolation is no activity-guided, the isolation process might be easily repeated with different initial activity assays, and v) as 'reverse metabolomics' is a general approach, it might be applied as well to further high-throughput screening (HTS) investigations like the identification of active compounds in mixture-based compound libraries in the field of combinatorial chemistry.

In comparison with QPAR and a devised PCA-based approach on LC-MS and FTICR-MS spectra of inactive extracts of the fungi *Hygrophorus* ssp. which have been spiked with three antibiotics in different concentrations AcorA has been proved to be superior over the PCA-based approach and to be as equally well suited for the identification of peaks of active compounds in complex natural extracts as QPAR.

In comparison with QPAR and a devised PCA-based approach on LC-MS and FTICR-MS spectra of inactive extracts of the fungi *Hygrophorus* which have been spiked with three antibiotics in different concentrations AcorA has been evidenced to be superior over the PCA-based approach and to be as equally well suited for the identification of peaks of active compounds in complex natural extracts as QPAR.

In two real cases, bioactive metabolites with an antibacterial activity were successfully identified. Besides some known and yet unknown prenylated compounds, the fungal metabolite scutigeral (**1**) with an IC$_{50}$ value of 2 µg/mL was identified using an UPLC/ESI-ion trap MS[2] comparison with a reference compound from extracts of fungi of the genera *Albatrellus*. From extracts of the basidiomycete *Hygrophorus latitabundus* 11,12-dihydroxy-12,13-dienoic acid (**3**) and 8,11-dihydroxy-9-octadecenoic acid (**4**) could be identified as most probable bioactive metabolites.

REFERENCES

1. Koehn, F.E. & Carter, G.T. (2005) The evolving role of natural products in drug discovery. *Nat. Rev. Drug Discov.* **4**, 206–220.

2. Newman, D.J. & Cragg, G.M. (2012) Natural products as sources of new drugs over the 30 years from 1981 to 2010. *J. Nat. Prod.* **75**, 311–335.

3. Ji, H.-F., Li, X.-J. & Zhang, H.-Y. (2009) Natural products and drug discovery. *EMBO Rep.* **10**, 194-200.

4. Newman, D.J. & Cragg, G.M. (2007) Natural products as sources of new drugs over the last 25 years. *J. Nat. Prod.* **70**, 461–477.

5. Peláez, F. (2006) The historical delivery of antibiotics from microbial natural products--can history repeat? *Biochem. Pharmacol.* **71**, 981–990.

6. Wright, G.D. (2012) Antibiotics: A new hope. *Chem. Biol.* **19**, 3–10.

7. Walsh, C. (2003) Where will new antibiotics come from? *Nat. Rev. Microbiol.* **1**, 65–70.

8. Fischbach, M.A. & Walsh, C.T. (2009) Antibiotics for emerging pathogens. *Science* **325**, 1089–1093.

9. Ingkaninan, K. Hazekamp, A., De Best, C.M., Irth, H., Tjaden, U.R., Van der Heijden, R., Van der Greef, J. & Verpoorte, R. (2000) The application of HPLC with on-line coupled UV/MS-biochemical detection for isolation of an acetylcholinesterase inhibitor from *Narcissus* 'Sir Winston Churchill'. *J. Nat. Prod.* **63**, 803–806.

10. Van Elswijk, D.A., Diefenbach, O., Van der Berg, S., Irth, H., Tjaden, U.R. & Van Der Greef, J. (2003) Rapid detection and identification of angiotensin-converting enzyme inhibitors by on-line liquid chromatography – biochemical detection, coupled to electrospray mass spectrometry. *J. Chromatogr. A* **1020**, 45–58.

11. Schobel, U. Frenay, M., Elswijk, D.A., Van; Mcandrews, J.M., Long, K.R., Olson, L.M. & Bobzin, S.C. (2001) High resolution screening of plant natural product extracts for estrogen receptor α and β3 binding activity using an online HPLC-MS biochemical detection system. *J. Biomol. Screen.* **6**, 291–303.

12. Schriemer, D.C., Bundle, D.R., Li, L. & Hindsgaul, O. (1998) Micro-scale frontal affinity chromatography with mass spectrometric detection: A new method for the screening of compound libraries. *Angew. Chem. Int. Ed.* **37**, 3383–3387.

13. Slon-Usakiewicz, J.J., Ng, W., Dai, J.-R., Pasternak, A. & Redden, P.R. (2005) Frontal affinity chromatography with MS detection (FAC–MS) in drug discovery. *Drug Dis. Today* **10**, 409–416.

14. Dumarey, M., van Nederkassel, A. M., Deconinck, E. & Vander Heyden, Y. (2008) Exploration of linear multivariate calibration techniques to predict the total antioxidant capacity of green tea from chromatographic fingerprints. *J. Chromatogr. A* **1192**, 81–88.

15. Nguyen Hoai, N., Dejaegher, B., Tistaert, C., Nguyen Thi Hong, V., Rivière, C., Chataigné, G., Phan Van, K., Chau Van, M., Quetin-Leclercq, J. & Vander Heyden, Y. (2009) Development of HPLC fingerprints for *Mallotus* species extracts and evaluation of the peaks responsible for their antioxidant activity. *J. Pharm. Biomed. Anal.* **50**, 753–763.

16. Rajalathi, T. & Kvalheim, O.M. (2011) Multivariate data analysis in pharmaceutics: A tutorial review. *Int. J. Pharm.* **417,** 280–290.

17. Trygg, J. & Wold, S. (2002) Orthogonal projections to latent structures (O-PLS). *J. Chemom.* **16**, 119–128.

18. Kvalheim, O.M. & Karstang, T.V. (1989) Interpretation of latent-variable regression models. *Chemom. Intell. Lab.* **7**, 39–51.

19. Kvalheim, O.M. (1990) Latent-variable regression models with higher-order terms: An extension of response modelling by orthogonal design and multiple linear regression. *Chemom. Intell. Lab.* **8**, 59–67.

20. Rajalahti, T., Arneberg, R., Kroksveen, A.C., Berle, M., Myhr, K.-M. & Kvalheim, O.M. (2009) Discriminating variable test and selectivity ratio plot: quantitative tools for interpretation and variable (biomarker) selection in complex spectral or chromatographic profiles. *Anal. Chem.* **81**, 2581-2590.

21. Rajalahti, T., Arneberg, R., Berven, F.S., Myhr, K.-M., Ulvik, R.J. & Kvalheim, O.M. (2009) Biomarker discovery in mass spectral profiles by means of selectivity ratio plot. *Chemom. Intell. Lab.* **95**, 35–48.

22. Chau, F.-T., Chan, H.-Y., Cheung, C., Xu, C.-J., Liang, Y. & Kvalheim, O.M. (2009) Recipe for uncovering the bioactive components in herbal medicine. *Anal. Chem.* **81**, 7217–7225.

23. Joyce, A.R. & Palsson, B.Ø. (2006) The model organism as a system: integrating "omics" data sets. *Nat. Rev. Mol. Cell Bio.* **7**, 198–210.

24. Lokhov, P.G. & Archakov, A.I. (2009) Mass spectrometry methods in metabolomics. *Biochem. Suppl. Ser. B Biomed. Chem.* **3**, 1–9.

25. Jolliffe, I.T. (2002) *Principal component analysis. Encycl. Stat. Behav. Sci.* (Springer New York, ISBN: 978-0-387-95442-4).

26. Pearson, K. (1901) On lines and planes of closest fit to systems of points in space. *Phil. Trans.* **1**, 559-572.

27. Michels, K. (2011) Entwicklung einer LC-MS basierten Methode zur Identifizierung von aktivitätsrelevanten Metaboliten in komplexen Mischungen. Dissertation, Martin-Luther University Halle-Wittenberg.

28. Veening, J., Smits, W.K., Leendert, W., Jongbloed, J.D.H. & Kuipers, O.P. (2004) Visualization of differential gene expression by improved cyan fluorescent protein and yellow fluorescent protein production in *Bacillus subtilis*. *Appl. Environ. Microbiol.* **70**, 6809–6815.

29. Smith, C.A., Want, E.J., O'Maille, G., Abagyan, R. & Siuzdak, G. (2006) XCMS: Processing mass spectrometry data for metabolite profiling using nonlinear peak alignment, matching, and identification. *Anal. Chem.* **78**, 779–787.

30. Deubel, A., Fandi, A.S., Sörgel, F. & Holzgrabe, U. (2006) Determination of erythromycin and related substances in commercial samples using liquid chromatography/ion trap mass spectrometry. *J. Chromatogr. A* **1136**, 39–47.

31. Pendela, M., Van den Bossche, L., Hoogmartens, J., Van Schepdael, A. & Adams, E. (2008) Combination of a liquid chromatography-ultraviolet method with a non-volatile eluent, peak trapping and a liquid chromatography-mass spectrometry method with a volatile eluent to characterise erythromycin related substances. *J. Chromatogr. A* **1180**, 108–121.

14

32. Lübken, T., Schmidt, J., Porzel, A., Arnold, N. & Wessjohann, L. (2004) Hygrophorones A–G: fungicidal cyclopentenones from *Hygrophorus* species (Basidiomycetes). *Phytochemistry* **65**, 1061-1071.

33. Gilardoni, G., Clericuzio, M., Tosi, S., Zanoni, G. & Vidari, G. (2007) Antifungal acylcyclopentenediones from fruiting bodies of *Hygrophorus chrysodon*. *J. Nat. Prod.* **70**, 137–139.

34. Farag, M.A., Porzel, A., Schmidt, J. & Wessjohann, L.A. (2012) Metabolite profiling and fingerprinting of commercial cultivars of *Humulus lupulus* L. (hop): a comparison of MS and NMR methods in metabolomics. *Metabolomics* **8**, 492–507.

35. Heinke, R., Schöne, P., Arnold, N., Wessjohann, L. & Schmidt, J. (2014) Metabolite profiling and fingerprinting of *Suillus* species (Basidiomycetes) by electrospray mass spectrometry. *Eur. J. Mass Spectrom.* **20**, 85.

36. Glauser, G., Veyrat, N., Rochat, B., Wolfender, J.-L. & Turlings, T.C.J. (2013) Ultra-high pressure liquid chromatography – mass spectrometry for plant metabolomics: A systematic comparison of high-resolution quadrupole-time-of-flight and single stage Orbitrap mass spectrometers. *J. Chromatogr. A* **1292**, 151–159.

37. Heinke, R., Arnold, N., Wessjohann, L. & Schmidt, J. (2013) Negative ion tandem mass spectrometry of prenylated fungal metabolites and their derivatives. *Anal. Bioanal. Chem.* **405**, 177–189.

38. Zechlin, L., Wolf, M., Steglich, W. & Anke, T (1981). Cristatsäure, ein modifiziertes Farnesylphenol aus Fruchtkörpern von *Albatrellus cristatus*. *Liebigs Ann. Chem.* **12**, 2099–2105.

39. Nilsson, T., Martínez, E., Manresa, A. & Oliw, E.H. (2010) Liquid chromatography/tandem mass spectrometric analysis of 7,10-dihydroxyocta-decenoic acid, its isotopomers, and other 7,10-di-hydroxy fatty acids formed by *Pseudomonas aeruginosa* 42A2. *Rapid Commun. Mass Spectrom.* **24**, 777–783.

40. Murphy, R.C., Fiedler, J. & Hevko, J. (2001) Analysis of nonvolatile lipids by mass spectrometry. *Chem. Rev.* **101**, 479–526.

41. Murphy, R.C., Barkley, R.M., Zemski Berry, K., Hankin, J., Harrison, K., Johnson, C., Krank, J., McAnoy, A., Uhlson, C. & Zarini, S. (2005) Electrospray ionization and tandem mass spectrometry of eicosanoids. *Anal. Biochem.* **346**, 1-42.

42. Garscha, U., Jernerén, F., Chung, D., Keller, N.P., Hamberg, M. & Oliw, E.H. (2007) Identification of dioxygenases required for *Aspergillus* development. Studies of products, stereochemistry, and the reaction mechanism. *J. Biol. Chem.* **282**, 34707-34718.

15

6.   New antibacterial active metabolites of *Albatrellus* species (Basidiomycetes) identified by activity correlation analysis

Ramona Heinke, Sebastian Stark, Annegret Laub, Anja Ehrlich, Norbert Arnold,
Jürgen Schmidt, Ludger Wessjohann*
Unpublished

Abstract

The antibacterial properties of fungal extracts of *Albatrellus* species were investigated. The growth of the Gram-positive bacterium *Bacillus subtilis* was well inhibited, while the effect against the Gram-negative bacterium *Aliivibrio fischeri* is only low to moderate. Furthermore, few extracts show cell proliferation inhibitory effects against the human prostate cancer cell line PC3 and the colon cancer cell line HT29. The results obtained by the *B. subtilis* assay were directly correlated with the MS-based metabolite profiles using the 'reverse metabolomics' approach. Besides the known antibacterially active prenylated compounds **1** and **2** a peak cluster corresponding to nitrogen-containing compounds (**39-44**) are found which correlate with the antibacterial activity against *B. subtilis*.

Keywords

'Reverse metabolomics'; activity correlation analysis (AcorA); Basidiomycetes, Albatrellus; antibacterial activity; electrospray ionization - mass spectrometry

New antibacterial active metabolites of *Albatrellus* species (Basidiomycetes) identified by activity correlation analysis

Ramona Heinke[1], Sebastian Stark[1,2], Annegret Laub[1], Anja Ehrlich[1],
Norbert Arnold[1], Jürgen Schmidt[1], Ludger Wessjohann[1*]

[1]*Leibniz Institute of Plant Biochemistry, Department of Bioorganic Chemistry, Weinberg 3, 06120 Halle/Saale, Germany, Tel: +49 (0) 345-55821301, Fax: +49 (0) 345-55821309*

[2]*Ascendis Pharma GmbH, Im Neuenheimer Feld 584, 69120 Heidelberg, Germany*

corresponding author: wessjohann@ipb-halle.de

unpublished

ABSTRACT

The antibacterial properties of fungal extracts of *Albatrellus* species were investigated. The growth of the Gram-positive bacterium *Bacillus subtilis* was well inhibited, while the effect against the Gram-negative bacterium *Aliivibrio fischeri* is only low to moderate. Furthermore, a few extracts show cell proliferation inhibitory effects against the human prostate cancer cell line PC3 and the colon cancer cell line HT29. The results obtained by the *B. subtilis* assay were directly correlated with the MS-based metabolite profiles using the 'reverse metabolomics' approach. Besides the known antibacterially active prenylated compounds **1** and **2**, a peak cluster corresponding to nitrogen-containing compounds (**39-44**) was found which correlate with the antibacterial activity against *B. subtilis*.

KEYWORDS

'Reverse metabolomics', activity correlation analysis (AcorA), Basidiomycetes, *Albatrellus*, antibacterial activity, electrospray ionization - mass spectrometry

INTRODUCTION

The genus *Albatrellus* S.F. Gray belongs to the family *Albatrellaceae* (Russulales), mainly found in the temperate forests of the Northern hemisphere. The terrestrial medium to large fleshy fruiting bodies of various colors are mostly mycorrhizal partners of deciduous and coniferous trees, while some may be wood-decaying taxa. Most species are growing in montane and sub-alpine woodlands. The basidiomes are stipitate (either central or eccentric to lateral), a universal veil and partial veil are absence. The pileus surface is glabrous to felted, and the hymenophore on the lower surface of basidiocarps is poroid. The hyphal system is monomitic with simple septa or clamp connections. The basidiospores of *Albatrellus* spp. are smooth, broadly ellipsoid to subglobose, amyloid to non-amyloid (negative in Melzer's reagent).
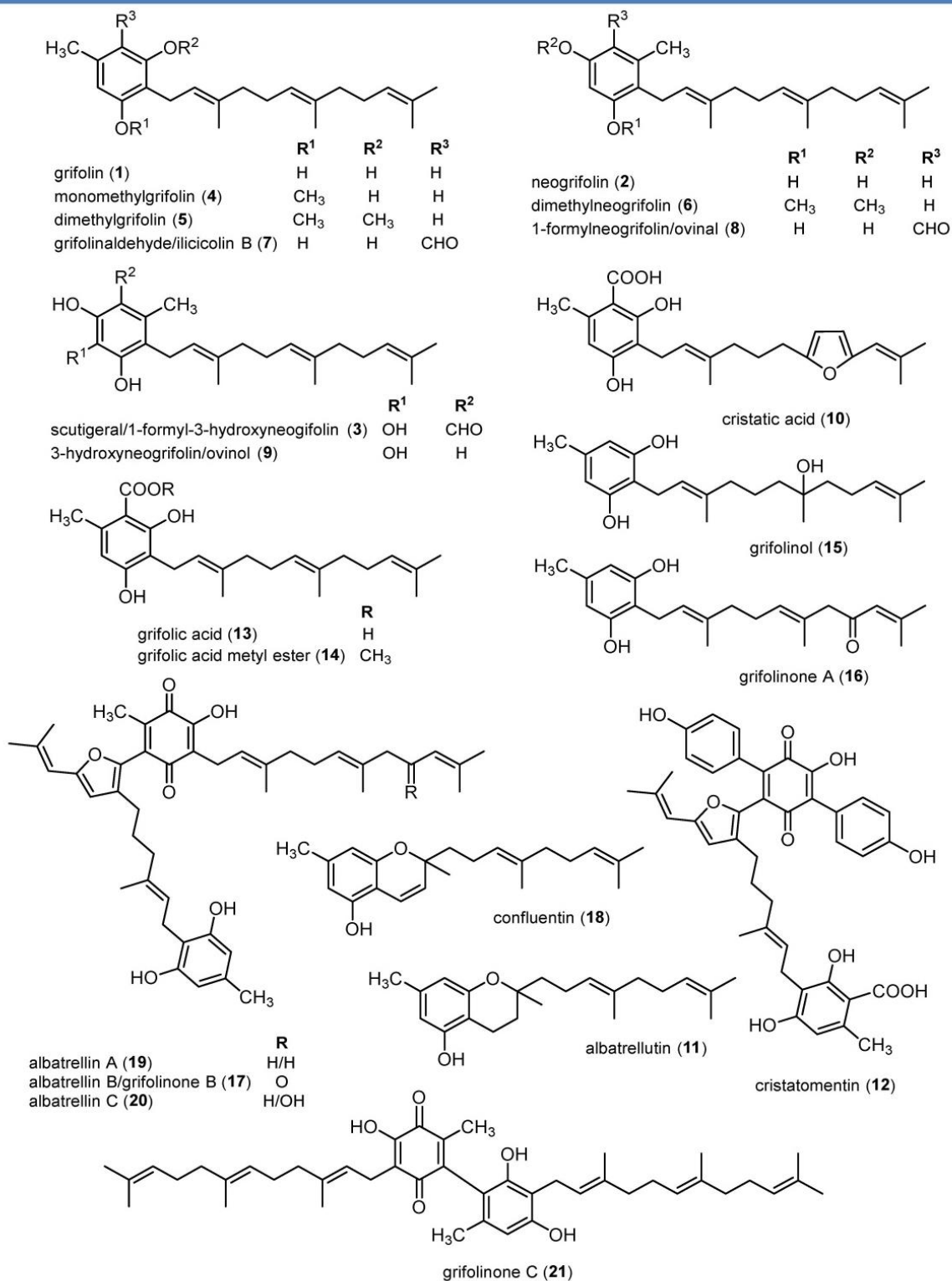
Originally, species of *Albatrellus* has been classified in the order Polyporales. Recent studies based on phylogenetic analyses of sequence data from the internal transcribed spacer (ITS) region of nuclear ribosomal DNA showed that the genus *Albatrellus* is polyphyletic and consists of two separate groups with affinities to the polyporoid clade and the russuloid clade.[1–3] The ITS phylogeny in recent studies supports a close relationship among *A. citrinus* Ryman, *A. subrubescens* (Murrill) Pouzar, and *A. ovinus* (Schaeff.) Kotl. & Pouzar, all belong to the russuloid claid.[3–5] In contrast to the most members of the genus *Albatrellus*, the ITS sequences of *A. syringae* (Parmasto) Pouzar are perspicuously different from the other species of *Albatrellus* and placed in the polyporoid clade.[4–8]

Next to morphological features and DNA analyses, also the chemical characters are helpful

1

for a (chemo-) taxonomic classification. Exemplary farnesylated phenols isolated from the fruiting bodies of species of the genus *Albatrellus* are naturally occurring constituents (Figure 1).


	R¹	R²	R³
grifolin (**1**)	H	H	H
monomethylgrifolin (**4**)	CH₃	H	H
dimethylgrifolin (**5**)	CH₃	CH₃	H
grifolinaldehyde/ilicicolin B (**7**)	H	H	CHO

	R¹	R²	R³
neogrifolin (**2**)	H	H	H
dimethylneogrifolin (**6**)	CH₃	CH₃	H
1-formylneogrifolin/ovinal (**8**)	H	H	CHO

	R¹	R²
scutigeral/1-formyl-3-hydroxyneogifolin (**3**)	OH	CHO
3-hydroxyneogrifolin/ovinol (**9**)	OH	H

	R
grifolic acid (**13**)	H
grifolic acid metyl ester (**14**)	CH₃

cristatic acid (**10**)

grifolinol (**15**)

grifolinone A (**16**)

	R
albatrellin A (**19**)	H/H
albatrellin B/grifolinone B (**17**)	O
albatrellin C (**20**)	H/OH

confluentin (**18**)

albatrellutin (**11**)

cristatomentin (**12**)

grifolinone C (**21**)

Figure 1. Structural formulas of isolated prenylated metabolites from *Albatrellus* species.

So, grifolin (**1**), first isolated in 1950 by Hirata and Nakanishi from *A. confluens* (Alb. & Schwein.) Kotl. & Pouzar,[9,10] and its isomer neogrifolin (**2**) are typical components of *Albatrellus* species. In addition, the yellow-colored scutigeral (**3**) being responsible for the red-brown color reaction of the fruiting body with aqueous alkali could be identified as a further main constituent of *A. ovinus* and *A. subrubescens*. Furthermore, both neogrifolin (**2**) and scutigeral (**3**) have an unusual position of the farnesyl moiety inserted between the *C*-methyl and OH group. In other known natural products of this type the prenyl side chain is always located between the two OH groups of orcinol or orsellinaldehyde moiety.[11] Further chemical investigations of several *Albatrellus* species has resulted in other grifolin derivatives like monomethylgrifolin (**4**), dimethylgrifolin (**5**) and dimethylneogrifolin (**6**),[12] as well as grifolinaldehyde (ilicicolin B, **7**), 1-formylneogrifolin (**8**), and 3-hydroxyneogrifolin (**9**).[13,14] *A. cristatus* (Schaeff.) Kotl. & Pouzar contains cristatic acid (**10**), a farnesylphenol with a modified side chain[15] and albatrellutin (**11**).[16] Moreover, cristatomentin (**12**) was also isolated from fruiting bodies of *A. cristatus*. A morphologically closely related American *Albatrellus* species contains grifolic acid (**13**) instead of cristatic acid

(**10**). Grifolic acid (**13**) is also a major component of the Japanese *A. dispansus* (Lloyd) Canf. & Gilb. along with grifolin (**1**), grifolic acid methyl ester (**14**), and grifolinol (**15**).[17] Grifolinones A (**16**) and B (= albatrellin B, **17**) isolated from the inedible *A. caeruleoporus* (Peck) Pouzar[18] or confluentin (**18**) and the dimeric grifolin derivatives albatrellin A (**19**), albatrellin B (= grifolinone B, **17**), albatrellin C (**20**) and grifolinone C (**21**) from *A. confluens* demonstrate the structural diversity of farnesylated phenols in the genus *Albatrellus*. Recent studies on *A. caeruleoporus* have been shown that further farnesylphenols could be isolated from fruiting bodies including eight neogrifolin derivatives (**22-29**) and one new grifolin analogue (**30**) (Figure 2).[19]

Some farnesylphenols such as grifolin (**1**), neogrifolin (**2**), and their derivatives possess a wide range of interesting biological activities like antioxidative,[13] anti-inflammatory,[18] plant growth inhibitory activity,[20] tyrosinase inhibition,[21] activity on vanilloid[22,23] and dopamine receptors,[14] cytotoxic and tumor growth inhibitory effects[24–28] as well as hypocholesterolemic[29] and antimicrobial properties.[9,15,17,30] Among them some metabolites exhibit antibacterial activities which are shown in Table 1.
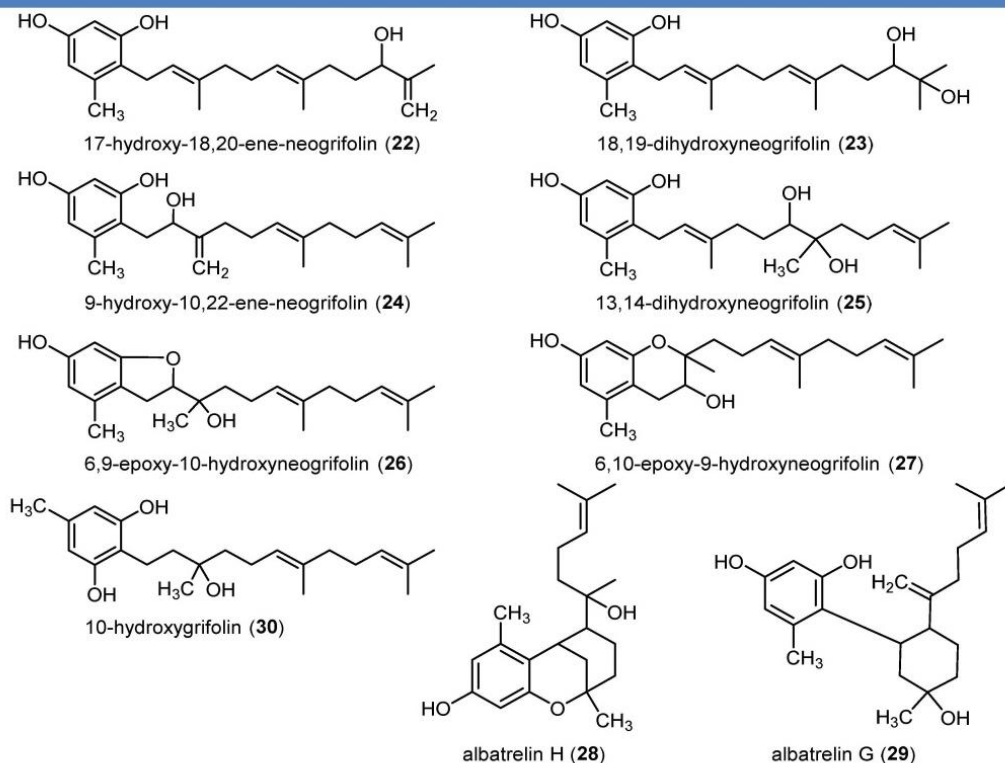
Figure 2. Structural formulas of isolated prenylated metabolites from *Albatrellus caeruleoporus*.[19]

17-hydroxy-18,20-ene-neogrifolin (**22**)

18,19-dihydroxyneogrifolin (**23**)

9-hydroxy-10,22-ene-neogrifolin (**24**)

13,14-dihydroxyneogrifolin (**25**)

6,9-epoxy-10-hydroxyneogrifolin (**26**)

6,10-epoxy-9-hydroxyneogrifolin (**27**)

10-hydroxygrifolin (**30**)

albatrelin H (**28**)

albatrelin G (**29**)

Table 1. Antibacterial activities of farnesyl phenols isolated from *Albatrellus* species described in literature.[15,17,30-32]

Compound	Activity against Gram-positive bacteria	Activity against Gram-negative bacteria
1	*Bacillus cereus* (MIC = 10 µg/mL)[31] *Enterococcus faecalis* (MIC = 0.5 µg/mL)[31] *Bacillus brevis* ([a]12 mm [c = 100 µg])[15] *Bacillus subtilis* ([a]11 mm [c = 100 µg])[15] *Staphylococcus aureus* ([a]19 mm [c = 50 µg])[17] MRSA[30]	No activity against *Escherichia coli* K12[15] *Escherichia coli* ([a]27 mm [c = 50 µg])[17] *Salmonella enteritidis* ([a]18 mm [c = 50 µg])[17] *Pseudomonas aeruginosa* ([a]20 mm [c = 50 µg])[17] *Klebsiella pneumoniae* ([a]40 mm [c = 50 µg])[17]
2	*Bacillus cereus* (MIC = 20 µg/mL)[31] *Enterococcus faecalis* (MIC = 0.5 µg/mL)[31] MRSA[30]	
3	MRSA[30]	
7	No activity against Gram-positive bacteria[32]	No activity against Gram-negative bacteria[32]
10	*Bacillus brevis* ([a]16 mm [c = 100 µg])[15] *Bacillus subtilis* ([a]17 mm [c = 100 µg])[15]	No activity against *Escherichia coli* K12[15]
13	*Bacillus brevis* ([a]12 mm [c = 100 µg])[15] *Bacillus subtilis* ([a]14 mm [c = 100 µg])[15] *Staphylococcus aureus* ([a]27 mm [c = 50 µg])[17] MRSA[30]	No activity against *Escherichia coli* K12[15] *Escherichia coli* ([a]30 mm [c = 50 µg])[17] *Salmonella enteritidis* ([a]28 mm [c = 50 µg])[17] *Pseudomonas aeruginosa* ([a]27 mm [c = 50 µg])[17] *Klebsiella pneumoniae* ([a]44 mm [c = 50 µg])[17]
14	*Staphylococcus aureus* ([a]15 mm [c = 50 µg])[17] MRSA[30]	*Escherichia coli* ([a]20 mm [c = 50 µg])[17] *Salmonella enteritidis* ([a]26 mm [c = 50 µg])[17] *Pseudomonas aeruginosa* ([a]16 mm [c = 50 µg])[17] *Klebsiella pneumoniae* ([a]42 mm [c = 50 µg])[17]
15	Weak activity against MRSA[30]	
18	*Bacillus cereus* (MIC = 20 µg/mL)[31] *Enterococcus* faecalis (MIC = 1 µg/mL)[31]	

[a] diameters of inhibitory zone obtained by the disk diffusion test

MIC = minimum inhibitory concentration; MRSA = Methicillin-resistant *Staphylococcus aureus*
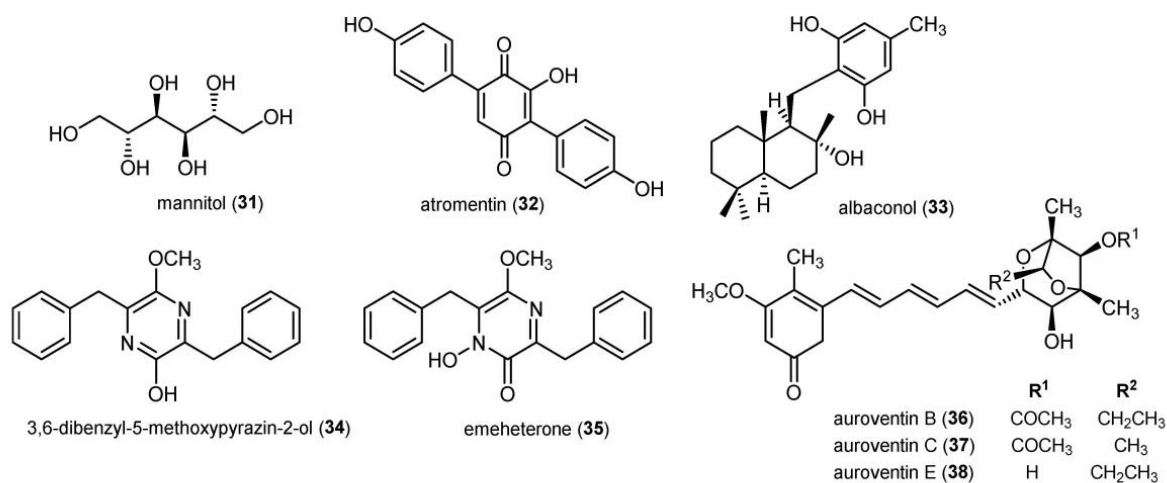
Figure 3. Structural formulas of isolated non-prenylated metabolites from *Albatrellus* species.

mannitol (**31**)

atromentin (**32**)

albaconol (**33**)

3,6-dibenzyl-5-methoxypyrazin-2-ol (**34**)

emeheterone (**35**)

	R¹	R²
auroventin B (**36**)	COCH₃	CH₂CH₃
auroventin C (**37**)	COCH₃	CH₃
auroventin E (**38**)	H	CH₂CH₃

Further constituents (Figure 3) isolated from in *Albatrellus* species are mannitol (**31**), atromentin (**32**), albaconol (**33**) and nitrogen containing compounds like the pyrazine derivatives **34** and **35**, hitherto isolated from *A. confluens* as well as auroventine (**36**-**38**).[33–35] Moreover, cleistanthane-type diterpenes, isocoumarines and polyesters are metabolites which can be found in cultures of *A. confluens*.[36] The review paper of Quang et al. (2006) give an overview of the distribution and the biological activities of grifolin derivatives from *Albatrellus* species.[37]

In continuation of our investigations concerning antibacterial activities, the ethyl acetate, methanolic and acidified acetone extracts of seven *Albatrellus* species from different geographical regions and habitats, including the mycelial culture of *A. syringae*, were analyzed. In addition to the antibacterial properties, the cytotoxic properties were determined using a cell proliferation assay with two different cell lines.

For the *ab initio* identification of potential antibacterially active fungal metabolites, the 'reverse metabolomics' method based on activity correlation analysis (AcorA) was applied. Therefore, the metabolite profiles obtained by liquid chromatography/electrospray ionization mass spectrometry (LC/ESI-MS) and direct infusion electrospray ionization Fourier transform ion cyclotron resonance mass spectrometry (ESI-FTICR-MS) with antibacterial activity data against *B. subtilis* were correlated.

EXPERIMENTAL

Fungal materials and culture of fungi

An overview of specimens used in the different studies is given in the supporting information in Table S1. Voucher specimens are deposited at the Leibniz Institute of Plant Biochemistry Halle, Germany (IPB). Selected strain [*A. syringae* KSH 873] from the culture collection of the IPB were grown in Petri dishes containing 20 mL Moser-b medium.[38]

Extraction and sample preparation

Air-dried fruiting bodies of *Albatrellus* spp. were extracted three times under ultrasonication with methanol (MeOH), ethyl acetate (EE), or hydrochloric acetone (Ac/HCl). The agar of three petri dishes was cut into pieces and divided into two extraction approaches. Each approach was extracted thrice with ethyl acetate, or methanol under ultrasonication. The combined methanolic extracts were reduced to the aq. phase and

partitioned successively with ethyl acetate (LLEE) and water (LLW). After evaporation to dryness *in vacuo* the dry extracts were dissolved in methanol and processed with Chromabond® C8 cartridge (Macherey-Nagel) using methanol as eluent for the antibacterial/antiproliferative testing and MS measurements.

Reagents and standards

Authentic compounds (**2**, **3**) were kindly provided by Prof. Dr. Dr. h.c. Wolfgang Steglich (Ludwig-Maximilians-University, Munich). Stock solutions were prepared in methanol (1 mg ml^{-1}).

Antibacterial bioassay

The biological activities of the crude extracts and authentic reference compounds against Gram-positive bacteria *Bacillus subtilis* were determined with a quantitative fluorescence-based antibacterial growth inhibition assay.[39] The fluorescence was measured on a microtiter plate reader GENios Pro (Fa. Tecan, excitation, 510 nm; emission, 535 nm). The *B. subtilis* strain 168 (PAbrB-IYFP) was maintained on TY (tryptone-yeast extract) medium supplemented with 1 % Bacto-tryptone, 0.5 % Bacto-yeast extract, 1 % NaCl and chloramphenicol (5 µg/ml).[40]

The *Aliivibrio fischeri* assay is based on the measurement of the inhibition of bacterial luminescence against a negative control. Bacteria were pregrown on a saline BOSS medium (3 % NaCl w/w) whereby at a certain population density, bacterial luminescence will start. The bacterial suspension was diluted, distributed into 96-well microtiter plates and the respective compounds were applied as a concentration series as solutions in DMSO/medium (2 % v/v) and mixed. The luminescence of bacteria treated with the respective compounds was measured after 1 h (acute toxicity) and after 24 h incubation (general toxicity) at 23°C in the dark, in relation to controls of untreated bacteria.

Cell proliferation assay

The determination of cell proliferation by XTT method, the Cell Proliferation Kit II (Roche) was used. The human prostate cancer cell line PC3 and the colon cancer cell line HT29 were maintained in RPMI 1640 medium supplemented with 10 % fetal bovine serum, 1 % L-alanyl-l-glutamine (200 mM), 1 % penicillin/streptomycin and 1.6 % hepes (1 M). For the measurement of cell proliferation effects the same medium was used without antibiotics. For PC3 500 cells/well and for HT29 1500 cells/well were seeded overnight into 96-well plates and exposed to serial dilution of each compound for 3 days.

5

Mass spectrometry

The positive and negative ion high-resolution ESI mass spectra were obtained from a Bruker Apex III FTICR mass spectrometer (Bruker Daltonics, Billerica, USA) equipped with an Infinity™ cell, a 7.0-Tesla superconducting magnet (Bruker, Karlsruhe, Germany), a radio frequency-only hexapole ion guide and an external APOLLO electrospray ion source (Agilent; off axis spray; negative ion mode: voltages: endplate, 3700 V; capillary, 4200 V; capillary exit, -100 V; skimmer 1, -15.0 V; skimmer 2, -12.0 V; positive ion mode - 3700 V; capillary, -4.200 V; capillary exit, 100 V; skimmer 1, 15.0 V; skimmer 2, 12.0 V). Nitrogen was used as drying gas at 150°C. The sample solutions were introduced continuously via a syringe pump with a flow rate of 120 µl h^{-1}. The mass spectra were evaluated by the Bruker software XMASS 7.0.8.

The negative ion high resolution ESI mass spectra were obtained from an Orbitrap Elite mass spectrometer (Thermofisher Scientific, Bremen, Germany) equipped with an HESI electrospray ion source (spray voltage 4.0 kV; capillary temperature 275°C, source heater temperature 200°C; FTMS resolution 30.000). Nitrogen was used as sheath gas. The MS system is coupled with an UHPLC system (Dionex UltiMate 3000, Thermo Scientific), equipped with a RP8 column (50 mm x 2.1 mm, 1.9 µm particle size, Hypersil GOLD C8, Thermo Scientific, column temperature 30°C). For the UHPLC a gradient system was used starting from water/acetonitrile 50:50 (each of them containing 0.2 % formic acid), holding 0.2 min, then to 0:100 within 16.3 min and then hold on 100 % acetonitrile for further 6.5 min; flow rate 150 µl min^{-1}. The injection volume of the crude extracts was 2 µL. The collision induced dissociation (CID) MS^n measurements were performed using the normalized collision energy of 35-45 % (see Table S2). The instrument was externally calibrated by the Pierce® ESI negative ion calibration solution (product number 88324) from Thermofisher Scientific, Rockford, IL, 61105 USA). The data were evaluated by the Xcalibur software 2.7 SP1.

MS data processing and activity correlation analysis (AcorA)

The conversion of the ESI-FTICR-MS files to mzdata format were carried out by using ProteoWizard in both cases. Data were processed using XCMS for peakpicking and alignment. The software-package XCMS was implemented in R (version 2.10.0). The used parameter for the peakpicking and alignment are following for ESI-FTICR-MS: method='MSV', SNR.method= 'data.mean', winSize.noise=500, peakThr=80000, snthresh=3, amp.Th=0.005, scales=c(1,seq(7,9,3)); minsamp=2, mzppm=7. The data output effected as aligned data matrix. The results were viewed as Excel table.

For the identification of antibacterially active metabolites of *Albatrellus* spp. extracts were analyzed with the 'reverse metabolomics' approach using the AcorA technique. The activity correlation analysis (AcorA) represents a mathematical method for predicting those peaks resulting from spectroscopic or chromatographic investigations of complex crude extracts which are depicted potentially active compound of a corresponding extract.[40,41]

RESULTS AND DISCUSSION

The fungal extracts of *Albatrellus* species were investigated for their growth inhibitory effect against the Gram-positive bacterium *Bacillus subtilis* as well as the Gram-negative bacterium *Aliivibrio fischeri*. Therefore, fresh and dried fruiting bodies of *A. citrinus*, *A. cristatus*, *A. hirtus* (Schaeff.) Kotl. & Pouzar, *A. ovinus*, *A. subrubescens* and *A. ssp.* (Table S1) were extracted with ethyl acetate, methanol and hydrochloric acetone. Furthermore, extracts of the mycelial culture of *A. syringae* were analyzed. A fluorescence-based bioassay was used to determine the growth inhibition of *B. subtilis*. For the determination of the inhibitory properties against *Aliivibrio fischeri* a luminescence-based microtiter plate assay was utilized. The results of the antibacterial assays are given in Tables S3-S7. In general, all extracts have remarkable activities between 60 % to 100 % ($c_{extract}$ = 50 µg/mL) against *B. subtilis* (Tables S3-S4, Figure 4) whereas most of the analyzed extracts show an acute toxicity after 1 h less than 50 % ($c_{extract}$ = 50 µg/mL) against *Aliivibrio fischeri* (Tables S6-S7). Moreover, a reduction of the bacteria number after 24 h have not be observed with exception of few ethyl acetate extracts of *A. hirtus* (1, 2), *A. ovinus* (3, 4, 5), *A. subrubescens* (5), *A. ssp.* (1, 2) as well as hydrochloric acetone extracts of *A. ovinus* (2, 3) and *A. hirtus* (1) with moderate activities around 50 %. In many cases the extracts increase the bacterial luminescence (values > 100 %). This effect can be explained by metabolites which promote the bacterial vitality such as glycosides. A concentration-dependent activity of *Albatrellus* extracts against *B. subtilis* is obviously (Figure 4).
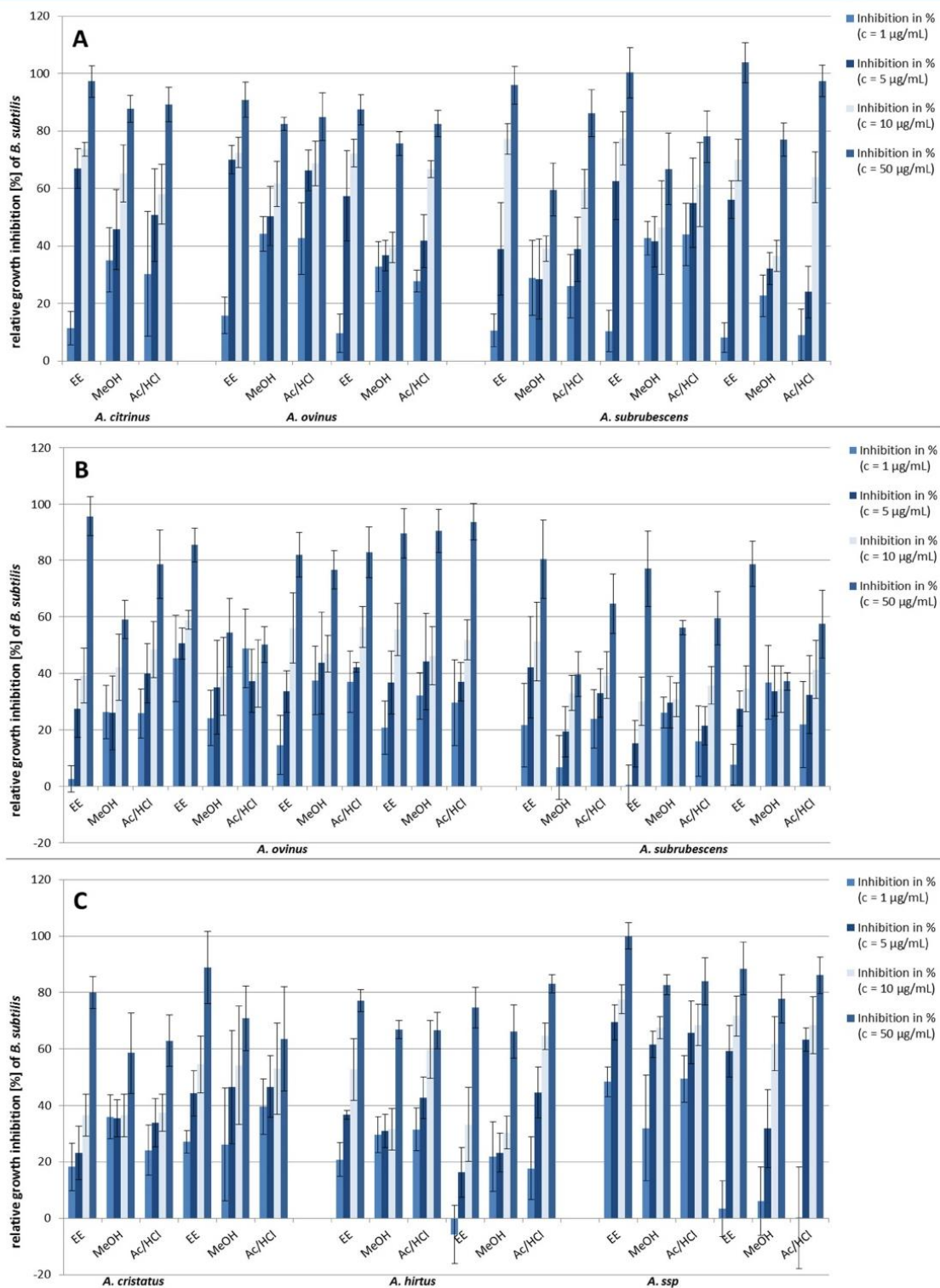
Figure 4. Biological activities (relative growth inhibition [%] of *Bacillus subtilis*) of the ethyl acetate (EE), methanol (MeOH), and hydrochloric acetone (Ac/HCl) extract aliquots of *Albatrellus* species **A**: extracts of fresh fruiting bodies; **B**: extracts of dried material from *A. ovinus* and *A. subrubescens*; **C**: extracts of dried fruiting bodies of *A. cristatus*, *A. hirtus* and *A. ssp*.in the concentrations of 1, 5, 10 and 50 µg/mL.

It should be noted that the activities of extracts derived from fresh material are slightly more active than those from dried fruiting bodies at the highest tested concentration of $c_{extract}$ = 50 µg/mL with a few exceptions like the activities of the extracts from *A. ssp.* The observed differences between the growth inhibitory potential of the analyzed extracts are larger at a concentration of $c_{extract}$ = 10 µg/mL. While the extracts of the fresh fungal fruiting bodies and from *A. ssp.* exhibit high activities between 60 % to 80 % growth inhibition, the extracts of the dried material show inhibitions between 30 % to 60 %. The results obtained by the *B. subtilis* assay were directly correlated with the MS-based metabolite profiles using the a new approach called 'reverse metabolomics'.[40,41] Therefore, the metabolite profiles of the *Albatrellus* extracts were determined in triplicate by UPLC/ESI-MS and ESI-FTICR-MS both in the positive and negative ion mode. After pre-processing the MS data were correlated with the bioactivities against *B. subtilis* for the concentrations $c_{extract}$ = 50 µg/mL. Based on this activity relevant peak clusters could be identified using an activity correlation analysis (AcorA). Table 2 shows the top-20 ranked peaks from the hit list of the negative ion ESI-FTICR-MS data out of 508 aligned peaks which exhibit a positive correlation with the bioactivity profiles against *B. subtilis* for $c_{extract}$ =50 µg/mL. Prenylated metabolites such as grifolin (**1**) and/or neogrifolin (**2**) at *m/z* 327.2332 ([M-H]⁻, calcd. *m/z* 327.2330 for $C_{22}H_{31}O_2^-$) correlate on rank 3 of the hit list together with its isotope peak at *m/z* 328.2365 with a correlation coefficient of 0.44. This result is in agreement to the literature (Table 1)[15,17,30,31] where both compounds are described as antibacterially active metabolites of *Albatrellus* species. A further prenylated compound at *m/z* 343.2279 ([M-H]⁻, calcd. *m/z* 343.2279 for $C_{22}H_{31}O_3^-$) showing a correlation on rank 2 (correlation coefficient of 0.46) probably corresponds to a hydroxylated neogrifolin (**9**) or grifolin. The high-resolution MS² data (Table 3 and S2) confirm the presence of a farnesyl side chain and the functional groups at the aromatic moiety.[42] Interestingly, a peak cluster of nitrogen-containing metabolites at *m/z* 424.2856 (**39**, [M-H]⁻, calcd. *m/z* 424.2857 for $C_{27}H_{38}NO_3^-$), *m/z* 438.3015 (**40**, [M-H]⁻, calcd. *m/z* 438.3014 for $C_{28}H_{40}NO_3^-$), *m/z* 472.2856 (**41**, [M-H]⁻, calcd. *m/z* 472.2857 for $C_{31}H_{38}NO_3^-$), *m/z* 500.3023 (**42**, [M-H]⁻, calcd. *m/z* 500.3018 for $C_{29}H_{42}NO_6^-$), *m/z* 514.3179 (**43**, [M-H]⁻, calcd. *m/z* 514.3174 for $C_{30}H_{44}NO_6^-$) and *m/z* 548.3019 (**44**, [M-H]⁻, calcd. *m/z* 548.3018 for $C_{33}H_{42}NO_6^-$) also correlates in the hit list. These

metabolites were further investigated with high-resolution tandem mass spectrometry. The characteristic fragment ions are listed in Table 3. Typical losses of a C_5- and a C_{10}-unit as well as the loss of the whole side chain (C_{14}-unit) forming a benzyl anion are characteristic for farnesylated aromatic compounds without modifications on the prenyl side chain. Losses of H_2O and CO are observable for phenolic compounds. Moreover, the nitrogen-containing metabolites fragment in the MS² mode under collision-induced dissociation (CID) to the key ions **a**, **b**, **c**, **d** and **e**. The nitrogen-free key ion **a** at *m/z* 353.212 (calcd. *m/z* 353.2122 for $C_{23}H_{29}O_3^-$) formally exhibits the same elemental composition as the [M-H-H_2O]⁻ ion of scutigeral (**3**). Therefore, the nitrogen-containing metabolites are probably structurally related to scutigeral (**3**). The other nitrogen-containing fragment ions **b** (*m/z* 312.160, calcd. *m/z* 312.1605 for $C_{19}H_{22}NO_3^-$), **c** (244.098, calcd. *m/z* 244.0979 for $C_{14}H_{14}NO_3^-$), **d** (*m/z* 230.082, calcd. *m/z* 230.0823 for $C_{13}H_{12}NO_3^-$), and **e** (*m/z* 178.051, calcd. *m/z* 178.0510 for $C_9H_8NO_3^-$) indicate that the nitrogen is connected to the aromatic moiety. In the MS² spectra of compounds **42**, **43** and **44** the loss of $C_2H_4O_3$ represents the dominant fragmentation. The MS³ spectra of the [M-H-$C_2H_4O_3$]⁻ of **42**, **43** and **44** are comparable with the MS² spectra of **39**, **40** and **41**. Hence, it is assumed that **42**, **43** and **44** represent glycolic acid adducts of **39**, **40** and **41**. Next to the compounds **39**-**44**, further a nitrogen-containing metabolite was detected. A further farnesylated compound at *m/z* 438.2647 ([M-H]⁻, calcd. *m/z* 438.2649 for $C_{27}H_{36}NO_4^-$) shows typical neutral losses of isoprene units as well as key ions **a**, **c**, **d** and **e**. The structural relationship is likely to the other nitrogen-containing metabolites. To our knowledge, except for the already mentioned pyrazine derivatives **34** and **35** nitrogen-containing compounds (**39**-**44** and **45**) are hitherto not described for *Albatrellus* species.

The hit list of the positive ion ESI-FTICR-MS data contains 64 and 92 out of 1846 aligned peaks exhibiting a positive correlation with the bioactivity profiles for $c_{extract}$ = 10 µg/mL and $c_{extract}$ = 50 µg/mL. In both cases clusters could be identified among the top-13 or top-10 ranked peaks which belong to prenylated compounds (Table S8 and S9). At *m/z* 395.2197 ([M+Na]⁺, calcd. *m/z* 395.2193 for $C_{23}H_{32}O_4Na^+$) correlates scutigeral (**3**) and/or grifolic acid (**13**) together with grifolin (**1**) and/or neogrifolin (**2**) at *m/z* 351.2296 ([M+Na]⁺, calcd. *m/z* 351.2193 for $C_{22}H_{32}O_2Na^+$) and probably hydroxylated neogrifolin (**9**) or grifolin at *m/z* 383.1986 ([M+K]⁺,

calcd. m/z 383.1983 for $C_{22}H_{32}O_3K^+$) and at m/z 367.2245 ([M+Na]$^+$, calcd. m/z 367.2244 for $C_{22}H_{32}O_3Na^+$). It could be shown that these compounds also correlate in the positive ion ESI-FTICR-MS data with the bioactivity profile of fresh fruiting bodies of *Albatrellus* species.[41]

Table 2. Hit list of the top-20 ranked peaks based on negative ion ESI-FTICR-MS data correlated with the antibacterial bioactivity profiles against *B. subtilis* of the *Albatrellus* extracts ($c_{extract}$ = 50 µg/mL).

Rank	Spearman correlation coefficient	[M-H]$^-$ (m/z)	elemental composition	DBE	Error [ppm]	possible compound
1	0.49	289.2173	$C_{19}H_{29}O_2^-$	5.5	0.01	Not determined
2	0.46	343.2279	$C_{22}H_{31}O_3^-$	7.5	0.3	Hydroxyneogrifolin (**9**)
3	0.44	327.2332	$C_{22}H_{31}O_2^-$	7.5	0.8	Grifolin(**1**)/Neogrifolin (**2**)
4	0.43	311.2229				Not determined
5	0.42	500.3023	$C_{29}H_{42}NO_6^-$	9.5	1.1	**42**
6	0.42	424.2856	$C_{27}H_{38}NO_3^-$	9.5		**39**
7	0.42	514.3179	$C_{30}H_{44}NO_6^-$	9.5	1.0	**43**
8	0.40	328.2365	$C_{21}{}^{13}C_1H_{31}O_2^-$			Isotope peak of m/z 327.2332
9	0.40	669.4545				Not determined
10	0.40	684.4362				Not determined
11	0.39	344.2312	$C_{21}{}^{13}C_1H_{31}O_3^-$			Isotope peak of m/z 343.2279
12	0.39	548.3019	$C_{33}H_{42}NO_6^-$	13.5	0.3	**44**
13	0.38	221.1549				Not determined
14	0.38	339.2336				Not determined
15	0.37	472.2856	$C_{31}H_{38}NO_3^-$	13.5	0.3	**41**
16	0.37	290.2206				Not determined
17	0.36	683.4326	$C_{44}H_{59}O_6^-$	15.5	1.3	Not determined
18	0.35	438.3015	$C_{28}H_{40}NO_3^-$	9.5	0.3	**40**
19	0.35	342.2155				Not determined
20	0.35	399.2179				Not determined

Table 3. Characteristic high resolution fragment ions of farnesylated and nitrogen-containing metabolites of *Albatrellus* extracts measured in the negative ion mode under electrospray ionization conditions.

	farnesylated compounds				nitrogen-containing compounds			
	MS^2 mode				MS^2 mode			
NCE [%]	45	35	40	45	45			
No.	**3**	**2**	**9**	**7/8**	**39**	**40**	**41**	**45**
RT [min]	13.79	12.06	12.10	15.02	12.56	14.01	13.54	13.43
Ion								
[M-H]$^-$	**371.2226** (C$_{23}$H$_{31}$O$_4^-$, 1.1)	**327.2340** (C$_{22}$H$_{31}$O$_2^-$, 3.2)	**343.2275** (C$_{22}$H$_{31}$O$_3^-$, 0.8)	**355.2272** (C$_{23}$H$_{31}$O$_3^-$, 1.9)	**424.2856** (C$_{27}$H$_{38}$NO$_3^-$, 0.2)	**438.3013** (C$_{28}$H$_{40}$NO$_3^-$, 0.3)	**472.2853** (C$_{31}$H$_{38}$NO$_3^-$, 0.8)	**438.2647** (C$_{27}$H$_{36}$NO$_4^-$, 0.6)
[M-H-H$_2$O]$^-$	353.2123 (0.4, C$_{23}$H$_{29}$O$_3^-$, 0.3)	309.2221 (22.7, C$_{22}$H$_{29}$O$^-$, 1.0)	325.2173 (3.4, C$_{22}$H$_{29}$O$_2^-$, 0.1)	337.2167 (1.5, C$_{23}$H$_{29}$O$_2^-$, 1.8)	406.2749 (28.2, C$_{27}$H$_{36}$NO$_2^-$, 0.7)	420.2905 (38.7, C$_{28}$H$_{38}$NO$_2^-$, 0.8)	454.2740 (17.0, C$_{31}$H$_{36}$NO$_2^-$, 2.6)	420.2541 (1.4, C$_{27}$H$_{34}$NO$_3^-$, 0.7)
[M-H-CO]$^-$	343.2280 (14.6, C$_{22}$H$_{31}$O$_3^-$, 0.3)	299.2378 (1.0, C$_{21}$H$_{31}$O$^-$, 0.8)	315.2329 (18.7, C$_{21}$H$_{31}$O$_2^-$, 0.2)	327.2325 (28.0, C$_{22}$H$_{31}$O$_2^-$, 1.3)	396.2904 (31.2, C$_{26}$H$_{38}$NO$_2^-$, 0.9)	410.3062 (30.5, C$_{27}$H$_{40}$NO$_2^-$, 0.7)	444.2903 (6.4, C$_{30}$H$_{38}$NO$_2^-$, 1.1)	410.2697 (27.6, C$_{26}$H$_{36}$NO$_3^-$, 1.0)
[M-H-C$_5$H$_9$]$^{\cdot-}$	302.1525 (24.3, C$_{18}$H$_{22}$O$_4^{\cdot-}$, 0.3)	258.1620 (1.3, C$_{17}$H$_{22}$O$_2^{\cdot-}$, 2.0)	274.1574 (24.8, C$_{17}$H$_{22}$O$_3^{\cdot-}$, 0.1)	286.1570 (4.2, C$_{18}$H$_{22}$O$_3^{\cdot-}$, 1.5)	355.2145 (31.4, C$_{22}$H$_{39}$NO$_3^{\cdot-}$, 2.1)	369.2302 (33.4, C$_{23}$H$_{31}$NO$_3^{\cdot-}$, 2.1)	403.2148 (7.7, C$_{26}$H$_{29}$NO$_3^{\cdot-}$, 1.2)	369.1935 (1.3, C$_{22}$H$_{27}$NO$_4^{\cdot-}$, 2.8)
[M-H-C$_{10}$H$_{17}$]$^{\cdot-}$	234.0898 (100.0, C$_{13}$H$_{14}$O$_4^{\cdot-}$, 0.2)	189.0921 (8.7, C$_{12}$H$_{13}$O$_2^-$, 0.1)	206.0949 (0.2, C$_{12}$H$_{14}$O$_3^{\cdot-}$, 0.4)	218.0948 (48.1, C$_{13}$H$_{14}$O$_3^{\cdot-}$, 0.3)	287.1526 (100.0, C$_{17}$H$_{21}$NO$_3^{\cdot-}$, 0.5)	301.1682 (85.0, C$_{18}$H$_{23}$NO$_3^{\cdot-}$, 0.5)	335.1526 (40.2, C$_{21}$H$_{21}$NO$_3^{\cdot-}$, 0.4)	301.1317 (35.2, C$_{17}$H$_{19}$NO$_4^{\cdot-}$, 0.9)
[M-H-C$_{14}$H$_{23}$]$^{\cdot-}$	180.0429 (52.5, C$_9$H$_8$O$_4^{\cdot-}$, 0.7)	135.0452 (100.0, C$_8$H$_7$O$_2^-$, 0.5)	152.0480 (100.0, C$_8$H$_8$O$_3^{\cdot-}$, 0.5)	164.0478 (100.0, C$_9$H$_8$O$_3^{\cdot-}$, 0.3)	233.1058 (71.5, C$_{13}$H$_{15}$NO$_3^{\cdot-}$, 0.2)	247.1214 (50.3, C$_{14}$H$_{17}$NO$_3^{\cdot-}$, 0.2)	281.1057 (13.4, C$_{17}$H$_{15}$NO$_3^{\cdot-}$, 0.1)	247.0850 (29.8, C$_{13}$H$_{13}$NO$_4^{\cdot-}$, 0.1)
a					353.2121 (54.5, C$_{23}$H$_{29}$O$_3^-$, 0.4)	353.2120 (100.0, C$_{23}$H$_{29}$O$_3^-$, 0.5)	353.2116 (44.2, C$_{23}$H$_{29}$O$_3^-$, 1.7)	353.2120 (2.7, C$_{23}$H$_{29}$O$_3^-$, 0.7)
b					312.1604 (62.0, C$_{19}$H$_{22}$NO$_3^-$, 0.5)	312.1604 (57.3, C$_{19}$H$_{22}$NO$_3^-$, 0.2)	312.1605 (52.9, C$_{19}$H$_{22}$NO$_3^-$, 0.1)	312.1239 (5.4, C$_{18}$H$_{18}$NO$_4^-$, 0.7)
c					244.0979 (46.7, C$_{14}$H$_{14}$NO$_3^-$, 0.3)	244.0979 (40.0, C$_{14}$H$_{14}$NO$_3^-$, 0.2)	244.0980 (19.5, C$_{14}$H$_{14}$NO$_3^-$, 0.3)	244.0979 (2.4, C$_{14}$H$_{14}$NO$_3^-$, 0.1)
d					230.0823 (53.2, C$_{13}$H$_{12}$NO$_3^-$, 0.1)	230.0823 (35.2, C$_{13}$H$_{12}$NO$_3^-$, 0.2)	230.0824 (11.3, C$_{13}$H$_{12}$NO$_3^-$, 0.4)	230.0821 (2.0, C$_{13}$H$_{12}$NO$_3^-$, 0.7)
e					178.0510 (29.7, C$_9$H$_8$NO$_3^-$, 0.3)	178.0511 (23.1, C$_9$H$_8$NO$_3^-$, 0.8)	n.d.	178.0511 (1.0, C$_9$H$_8$NO$_3^-$, 0.7)

(relative intensity [%], elemental composition, error [ppm])

In addition to the antibacterial bioassays the cell proliferation inhibitory activities against the human prostate cancer cell line PC3 and the colon cancer cell line were analyzed (Tables S10-S12). Figure 5 shows the activities of the most promising *Albatrellus* extracts. The ethyl acetate extracts of the fresh fruiting bodies of *A. citrinus* and *A. ovinus* (1 and 2) and dried material of *A. hirtus* as well as the hydrochloric acetone extracts of *A. ovinus* 1 and *A. ovinus* 2 inhibit the cell proliferation of PC3 cells in the range of 60 % to 80 % ($c_{extract}$ = 50 µg/mL). However, far less extracts have cell proliferation inhibitory effects on HT29 cells. The ethyl acetate

and hydrochloric acetone extracts of *A. hirtus* are the most active ones with inhibitions between 65 % and 75 %. The ethyl acetate extracts of *A. citrinus* (54.8 % cell proliferation inhibition) as well as *A. ovinus* 1 and *A. ovinus* 2 (ethyl acetate and hydrochloric acetone extracts) show a moderate activity in the cell proliferation of HT29 cells between 20 % and 40 %. On the other hand, negatively measured values in the cell proliferation assay of extracts of *A. cristatus* and *A. subrubescens* indicate a cell proliferation promoting effect of these extracts against the colon cancer cell line HT29.
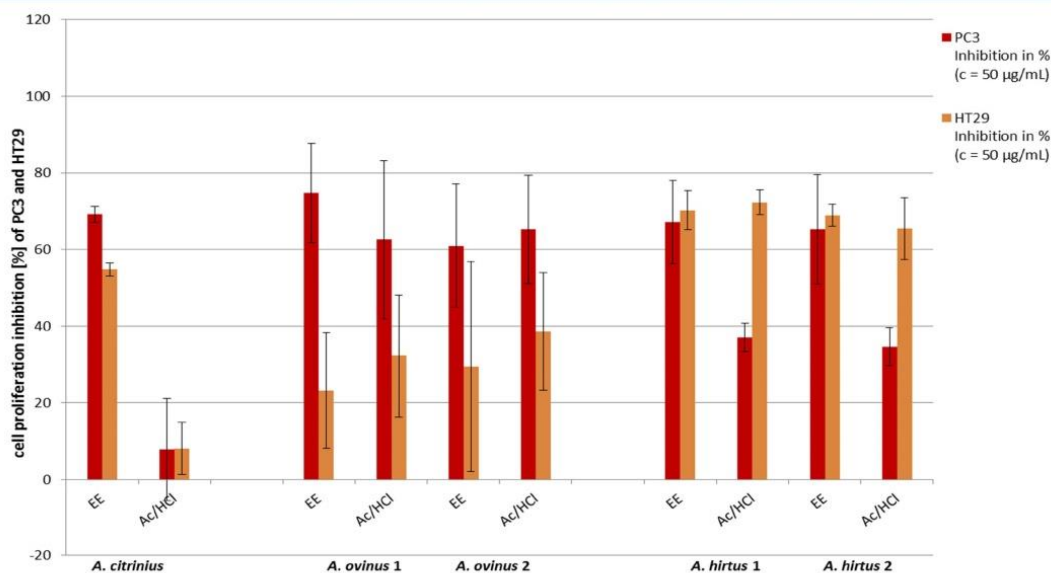
Figure 6. Biological activities (cell proliferation inhibition [%] of PC3 – red and HT29 – orange) of the ethyl acetate (EE) and hydrochloric acetone (Ac/HCl) extract aliquots of *A. citrinus, A. ovinus* 1 and 2 as well as *A. hirtus* 1 and 2 in the concentrations of 50 µg/mL.

Because of the exceptional position in terms of the ITS sequences *A. syringae* are considered separately. The ethyl acetate extract exhibits a significant antibacterial activity against *B. subtilis* (Table S5, Figure 6) as shown by a growth inhibition of 86.0 % at a concentration of 50 µg/mL, whereas the more polar methanol extract are only moderate active (43.1 % growth inhibition). However, the inhibitory properties of both ethyl acetate and methanol extracts are comparable at the tested concentration of 1, 5 and 10 µg/mL crude extract. The ethyl acetate extract shows only a low cytotoxic effect against the human prostate cancer cell line PC3 and the colon cancer cell line HT29 (PC3: 8.1 % cell proliferation inhibition; HT29: 23.4 % cell proliferation inhibition, Table S12, Figure 6). The methanolic extract shows a slightly cell proliferation

promoting effect. After reducing of the methanol extract to the aqueous phase by liquid-liquid extraction the extract were partitioned between ethyl acetate (LLEE) and water (LLW). Both fractions were also analyzed with respect to their antibacterial and antiproliferative activities. In contrast to the methanol extract, the so obtained ethyl acetate fraction shows an increase of the growth inhibition of *B. subtilis* in all tested concentration. Also the cell proliferation inhibitory effect of the PC3 (28.5 %) and HT29 (36.5 %) cells is increased. Otherwise, the antibacterial effect of the water fraction is slightly lower compared with the activity of the methanol extract, although the cytotoxicity is increased to 12.4 % (PC3) and 9.4 % (HT29) in the cell proliferation inhibition assay at a concentration at 50 µg/mL.

11
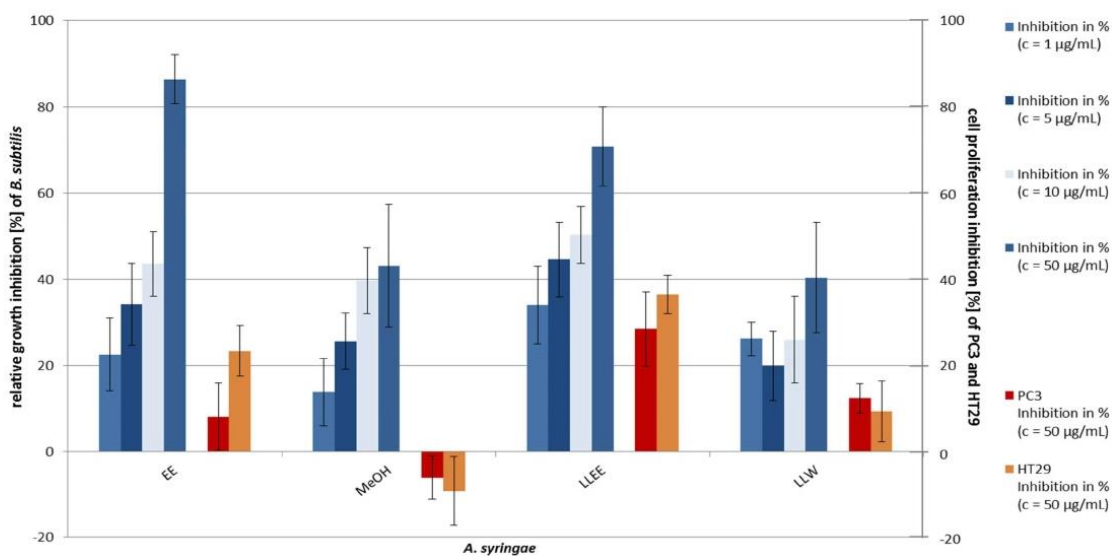
Figure 7. Antibacterial activities (relative growth inhibition [%] of *Bacillus subtilis* - blue) of the extract aliquots of *Albatrellus syringae* in the concentrations of 1, 5, 10 and 50 µg/mL and cell proliferation inhibitory effects in % (against PC3 – red and HT29 - orange) of those extract in the concentration of 50 µg/mL.

CONCLUSIONS

Crude extracts of *Albatrellus* species were investigated regarding their antibacterial activity against the Gram-positive bacterium *Bacillus subtilis* and Gram-negative bacterium *Aliivibrio fischeri*. The analyzed extracts remarkably inhibit the growth of *B. subtilis*, whereas the inhibitory potential of the *Albatrellus* extracts against *Aliivibrio fischeri* are only low to moderate. Also the used extraction solvents influenced the biological activity. Normally, the ethyl acetate and hydrochloric acetone extracts were more active than the methanolic ones. Furthermore, the cell proliferation inhibition was investigated. Thereby, the extracts of the fresh fruiting bodies of *A. citrinus* and *A. ovinus* and dried material of *A. hirtus* show the highest inhibitory effect on the human prostate cancer cell line PC3 and the colon cancer cell line HT29, whereas the extracts of *A. cristatus* and *A. subrubescens* promote the cell proliferation at a concentration of 50 µg/mL.

Using a new approach called 'reverse metabolomics' activity correlation analysis (AcorA) a number of possible antibacterially active metabolites like grifolin (**1**) and neogrifolin (**2**) were predicted. Furthermore, a new interesting group of nitrogen-containing (**39**-**44**) compounds correlates with the antibacterial activity against *B. subtilis*. Structural relationship of the nitrogen-containing metabolites (**39**-**44**) to scutigeral (**3**) can be assumed based on

fragmentation studies with high resolution ESI mass spectrometry (Table 3).

Moreover, extracts of the mycelial culture of *A. syringae* were tested. The lipophilicity of the extraction solvents are also relevant and influence the biological activity. The results show that the more lipophilic extracts exhibit higher antibacterial and antiproliferative properties than the more polar ones.

Extracts of *Albatrellus* species exhibit a highly significant activity against *B. subtilis* and also few extracts have cell proliferation inhibition. The new approach also demonstrates that hitherto structurally non-identified metabolites could be determined as bioactive compounds with high probability. However, these compounds have to be isolated to clarify both the structure and the antibacterial activity unambiguously.

12

REFERENCES

1. Gardes, M. & Bruns, T.D. (1996) Community structure of ectomycorrhizal fungi in a *Pinus muricata* forest: above- and below-ground views. *Can. J. Bot.* **74**, 1572–1583.

2. Greslebin, A., Nakasone, K.K. & Rajchenberg, M. (2004) Rhizochaete, a new genus of phanerochaetoid fungi. *Mycologia* **96**, 260–71.

3. Larsson, E. & Larsson, K.-H. (2003) Phylogenetic relationships of russuloid basidiomycetes with emphasis on aphyllophoralean taxa. *Mycologia* **95**, 1037–65.

4. Binder, M., Hibbett, D.S., Larsson, K.-H., Larsson, E., Langer, E. & Langer, G. (2005) The phylogenetic distribution of resupinate forms across the major clades of mushroom forming fungi (Homobasidiomycetes). *Syst. Biodivers.* **3**, 113–157.

5. Cui, B.K., Wang, Z. & Dai, Y.C. (2008) *Albatrellus piceiphilus* sp. nov. on the basis of morphological and molecular characters. *Fungal Divers.* **28**, 41-48.

6. Bruns, T.D., Szaro, T.M., Gardes, M., Cullings, K.W., Pan, J.J., Taylor, D.L., Horton, T.R., Kretzer, A., Garbelotto, M. & Liss, Y. (1998) A sequence database for the identification of ectomycorrhizal basidiomycetes by phylogenetic analysis. *Mol. Ecol.* **7**, 257–272.

7. Binder, M. & Hibbett, D.S. (2002) Higher-level phylogenetic relationships of Homo-basidiomycetes (mushroom-forming fungi) inferred from four rDNA regions. *Mol. Phylogenet. Evol.* **22**, 76–90.

8. Ryman, S., Fransson, P., Johannesson, H. & Danell, E. (2003) *Albatrellus citrinus* sp. nov., connected to *Picea abies* on lime rich soils. *Mycol. Res.* **107**, 1243–1246.

9. Hirata, Y. & Nakanishi, K. (1950) Grifolin, an antibiotic from a Basidiomycete. *J. Biol. Chem.* **184**, 135–143.

10. Goto, T., Kakisawa, H. & Hirata, Y. (1963) The structure of grifolin, an antibiotic from a basidiomycete. *Tetrahedron* **19**, 2079–2083.

11. Besl, H., Höfle, G., Jendrny, B., Jägers, E. & Steglich, W. (1977) Pilzpigmente, XXXI. Farnesylphenole aus *Albatrellus* Arten (Basidiomycetes). *Chem. Ber.* **110**, 3770–3776.

12. Vrkoč, J., Buděšinsky, M. & Dolejš, L. (1977) Phenolic from the Basidiomycete *Albatrellus ovinus*. *Phytochemistry* **16**, 1409–1411.

13. Nukata, M., Hashimoto, T., Yamamoto, I., Iwasaki, N., Tanakab, M. & Asakawa, Y. (2002) Neogrifolin derivatives possessing anti-oxidative activity from the mushroom *Albatrellus ovinus*. *Phytochemistry* **59**, 731–737.

14. Dekermendjian, K., Shan, R., Nielsen, M., Stadler, M., Sterner, O. & Witt, M.R. (1997) The affinity to the brain dopamine D1 receptor in vitro of triphenyl phenols isolated from the fruit bodies of *Albatrellus ovinus*. *Eur. J. Med. Chem.* **32**, 351-356.

15. Zechlin, L., Wolf, M., Steglich, W. & Anke, T. (1981) Cristatsäure, ein modifiziertes Farnesylphenol aus Fruchtkörpern von *Albatrellus cristatus*. *Liebigs Ann. Chem.* **12**, 2099–2105.

16. Zhang, A.-L., Xu, T., Gao, J.-M., Bai, M.-S., Zhang, G., Liu, H.-W., Li, S.-Q. & Konishi, Y. (2009) Chemical constituents from the fruiting bodies of the basidiomycete *Albatrellus* sp. *Heterocycles* **78**, 1807–1813.

17. Hashimoto, T., Quang, D.N., Nukada, M. & Asakawa, Y. (2005) Isolation, synthesis and biological activity of grifolic acid derivatives from the inedible mushroom *Albatrellus dispansus*. *Heterocycles* **65**, 2431–2439.

18. Quang, D. N. Hashimoto, T., Arakawa, Y., Kohchi, C., Nishizawa, T., Soma, G.-I. & Asakawa, Y. (2006) Grifolin derivatives from *Albatrellus caeruleoporus*, new inhibitors of nitric oxide production in RAW 264.7 cells. *Bioorg. Med. Chem.* **14**, 164–168.

19. Liu, L.-Y., Li, Z.-H., Wang, G.-Q., Wei, K. Dong, Z.-J., Feng, T., Li, G.-T., Li, Y. & Liu, J.-K. (2014) Nine new farnesylphenols from the Basidiomycete *Albatrellus caeruleoporus*. *Nat. Products Bioprospect.* **4**, 119–128.

20. Ikeda, M., Kanou, H. & Nukina, M. (1989) Plant growth inhibitors from fruit bodies of *Polyporus confluens*. *Bull. Yamagata Univ. Agric. Sci.* **10**, 849–852.

21. Misasa, H., Matsui, Y., Uehara, H., Tanaka, H., Ishihara, M. & Shibata, H. (1992) Tyrosinase inhibitors from *Albatrellus confluens*. *Biosci. Biotech. Biochem.* **56**, 1660–1661.

22. Szallasi, A., Bíró, T., Szabó, T., Modarres, S., Petersen, M., Klusch, A., Blumberg, P. M., Krause, J. E. & Sterner, O. (1999) A non-pungent triprenyl phenol of fungal origin, scutigeral, stimulates rat dorsal root ganglion neurons via interaction at vanilloid receptors. *Brit. J. Pharmacol.* **126**, 1351–1358.

23. Hellwig, V., Nopper, R., Mauler, F., Freitag, J., Ji-Kai, L., Zhi-Hui, D. & Stadler, M. (2003) Activities of prenylphenol derivatives from fruitbodies of *Albatrellus* spp. on the human and rat vanilloid receptor 1 (VR1) and characterisation of the novel natural product, confluentin. *Arch. Pharm. Pharm. Med. Chem.* **2**, 119–126.

24. Yang, X.-L., Qin, C., Wang, F., Dong, Z.-J. & Ji-Kai, L. (2008) A new meroterpenoid pigment from the Basidiomycete *Albatrellus confluens*. *Chem. Biodivers.* **5**, 484–489.

13

25. Ye, M., Liu, J., Lu, Z., Zhao, Y., Liu, S., Li, L., Tan, M., Weng, X., Li, W. & Cao, Y. (2005) Grifolin, a potential antitumor natural product from the mushroom *Albatrellus confluens*, inhibits tumor cell growth by inducing apoptosis in vitro. *FEBS Lett.* **579**, 3437–3443.

26. Luo, X., Li, L., Deng, Q., Yu, X., Yang, L., Luo, F., Xiao, L., Chen, X., Ye, M., Liu, J. & Cao, Y. (2011) Grifolin, a potent antitumour natural product upregulates death-associated protein kinase 1 DAPK1 via p53 in nasopharyngeal carcinoma cells. *Eur. J. Cancer* **47**, 316–325.

27. Ye, M., Luo, X., Li, L., Shi, Y., Tan, M., Weng, X., Li, W., Liu, J. & Cao, Y. (2007) Grifolin, a potential antitumor natural product from the mushroom *Albatrellus confluens*, induces cell-cycle arrest in G1 phase via the ERK1/2 pathway. *Cancer Lett.* **258**, 199–207.

28. Jin, S., Pang, R.-P., Shen, J.-N., Huang, G., Wang, J. & Zhou, J.-G. (2007) Grifolin induces apoptosis via inhibition of PI3K/AKT signalling pathway in human osteosarcoma cells. *Apoptosis* **12**, 1317–1326.

29. Sugiyama, K., Tanaka, A., Kawagishi, H., Ojima, F., Sakamoto, H. & Ishiguro, Y. (1994) Hypocholesterolemic action of dietary grifolin on rats fed with a high-cholesterol diet. *Biosci. Biotech. Biochem.* **58**, 211–212.

30. Tokuyama, S., Horikawa, M., Morita, T., Hashimoto, T., Quang, D.N., Asakawa, Y. & Kawagishi, H. (2007) Anti-MRSA and antifungal compounds from the mushroom *Albatrellus dispansus* (Lloyd) Canf. et Gilb. (Aphyllophoromycetideae). *Int. J. Med. Mushrooms* **9**, 159–161.

31. Liu, X., Winkler, A.L., Schwan, W.R., Volk, T.J., Rott, M.A. & Monte, A. (2010) Antibacterial compounds from mushrooms I: A lanostane-type triterpene and prenylphenol derivatives from *Jahnoporus hirtus* and *Albatrellus flettii* and their activities against *Bacillus cereus* and *Enterococcus faecalis*. *Planta Med.* **76**, 182–185.

32. Takamatsu, S., Rho, M.-C., Masuma, R., Hayashi, M., Komiyama, K., Tanaka, H. & Omura, S. (1994) A novel testosterone 5α-reductase inhibitor, 8′,9′-dehydroascocholin produced by *Verticillium* sp. FO-2787. *Chem. Pharm. Bull.* **42**, 953–956.

33. Guo, H., Feng, T., Li, Z.-H. & Liu, J.-K. (2013) Ten new aurovertins from cultures of the basidiomycete *Albatrellus confluens*. *Nat. Products Bioprospect.* **3**, 8–13.

34. Zhi-Hui, D., Ze-Jun, D. & Ji-Kai, L. (2001) Albaconol, a novel prenylated resorcinol (= benzene-1,3-diol) from Basidiomycetes *Albatrellus confluens*. *Helv. Chim. Acta* **84**, 259-262.

35. Kawagishi, H., Tanaka, A., Sugiyama, K., Mri, H., Sakamoto, H., Ishiguro, Y., Kobayashi, K. & Uramato, M. (1996) A pyradine-derivative from the mushroom *Albatrellus confluens*. *Phytochemistry* **42**, 547–548.

36. Zhou, Z.-Y., Liu, R., Jiang, M-Y., Zhang, L., Niu, Y., Zhu, Y.-C., Dong, Z.-J. & Liu, J.-K. (2009) Two new cleistanthane diterpenes and a new isocoumarine from cultures of the basidiomycete Albatrellus confluens. *Chem. Pharm. Bull.* **57**, 975–978.

37. Quang, D. N., Hashimoto, T. & Asakawa, Y. (2006) Inedible mushrooms: A good source of biologically active substances. *Chem. Rec.* **6**, 79-99.

38. Moser, M. (1958) Die künstliche Mykorrhiza-Impfung an Forstpflanzen. 1. Erfahrungen bei der Reinkultur von Mykorrhizapilzen. *Forstwiss. Centralbl.* **77**, 32–40.

39. Veening, J., Smits, W.K., Leendert, W., Jongbloed, J.D.H. & Kuipers, O.P. (2004) Visualization of differential gene expression by improved cyan fluorescent protein and yellow fluorescent protein production in *Bacillus subtilis*. *Appl. Environ. Microbiol.* **70**, 6809–6815.

40. Michels, K. (2011) Entwicklung einer LC-MS basierten Methode zur Identifizierung von aktivitätsrelevanten Metaboliten in komplexen Mischungen. Disseration Martin-Luther University Halle-Wittenberg.

41. Michels, K., Haid, M., Gohr, A., Heinke, R., Schmidt, J., Arnold, N., Wessjohann, L. Reverse metabolomics – a correlation approach for the direct identification of active compounds in complex mixtures. **unpublished**.

42. Heinke, R., Arnold, N., Wessjohann, L. & Schmidt, J. (2013) Negative ion tandem mass spectrometry of prenylated fungal metabolites and their derivatives. *Anal. Bioanal. Chem.* **405**, 177-189.

14

7.   General discussion

Prenylated natural products are widely distributed in organisms such as plants, microorganisms and fungi. Prenylated secondary metabolites often exhibit biological activities different from their non-prenylated parent compounds. The present thesis is focused both to the identification of known and/or unknown bioactive prenylated compounds in complex mixtures derived from crude fungal extracts and metabolites being relevant as potential biomarkers in fungal species.

The fragmentation behavior of several prenylated plant and fungal metabolites and their derivatives were analyzed by liquid chromatography (LC)/electrospray tandem mass spectrometry (ESI-MS^n) in the positive and negative ion mode as a presumption for the identification / characterization of prenylated compounds in complex crude extracts. In case of furanocoumarins from Yemenite *Dorstenia* species it could be shown that not only a differentiation of the furanocoumarin skeleton (linear or angular) but also the determination of the type of prenylation (*O*- and *C*-prenylated or reverse *C*-prenylated) is possible.[153] Even the position of substitution (C-3 or C-8) can be characterized by MS/MS measurements using both an ion trap and triple quadrupole system under positive ion ESI conditions. While the MS^2 spectra of linear furanocoumarins (type **I** and **II**) display only a few specific key fragments, the angular ones (type **III**) exhibit a stronger fragmentation. Linear *C*-prenylated furanocoumarins and oxygenated *C*-prenylated furanocoumarins (type **IIa**) show a significant loss of C_4H_8 leading to a key ion of type **a**. An additional **b**-type ion corresponding to $[M+H-C_3H_6]^+$ ion can be observed in the MS^2 spectra of reverse *C*-prenylated coumarins. A ratio of the relative abundance [**b**]/[**a**] of greater than 0.5 seems to be a good indication for the presence of a reverse *C*-prenylation. Further MS^3 investigations of the **a**-type ion allow a differentiation of the position of a *C*-prenyl side chain. If the isoprenyl group is located at C-3, the abundance of the ion [**a**-$^•$CH$_3$] is larger than that of [**a**-CO]. In case of a substitution at C-8, the relation is inversely. The fragmentation of oxyprenylated furanocoumarin (type **IIb**) is dominated by a neutral loss of the complete isoprene unit (C_5H_8). Type **IIc** furanocoumarins with *C*- and *O*-prenylation display a similar fragmentation behavior as type **IIa** and **IIb** coumarins. All these results can be applied to the investigation of plant extracts of furanocoumarin-containing species.

Farnesylated and geranylgeranylated fungal metabolites show a typical MS/MS fragmentation pattern in the negative ion mode under ESI conditions. Both prenylated phenols and benzoquinones exhibit a characteristic fragmentation behavior. Typical successive losses of the isoprene units allow the identification of the chain length, whereas the loss of the complete isoprenoid side chain leading to an ion representing the benzyl moiety gives information about

the substitution pattern of the aromatic ring system. Consequently, losses of C_5H_9 (69 Da) or C_5H_8 (68 Da) can be observed, whereas the last fragmentation step is characterized by a loss of a C_4 unit forming a benzyl type anion. In case of prenylated benzoquinones, a characteristic radical anion at *m/z* 152 appears. Furthermore, the linear boviquinone-4 and the structurally related cyclic tridentoquinone show a quite different fragmentation pattern. In contrast to the other prenylated compounds, tridentoquinone exhibits a dominant loss of water, and successive losses of CO and CO_2. Moreover, the fragmentation behavior of the prenylated fungal metabolites was also analyzed in the positive ion mode (unpublished data). The mass spectral decomposition of benzoquinones is characterized by a dominant loss of water. The formation of a benzyl cation at *m/z* 155 could be detected with a relative abundance of 10%. The farnesylated phenols scutigeral ([M+H]$^+$, *m/z* 373) and neogrifolin ([M+H]$^+$, *m/z* 329) are characterized by the loss of the whole isoprenoid side chain leading to benzyl cations at *m/z* 181 and *m/z* 137 in the MS^2 spectra. The benzyl cations are further decomposed in the MS^3 by a dominant loss of H_2O. The results obtained by electrospray tandem mass spectrometry in the positive ion mode are different from those in the negative one. The typical consecutive losses of the isoprene units could not be observed in the positive ion mode under electrospray ionization conditions.

The results discussed both in Chapters 2 and 3 demonstrate that the combination of LC and ESI-MS^n represents a valuable tool for structural characterization and investigation of such prenylated metabolites. The derived fragmentation rules form the basis for the characterization of prenylated compounds from Basidiomycetes such as *Suillus* and *Albatrellus* species. Further investigations combine mass spectrometry and multivariate data analysis (MDA).

The metabolite profiles of fruiting bodies and mycelial cultures of four *Suillus* species were analyzed by ESI-FTICR-MS and UPLC/ESI-MS/MS. The possibility of classification of such extracts via principal component analysis (PCA), hierarchical cluster analysis (HCA) and orthogonal partial least square (OPLS) was demonstrated. Both PCA and HCA allow a visual separation of the analyzed *Suillus* species. Known and structurally related unknown prenylated compounds as well as oxygenated unsaturated C_{18} fatty acids could be identified using high resolution MS and MS/MS data. Moreover, OPLS-DA two class models show a clear differentiation of two compared *Suillus* species or different *Suillus* samples according to their biological origin (fruiting bodies or mycelial culture). Furthermore, based on S-plots and loading plots statistically significant biomarkers for some species could be identified, e.g. amitenone for *S. bovinus* and tridentoquinone for *S. tridentinus*. MS-based metabolite profiling and fingerprinting represent useful tools not only for classification of different species, but also to

distinghish various biological samples (fruiting bodies or mycelial culture), to find biomarkers or to characterize fungal extracts (Chapter 4).

Based on a combination of informatics, MS-based metabolite profiling and biological screening a new method called 'reverse metabolomics' allows a direct identification of antibacterially active prenylated metabolites in crude extracts without further isolation and purification steps. This approach using an activity-correlation-analysis ('AcorA') connects the analysis of mass spectral metabolite profiles with the antibacterial activity of *Albatrellus* extracts. The metabolite profiles were determined by two different MS methods (UPLC/ESI-MS/MS and ESI-FTICR-MS) in both negative and positive ion mode (low and high resolution mass spectrometry). A *Bacillus subtilis* growth inhibition assay was used for the determination of the bioactivity profiles. AcorA generates a hit list with predicted activity-relevant metabolites. The established fragmentation rules of the various prenylated compounds represent the basis for the identification / characterization of known and/or unknown prenylated metabolites. Chapter 5 presents the novel method and the results obtained by the investigations of *Albatrellus* extracts. In the course of this approach scutigeral and other prenylated compounds could be identified as possible antibacterial active-relevant prenylated metabolites. Scutigeral exhibiting an IC_{50} value of 2 µg/mL was identified by comparing the UPLC/ESI-MS/MS data from the crude *Albatrellus* extract with corresponding reference compound. Furthermore, the structurally related prenylated compounds exhibiting [M-H]$^-$ ions at *m/z* 343 and *m/z* 355 contain one formyl function or one hydroxyl group less than scutigeral at the aromatic moiety. Such clusters could indicate possible structure-activity relationships which have to be proved by further investigations. In a more detailed and comprehensive study of *Albatrellus* extracts, also farnesylated metabiltes such as grifolin, neogrifolin and scutigeral correlate with the antibacterial activity against *B. subtilis*. Interestingly, a peak cluster of nitrogen-containing compounds at *m/z* 424.2856 ([M-H]$^-$, calcd. *m/z* 424.2857 for $C_{27}H_{38}NO_3^-$), *m/z* 438.3015 ([M-H]$^-$, calcd. *m/z* 438.3014 for $C_{28}H_{40}NO_3^-$), *m/z* 472.2856 ([M-H]$^-$, calcd. *m/z* 472.2857 for $C_{31}H_{38}NO_3^-$), *m/z* 500.3023 ([M-H]$^-$, calcd. *m/z* 500.3018 for $C_{29}H_{42}NO_6^-$), *m/z* 514.3179 ([M-H]$^-$, calcd. *m/z* 514.3174 for $C_{30}H_{44}NO_6^-$) and *m/z* 548.3019 ([M-H]$^-$, calcd. *m/z* 548.3018 for $C_{33}H_{42}NO_6^-$) correlates in the hit list, too. Based on detailed fragmentation studies with high resolution ESI mass spectrometry on an Orbitrap system, a structural relationship between the nitrogen-containing metabolites and scutigeral can be assumed. Because of the characteristic losses of C_5-, C_{10}- and C_{14}-units forming a benzyl anion this metabolites could be farnesylated aromatic compounds without modifications on the prenyl side chain. Further losses of H_2O and CO justify a phenolic moiety. Next to the growth inhibitory effects of *Albatrellus* extracts against the Gram-positive bacterium *B. subtilis* also the antibacterial properties against the Gram-negative bacterium *Aliivibrio fischeri* were analyzed.

The analyzed extracts show remarkably inhibition effects of the growth of *B. subtilis,* whereas the inhibitory potential of the *Albatrellus* extracts against *Aliivibrio fischeri* are only low to moderate. Furthermore, the cell proliferation effects were investigated. The extracts of dried material of *A. hirtus* and of fresh fruiting bodies of *A. citrinus* and *A. ovinus* exhibit the highest inhibitory potential on the human prostate cancer cell line PC3 and the colon cancer cell line HT29. In contrast to that, the extracts of *A. cristatus* and *A. subrubescens* promote the cell proliferation at a concentration of 50 µg/mL.

The 'reverse metabolomics' approach was also applied to identify antibacterial metabolites in *Suillus* species. Therefore, the biological activity of the *Suillus* extracts used in Chapter 4 were analyzed with the *Bacillus subtilis* assay as described in Chapters 5 and 6 (unpublished data, 11.2.6). The *Suillus* extracts show less antibacterial activities than the *Albatrellus* extracts. For growth inhibition effects between 70% and 95% of the fruiting body extracts from *Suillus* species a concentration of 100 µg/mL MeOH is necessary, whereas a concentration of 50 µg/mL MeOH of *Albatrellus* extracts are sufficient for comparable effects (growth inhibition between 60% and 100%). In comparison to fruiting bodies, the mycelial cultures of *Suillus* species exhibit lower activities, with exception of the extract of *S. tridentinus*. For the AcorA procedure the metabolite profiles of the fruiting bodies were correlated with their antibacterial activities. The hit list of the negative ion ESI-FTICR-MS data contains 28 out of 268 aligned peaks (*m/z* range 100 to 1000). Of particular note was that the correlated peaks mainly occuring in the *S. tridentinus* extracts show lower correlation coefficient values (0.47 – 0.58) than in the AcorA hit lists of *Albatrellus* species. Two metabolites with a correlation coefficient of 0.49 can be classified as prenylated compounds (see Table S5 of Chapter 11.2.6). Their molecular formulas $C_{26}H_{34}O_4$ and $C_{26}H_{34}O_5$ were determined by ESI-FTICR-MS as *m/z* 409.2384 [M-H]$^-$ (calc. 409.3384 for $C_{26}H_{33}O_4^-$) and [M-H]$^-$ (calc. 425.2333 for $C_{26}H_{33}O_5^-$). The IC$_{50}$ value of *S. tridentinus* is ten to twenty times higher than the IC$_{50}$ value of scutigeral (2 µg/mL). AcorA investigations of *S. bovinus* extracts from both fruiting bodies and mycelial cultures lead to the identification of oxygenated unsaturated C_{18} fatty acids. 9-Oxo-10*E*,12*Z*-octadecadienoic acid (9-oxo-ODE, *m/z* 293.2122 [M-H]$^-$ (calc. 293.2122 for $C_{18}H_{29}O_3^-$) and 9,10,13-trihydroxy-11*E*-octadecenoic acid (9,10,13-11*E*-THOD, *m/z* 329.2334 [M-H]$^-$ (calc. 329.2333 for $C_{18}H_{33}O_5^-$) appear on rank three and four of the hit list (52 hits out of 914 aligned peaks, see Table S6 of Chapter 11.2.6). Moreover, further extracts of fruiting bodies and mycelial cultures were investigated and their antibacterial properties against the Gram-positive bacterium *Bacillus subtilis* were analyzed (unpublished data, 11.2.6).

In the thesis mass spectrometry was used as analytical method to investigate fragmentation patterns of prenylated metabolites. In further studies MS-based metabolomics and 'reverse

metabolomics' approaches were combined with bioinformatics tools to answer different biological questions. Based on previous fragmentation studies it was possible to identify known and/or unknown prenylated metabolites. In summary, the results of the thesis demonstrate not only the importance of interdisciplinary projects in natural product research, but also the potential of mass spectrometry and bioinformatics for the classification of species as well as for the identification of bioactive metabolites and biomarkers.

8.   Summary

This thesis is an interdisciplinary work combining analytical chemistry, biological activity testing and chemoinformatics. Firstly, fragmentation patterns for the identification/characterization of prenylated compounds were established using both positive and negative ion electrospray ionization mass spectrometry (ESI-MS). Secondly, MS-based metabolite profiling und fingerprinting investigations of *Suillus* species and multivariate data analysis (MDA) show the importance of simplifying and visualizing complex data to answer biological questions like classification of biological samples, the influence of geographical origins, and the identification of potential biomarkers. Thirdly, with the involvement of biological screening methods, informatic approaches such as activity correlation analysis (AcorA) allow the prediction of potentially bioactive-relevant compounds in complex mixtures like crude extracts without prior isolation. It could be shown, that mass spectrometry and detailed fragmentation studies as well as mass spectral data of reference compounds enable the identification of prenylated and nitrogen-containing natural products in biological samples.

9.   Zusammenfassung

Die in der vorliegenden Arbeit dargestellten Ergebnisse zur Metabolitenanalyse in verschiedene Makromyzeten basieren auf der Kombination von massenspektrometrischen Untersuchungen, biologischem Screening und Informatik. Als Voraussetzung für die Identifizierung/Charakterisierung wurden Fragmentierungsmuster prenylierter Verbindungen mittels Elektrospray-Tandemmassenspektrometrie im positiven und im negativen Ionenmodus analysiert. Die MS-basierten „Metabolomics"-Untersuchungen (Metaboliten-Profiling und „Fingerprinting") von *Suillus*-Extrakten und die Verwendung von multivariate Datenanalysen zeigen, dass die Vereinfachung und Visualisierung von komplexen Daten zur Beantwortung unterschiedlicher biologischer Fragestellungen von großer Bedeutung sind. Die präsentierten Resultate belegen, das nicht nur eine Klassifizierung von Arten und Unterscheidung von biologischen Proben möglich ist, sondern auch der Einfluss der geographischer Herkunft bestimmt und potenzielle Biomarker identifiziert werden können. Darüber hinaus konnte gezeigt werden, dass MS-basierte Metabolitenprofile und Bioaktivitäten aus biologischem Screening mit Hilfe von bioinformatische Ansätze wie der Aktivitätskorrelationsanalyse (AcorA) korreliert werden können und eine Vorhersage aktivitätsrelevanter Metaboliten in komplexen Gemischen ohne vorherige Reinigung und Isolierung erlauben. Umfangreichen massenspektrometrischen Fragmentierungsstudien und Daten der Referenzsubstanzen dienen als Grundlage für die Identifizierung von prenylierten und stickstoffhaltigen Metaboliten in biologischen Proben.

10. Outlook

On the basis of the presented results of this thesis future, efforts should include more classes of secondary fungal metabolites. The obtained spectral data including fragmentation studies can be a good basis for building up a reference database which allows a direct identification of natural product classes and/or facilitate the characterization of hitherto unknown compounds. Moreover, classical metabolomics approaches can be combined with new techniques like 'reverse metabolomics' which also includes biological screening and correlation analysis. For example, next to scutigeral other prenylated compounds predicted and identified with an antibacterial activity should be isolated from *Albatrellus* species to prove the biological activity and possible structure-activity relationships. Furthermore, in the field of metabolite profiling more species from different genera should be analyzed to identify those metabolites which are characteristic for a genus and can be assigned as biomarkers for a species. Additionally, it has to be proved if undetermined fungal fruiting bodies can be specified using only MS-based MDA.

11. Appendix

11.1 List of Figures and Tables

11.2   Supplementary material of publications

11.2.1   Analysis of furanocoumarins from Yemenite *Dorstenia* species by liquid chromatography/electrospray tandem mass spectrometry

This Supporting Information shows the results of mass spectral behavior of the furanocoumarins under positive ion electrospray conditions using a triple quatrupol system. The selected collision energies are given in Tables S1-S5. Table S1 contains the mass spectral data of the non-prenylated furanocoumarins (type I). Tables S2-S4 give an overview of the (+)-ESI-CID mass spectral data of the prenylated linear furanocoumarins of type IIa, IIb and IIc. Table S5 shows the (+)-ESI-CID-MS^2 data of the analyzed angular furanocoumarins (type III).

11.2.2 Negative ion electrospray tandem mass spectrometry of prenylated fungal metabolites and their derivatives

This Supporting Information shows the results of high resolution MS measurements under negative ion electrospray conditions using a LTQ Orbitrap system. Table S1 contains the negative ion ESI-MS^n data of the analyzed prenylated benzoquinones and Table S2 shows the negative ion ESI-MS^n data of the prenylated phenols.

11.2.3   Metabolite profiling and fingerprinting of *Suillus* species (Basidiomycetes) by electrospray mass spectrometry

This Supporting Information illustrates used biological samples and additional results of the principal component analysis (PCA) of fruiting bodies and mycelial culture. In Tables S1 an overview of specimens (collected fruiting bodies) is given used in the MS-based investigations of the metabolite profiles. Figure S1 shows the PCA Score Plots of PC1 and PC2 scores derived from UPLC/ negative ion MS data of fruiting bodies and mycelial cultures (**A**) of *Suillus bovinus*; (**B**) of *Suillus granulatus*; (**C**) of *Suillus variegatus*.

11.2.4   Reverse metabolomics – a correlation approach for the direct identification of active compounds in complex mixture

Katharina Michels, Mark Haid, André Gohr, Ramona Heinke, Jürgen Schmidt, Norbert Arnold, Ludger Wessjohann
Unpublished

This Supporting Information illustrates used biological samples, modification methods and additional results of activity and metabolite determinations in more detail. The Figures S-1 and S-2 show the results of the growth inhibition assay against *Bacillus subtilis*. In Tables S-1 and S-2 an overview of specimens is given used in the different investigations. Table S-3 showed the experimental set up of spiking the crude fungal extracts with different antibiotic mixtures and the corresponding relative growth inhibition (%) of *Bacillus subtilis*. In Table S-4 and S-6 are presented modification procedures to generate different extract aliquots of variants from *Hygrophorus* species. Tables S-5 and S-7 contain LC/ESI-MS^n data of identified metabolites of *Albatrellus* und *Hygrophorus* species.
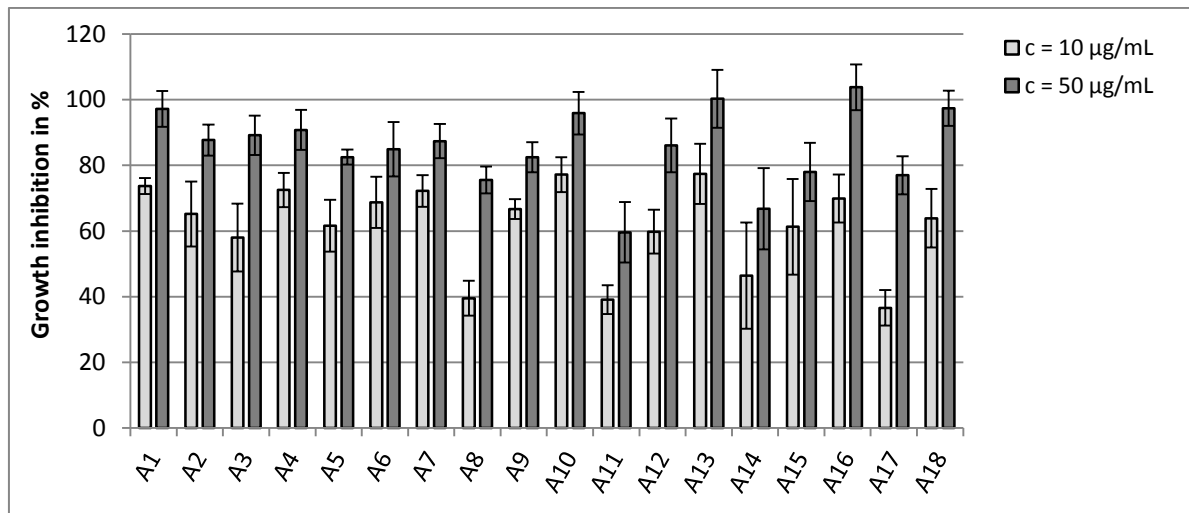
Figure S-1. Biological activities (relative growth inhibition [%] of *Bacillus subtilis*) of the ethylacetate, methanol and hydrochloric acetone extract aliquots of *Albatrellus* species $c_{extract}$ = 10 µg/mL (light grey) and $c_{extract}$ = 50 µg/mL (dark grey).
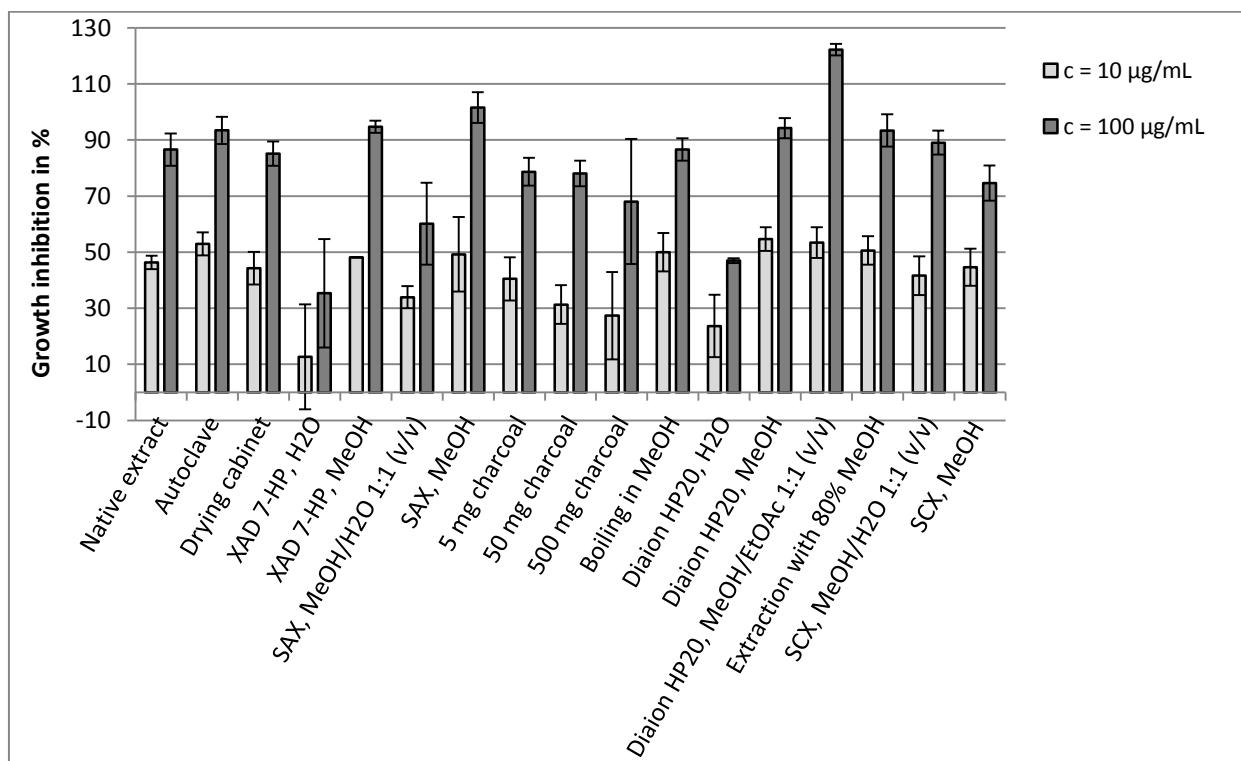
Figure S-2. Biological activities (relative growth inhibition of *Bacillus subtilis*) of the modified extract aliquots of *Hygrophorus latitabundus*.

Table S-1. Investigated *Hygrophorus* species with collection number, location, date, collector, kind of extraction, and extract No.

Fungal species	Collection	Location	Date	Collected and determined	Extraction	Extract No.
H. lucorum Kalchbr.	63/07 (fz)	near Freyburg, Saxony-Anhalt, Germany	10/30/07	Arnold	80% MeOH	H1
H. chrysodon (Batsch) Fr.	130/94 (fd)	near Uffenheim, Bavaria, Germany	09/26/94	Arnold	80% MeOH	H2
H. agathosmus (Fr.) Fr.	72/00 (fz)	near Ingolstadt, Bavaria, Germany	10/06/00	Arnold	100% EtOAc	H3
H. pustulatus (Pers.) Fr.	46/03 (fd)	near Neudorf, Saxony-Anhalt, Germany	11/25/03	Arnold	100% MeOH	H4
H. olivaceoalbus (Fr.) Fr.	Methanolic extract	Smaland, Sweden	09/17-24/07	Arnold	100% MeOH	H5
H. latitabundus Britzelm.	87/02 (fd)	near Bad Bibra, Saxony-Anhalt, Germany	11/13/02	Arnold		H6

fz, frozen collection; fd, freeze-dried collection

Table S-2. Investigated *Albatrellus* species with collection number, location, date, collector, kind of extraction, and extract No.

Fungal species	Collection	Location	Date	Collected and determined	Extraction	Extract No.
A. citrinus Ryman	7/11 (fr)	near Munich, Bavaria, Germany	09/19/11	-	100% EtOAc	A1
					100% MeOH	A2
					100% Ac/HCl	A3
A. ovinus (Schaeff.) Kotl. & Pouzar	63/11 (fr)	Pupplinger Au, Bavaria, Germany	10/22/11	Arnold	100% EtOAc	A4
					100% MeOH	A5
					100% Ac/HCl	A6
	64/11 (fr)	Pupplinger Au, Bavaria, Germany	10/22/11	Arnold	100% EtOAc	A7
					100% MeOH	A8
					100% Ac/HCl	A9
A. ovinus (Schaeff.) Kotl. & Pouzar / *subrubescens* (Murrill) Pouzar	66/11 (fr)	Oberbernbacher Wald, Bavaria, Germany	10/22/11	Arnold	100% EtOAc	A10
					100% MeOH	A11
					100% Ac/HCl	A12
	95/11 (fr)	Oberbernbacher Wald, Bavaria, Germany	11/23/11	Arnold	100% EtOAc	A13
					100% MeOH	A14
					100% Ac/HCl	A15
A. subrubescens (Murrill) Pouzar	28/10 (fr)	Pupplinger Au, Bavaria, Germany	10/03/10	Arnold	100% EtOAc	A16
					100% MeOH	A17
					100% Ac/HCl	A18

fr, fresh collection

Table S-3. Experimental set up of spiking the crude fungal extracts with different antibiotic mixtures and the corresponding relative growth inhibition (%) of *Bacillus subtilis* ($c_{extract}$ = 10 µg/mL).

Antibiotic mixture No.	c [µM in MeOH]			Combination with extract No.	Growth inhibition +/- s.d. [%]
	Amoxicillin	Erythromycin	Rifampicin		
1	10^{-2}	10^{-2}	100	H4	86 +/- 3
2	100	1	100	H5	92 +/- 1
3	0	10^{-2}	0	H5	22 +/- 12
4	10^{-2}	10	100	H5	86 +/- 5
5	10^{-2}	0	1	H3	28 +/- 2
6	100	10^{-2}	10^{-2}	H2	28 +/- 6
7	1	10^{-2}	0	H3	19 +/- 6
8	0	0	10^{-2}	H5	5 +/- 9
9	1	10	10^{-2}	H1	12 +/- 5
10	100	0	10^{-2}	H2	33 +/-5
11	0	10^{-2}	0	H4	19 +/- 6
12	100	10^{-2}	10^{-2}	H2	10 +/- 10
13	1	1	10^{-2}	H3	32 +/- 6
14	100	1	1	H1	21 +/- 1
15	1	10^{-2}	100	H1	88 +/- 3
16	0	0	100	H3	88 +/- 2
-	-	-	-	H1	12 +/- 5
-	-	-	-	H2	28 +/- 6
-	-	-	-	H3	27 +/- 3
-	-	-	-	H4	25 +/- 5
-	-	-	-	H5	37 +/- 1

s.d. – standard deviation

Table S-4. Applied modification procedures to generate different extract of variants from *H. chrysodon* H2.

Modification No.	Modification method
M1	Native without antibiotics
M2	Autoclave, $T = 394$ K, 20 min
M3	Drying cabinet, $T = 423$ K 30 min
M4	XAD 7-HP, elution with H_2O, MeOH and MeOH/EtOAc 1:1 (*v/v*)
M5	SAX, elution with MeOH/H_2O 1:1 (*v/v*) and MeOH
M6	5 mg charcoal, 5 min
M7	50 mg charcoal, 5 min
M8	500 mg charcoal, 5 min
M9	Boiling in MeOH ($T = 341$ K), 15 min
M10	Diaion HP20, elution with H_2O, MeOH and MeOH/EtOAc 1:1 (*v/v*)
M11	Native with antibiotics
M12	SCX, elution with MeOH/H_2O 1:1 (*v/v*) and MeOH

SAX/SCX – strong anion/kation exchange resin

Table S-5. Negative ion LC/ESI-IT-MS^2 data of prenylated metabolites from *Albatrellus* species.

Compound	RT [min]	[M-H]$^-$ (*m/z*)	Scan mode [*m/z*]	MS^2 *m/z* [relative intensity (%)]
grifolic acid (**2**)	6.4	371	MS^2 [**371**]	371 ([M-H]$^-$, 2), 353 ([M-H-H_2O]$^-$, 14), **327** ([M-H-CO_2]$^-$, **100**), 259 ([M-H-CO_2-C_5H_8]$^-$, 2), 234 (6), 191 ([M-H-CO_2-2C_5H_8]$^-$, 7), 135 ([M-H-CO_2-2C_5H_8-C_4H_8]$^-$, 8), 123 (5)
hydroxylated neogrifolin or grifolin	6.6	343	MS^2 [**343**]	343 ([M-H]$^-$, 27), 315 ([M-H-CO]$^-$, 10), 274 ([M-H-$^\bullet$$C_5H_9$]$^-$, 49), 259 (10), 206 ([M-H-$^\bullet$$C_5H_9$-$C_5H_8$]$^-$, 53), 191 ([M-H-$^\bullet$$C_5H_9$-$C_5H_8$-$^\bullet$Me]$^-$, 13), 165 (21), 163 ([M-H-$^\bullet$$C_5H_9$-$C_5H_8$-CO-$^\bullet$Me]$^-$, 32), **152** ([M-H-$^\bullet$$C_5H_9$-$C_5H_8$-$C_4H_6$]$^-$, **100**), 151 (81), 123 (11)
formyl-neogrifolin or -grifolin	7.3	355	MS^2 [**355**]	355 ([M-H]$^-$, 48), 327 ([M-H-CO]$^-$, 14), 286 ([M-H-$^\bullet$$C_5H_9$]$^-$, 14), 271 (22), 218 ([M-H-$^\bullet$$C_5H_9$-$C_5H_8$]$^-$, 71), **203** ([M-H-$^\bullet$$C_5H_9$-$C_5H_8$-$^\bullet$Me]$^-$, **100**), 190 ([M-H-$^\bullet$$C_5H_9$-$C_5H_8$-CO]$^-$, 16), 189 (53), 175 ([M-H-$^\bullet$$C_5H_9$-$C_5H_8$-CO-$^\bullet$Me]$^-$, 72), 164 ([M-H-$^\bullet$$C_5H_9$-$C_5H_8$-$C_4H_6$]$^-$, 97), 136 ([M-H-$^\bullet$$C_5H_9$-$C_5H_8$-$C_4H_6$-CO]$^-$, 5)
scutigeral (**1**)	7.0	371	MS^2 [**371**]	371 ([M-H]$^-$, 21), 343 ([M-H-CO]$^-$, 6), 302 ([M-H-$^\bullet$$C_5H_9$]$^-$, 26), 287 (12), **234** ([M-H-$^\bullet$$C_5H_9$-$C_5H_8$]$^-$, **100**), 219 ([M-H-$^\bullet$$C_5H_9$-$C_5H_8$-$^\bullet$Me]$^-$, 93), 206 ([M-H-$^\bullet$$C_5H_9$-$C_5H_8$-CO]$^-$, 17), 205 (30), 191 ([M-H-$^\bullet$$C_5H_9$-$C_5H_8$-CO-$^\bullet$Me]$^-$, 35), 180 ([M-H-$^\bullet$$C_5H_9$-$C_5H_8$-$C_4H_6$]$^-$, 47), 152 ([M-H-$^\bullet$$C_5H_9$-$C_5H_8$-$C_4H_6$-CO]$^-$, 6)

Table S-6. Applied modification procedures to generate different extract of variants from *H. latitabundus* H6*.

Modification No.	Modification method
M1	Native without antibiotics
M2	Autoclave, T = 394 K, 20 min
M3*	Drying cabinet, T = 373 K 30 min
M4*	XAD 7-HP, elution with H_2O and MeOH
M5	SAX, elution with MeOH/H_2O 1:1 (*v/v*) and MeOH
M6	5 mg charcoal, 5 min
M7	50 mg charcoal, 5 min
M8	500 mg charcoal, 5 min
M9	Boiling in MeOH (T = 341 K), 15 min
M10	Diaion HP20, elution with H_2O, MeOH and MeOH/EtOAc 1:1 (*v/v*)
M11*	Extraction with 80% MeOH
M12	SCX, elution with MeOH/H_2O 1:1 (*v/v*) and MeOH

SAX/SCX – strong anion/kation exchange resin

Table S-7. Negative ion LC/ESI-IT-MS^n and negative ion LC/ESI-QTOF-MS^2 data of the oxidized fatty acids **1** and **2**.

Compound	[M-H]$^-$ (*m/z*)	Scan mode [*m/z*]	ESI-IT-MS^n: *m/z* [relative intensity (%)]	ESI-QTOF-MS^2: *m/z* [elemental composition]
11,12-dihydroxy-12,13-dienoic acid (**3**)	311	MS^2 [**311**]	35% NCE: 311 ([M-H]$^-$, <3), **293** ([M-H-H_2O]$^-$, **100**), 277 (60), 269 (<3)	25 eV: 311.2203 ([M-H]$^-$, $C_{18}H_{31}O_4^-$), 293.2103 ([M-H-H_2O]$^-$, $C_{18}H_{29}O_3^-$), 275.1969 ($C_{18}H_{27}O_2^-$), 265.2184 ($C_{17}H_{29}O_2^-$), 249.2199 ($C_{17}H_{29}O^-$), 211.11325 ($C_{12}H_{19}O_3^-$), 199.1323 ($C_{11}H_{19}O_3^-$), 197.1184 ($C_{11}H_{17}O_3^-$), 181.1237 ($C_{11}H_{17}O_2^-$), 169.1231 ($C_{10}H_{17}O_2^-$), 113.0960 ($C_7H_{13}O^-$)
		MS^3 [311 → **293**]	35% NCE: 293 (**100**), 275 (18), 249 (55), 179 (<3), 177 (10), 155 (8), 113 (35)	
8,11-dihydroxy-9-octadecenoic acid (**4**)	313	MS^2 [**313**]	35% NCE: 313 ([M-H]$^-$, <3), **295** ([M-H-H_2O]$^-$, **100**)	30 eV: 313.2355 ([M-H]$^-$, $C_{18}H_{33}O_4^-$), 295.2285 ([M-H-H_2O]$^-$, $C_{18}H_{31}O_3^-$), 251.2342 ($C_{17}H_{31}O^-$), 183.1022 ($C_{10}H_{15}O_3^-$), 165.1280 ($C_{11}H_{17}O^-$), 155.1427 ($C_{10}H_{19}O^-$), 139.1117 ($C_9H_{15}O^-$), 137.0957 ($C_9H_{13}O^-$), 127.1117 ($C_8H_{15}O^-$), 111.0794 ($C_7H_{11}O^-$)
		MS^3 [313 → **295**]	35% NCE: **295** (**100**), 277 (60), 251 (30), 183 (10), 171 (5), 165 (15), 155 (30), 139 (5), 137 (5), 127 (5), 111 (12)	

11.2.5 New antibacterial active metabolites of Albatrellus species (Basidiomycetes) identified by activity correlation analysis

Ramona Heinke, Sebastian Stark, Annegret Laub, Anja Ehrlich, Norbert Arnold, Jürgen Schmidt, Ludger Wessjohann
Unpublished

This Supporting Information illustrates used biological samples, results of activity and metabolite determinations in more detail. Table S1 give an overview of specimens used in the investigations. Table S2 contain UHPLC/negative ion ESI-HR-MS^n data of metabolites of *Albatrellus* species. Tables S3-S5 show the results of the growth inhibition assay against *Bacillus subtilis*. Tables S6 and S7 show the effects of the analysed extracts on the bacterial vitality measured with a luminescence assay. The hit lists of peaks exhibiting a positive correlation of the bioactivity against *B. subtilis* ($c_{extract}$ = 10 µg/mL and $c_{extract}$ = 50 µg/mL) with the positive ion ESI-FTICR-MS data are given in Tables S8 and S9. The cell proliferation inhibitory effects against the human prostate cancer cell line PC3 and the colon cancer cell line HT29 of the analyzed *Albatrellus* extracts are shown in Tables S10-S12.

Table S1. Collection number and origin of the investigated *Albatrellus* species

Fungal species	Collection	Location	Date	Collected and determined
***Albatrellus citrinus* Ryman**				
A. citrinus	7/11 (fr)	near Munich, Bavaria, Germany	09/19/11	-
***Albatrellus cristatus* (Schaeff.) Kotl. & Pouzar**				
A. cristatus 1	191/95 (dr)	near Regensburg, Bavaria, Germany	10/11/95	Besl
A. cristatus 2	84/94 (dr)	Pupplinger Au, Bavaria, Germany	09/21/94	Arnold
***Albatrellus hirtus* (Schaeff.) Kotl. & Pouzar**				
A. hirtus 1	5/2002 (dr)	USA	10/16/02	Arnold
A. hirtus 2	18/2002 (dr)	USA	10/18/02	Arnold
***Albatrellus ovinus* (Schaeff.) Kotl. & Pouzar**				
A. ovinus 1	63/11 (fr)	Pupplinger Au, Bavaria, Germany	10/22/11	Arnold
A. ovinus 2	64/11 (fr)	Pupplinger Au, Bavaria, Germany	10/22/11	Arnold
A. ovinus 3	328/95 (dr)	Pupplinger Au, Bavaria, Germany	09/24/95	Arnold
A. ovinus 4	111/95 (dr)	KEH/Paintner Forst	09/22/95	Besl
A. ovinus 5	234/96 (dr)	Pupplinger Au, Bavaria, Germany	09/13/96	Arnold
A. ovinus 6	K-Ö/46 (ly)	Kaltenbrunn, Bavaria, Germany	09/-/88	-
***Albatrellus subrubescens* (Murrill) Pouzar**				
A. subrubescens 1	66/11 (fr)	Oberbernbacher Wald, Bavaria, Germany	10/22/11	Arnold
A. subrubescens 2	95/11 (fr)	Oberbernbacher Wald, Bavaria, Germany	11/23/11	Arnold
A. subrubescens 3	28/10 (fr)	Pupplinger Au, Bavaria, Germany	10/03/10	Arnold
A. subrubescens 4	113/95 (dr)	Pupplinger Au, Bavaria, Germany	09/24/95	Arnold
A. subrubescens 5	K-Ö/44 (ly)	Kaltenbrunn, Bavaria, Germany	09/-/88	-
A. subrubescens (cf)	341/95 (dr)	Kaltenbrunn, Bavaria, Germany	10/09/92	Arnold
Albatrellus species				
A. ssp. 1	K-Ö/20 (dr)	USA/Highlands	-/-/86	-
A. ssp. 2	K-Ö/51 (dr)	USA/Highlands	09/-/90	-
***Albatrellus syringae* (Parmasto) Pouzar**				
A. syringae	KSH873 (my)	CBS 728.85		

dr = air-dried; fr = fresh; my = mycelial culture; ly = freeze-dried

Table S2. Compounds assigned in *Albatrellus* species extracts by UHPLC/ negative ion ESI-HR-MS^n.

No.	compound	RT [min]	[M-H]$^-$ (*m/z*)	Scan mode	NCE [%]	*m/z* [relative Intensity (%), elemental composition, error (ppm)]
2	neogrifolin	12.03	327.2340	MS		327.2340 ($C_{22}H_{31}O_2^-$, 3.2)
				MS^2 [**327**]	35	327 ($C_{22}H_{31}O_2^-$), 309.2218 (22.7, $C_{22}H_{29}O^{-}$,1.9), 299.2369 (1.0, $C_{21}H_{23}O^-$, 3.8), 285.2222 (10.8, $C_{20}H_{29}O^-$, 0.6), 189.0921 (8.7, $C_{12}H_{14}O_2^{-\cdot}$, 0.1), 175.0763 (4.0, $C_{11}H_{11}O_2^-$, 0.5), 135.0452 (**100.0**, $C_8H_7O_2^{-\cdot}$, 0.5), 123.0452 (21.5, $C_7H_7O_2^-$, 0.2)
9	hydroxylated neogrifolin or grifolin	12.08	343.2276	MS		343.2276 ($C_{22}H_{31}O_3^-$; 0.7)
				MS^2 [**343**]	40	343 ($C_{22}H_{31}O_3^-$), 325.2172 (3.4, $C_{22}H_{29}O_2^-$, 0.4), 315.2328 (18.7, $C_{21}H_{31}O_2^-$, 0.5), 274.1573 (24.8, $C_{17}H_{22}O_3^{-\cdot}$, 0.5), 206.0949 (0.2, $C_{12}H_{14}O_3^{-\cdot}$, 0.2), 152.0480 (**100.0**, $C_8H_8O_3^{-\cdot}$, 0.4), 123.0453 (5.9, $C_7H_7O_2^-$, 0.9)
7 or 8	aldehyde of grifolin or neogrifolin	15.02	355.2722	MS		355.2722 ($C_{23}H_{31}O_3^-$; 2.0)
				MS^2 [**355**]	45	355 ($C_{23}H_{31}O_3^-$), 337.2168 (1.5, $C_{23}H_{29}O_2^-$, 1.6), 327.2325 (28.0, $C_{22}H_{31}O_2^-$, 1.4), 309.2220 (13.9, $C_{22}H_{29}O^-$, 1.1), 286.1570 (4.2, $C_{18}H_{22}O_3^{-\cdot}$, 1.5), 271.1337 (9.0, $C_{17}H_{19}O_3^-$, 0.9), 218.0948 (48.1, $C_{13}H_{14}O_3^{-\cdot}$, 0.3), 203.0712 (50.7, $C_{12}H_{11}O_3^-$, 0.8), 189.0556 (23.4, $C_{11}H_9O_3^-$, 0.7), 175.0400 (37.5, $C_{10}H_7O_3^-$, 0.3), 164.0478 (**100.0**, $C_9H_8O_3^{-\cdot}$, 0.3), 136.0529 (5, $C_8H_8O_2^-$, 0.2)
3	scutigeral	13.79	371.2226	MS		371.2226 ($C_{23}H_{31}O_4^-$; 0.6)
				MS^2 [**371**]	45	371 ($C_{23}H_{31}O_4^-$), 353.2123 (0.4, $C_{23}H_{29}O_3^-$, 0.3), 343.2280 (14.6, $C_{22}H_{31}O_3^-$, 0.3), 302.1525 (24.3, $C_{18}H_{22}O_4^{-\cdot}$, 0.4), 287.1290 (14.1, $C_{17}H_{19}O_4^{-\cdot}$, 0.5), 234.0898 (**100.0**, $C_{13}H_{14}O_4^{-\cdot}$, 0.3), 219.0664 (97.6, $C_{12}H_{11}O_4^{-\cdot}$, 0.4), 206.0589 (15.2, $C_{11}H_{10}O_4^{-\cdot}$, 2.1), 205.0508 (23.4, $C_{11}H_9O_4^-$, 0.7), 191.0351 (31.0, $C_{10}H_7O_4^-$, 0.7), 180.0430 (52.5, $C_9H_8O_4^{-\cdot}$, 0.9), 152.0481 (27.4, $C_8H_8O_3^{-\cdot}$, 1.2)
39		12.56	424.2853	MS		424.2853 ($C_{27}H_{38}NO_3^-$, 1.0)
				MS^2 [**424**]	45	424 ($C_{27}H_{38}NO_3^-$), 406.2749 (28.2, $C_{27}H_{36}NO_2^-$, 0.7), 396.2904 (31.2, $C_{26}H_{38}NO_2^-$, 0.9), 381.2304 (33.3, $C_{24}H_{31}NO_3^{-\cdot}$, 1.3), 368.2227 (73.5, $C_{23}H_{30}NO_3^-$, 1.1), 367.2149 (17.9, $C_{23}H_{29}NO_3^{-\cdot}$, 1.1), 355.2320 (37.1, $C_{23}H_{31}O_3^-$, 11.6), 355.2145 (31.4, $C_{22}H_{29}NO_3^{-\cdot}$, 2.1), 353.2121 (**a**, 54.5, $C_{23}H_{29}O_3^-$, 0.4), 340.1913 (27.3, $C_{21}H_{26}NO_3^-$, 1.7), 312.1604 (**b**, 62.0, $C_{19}H_{22}NO_3^-$, 0.5), 300.1603 (24.4, $C_{18}H_{22}NO_3^-$, 0.8), 298.1447 (34.0, $C_{18}H_{20}NO_3^-$, 0.4), 287.1526 (**100.0**, $C_{17}H_{21}NO_3^{-\cdot}$, 0.5), 286.1446 (41.7, $C_{17}H_{20}NO_3^-$, 1.0), 272.1291 (90.0, $C_{16}H_{18}NO_3^-$, 0.4), 244.0979 (**c**, 46.7, $C_{14}H_{14}NO_3^{-\cdot}$, 0.3), 233.1058 (71.5, $C_{13}H_{15}NO_3^{-\cdot}$, 0.2), 230.0823 (**d**, 53.2, $C_{13}H_{12}NO_3^-$, 0.1), 218.0823 (9.0, $C_{12}H_{12}NO_3^{-\cdot}$, 0.04), 202.0509 (8.0, $C_{11}H_8NO_3^-$, 0.4), 190.0510 (12.0, $C_{10}H_8NO_3^{-\cdot}$, 0.4), 178.0510 (**e**, 29.7, $C_9H_8NO_3^{-\cdot}$, 0.3)

Table S2. Continued

40	14.01	438.3013	MS		438.3013 ($C_{28}H_{40}NO_3^-$, 0.2)
			MS^2 [**438**]	45	438 ($C_{28}H_{40}NO_3^-$), 420.2905 (38.7, $C_{28}H_{38}NO_2^-$, 0.8), 410.3062 (30.5, $C_{27}H_{40}NO_2^-$, 0.7), 369.2302 (33.4, $C_{23}H_{31}NO_3^{-\cdot}$, 2.1), 353.2120 (**a**, **100.0**, $C_{23}H_{29}O_3^-$, 0.5), 312.1604 (**b**, 57.3, $C_{19}H_{22}NO_3^{-\cdot}$, 0.2), 301.1682 (85.0, $C_{18}H_{23}NO_3^{-\cdot}$, 0.5), 272.1293 (7.0, $C_{16}H_{18}NO_3^-$, 0.3), 247.1214 (50.3, $C_{14}H_{17}NO_3^{-\cdot}$, 0.2), 244.0979 (**c**, 40.0, $C_{14}H_{14}NO_3^-$, 0.2), 230.0823 (**d**, 35.2, $C_{13}H_{12}NO_3^-$, 0.2), 178.0511 (**e**, 23.1, $C_9H_8NO_3^-$, 0.8)
45	13.44	438.2647	MS		438.2647 ($C_{27}H_{36}NO_4^-$, 0.6)
			MS^2 [**438**]	45	438 ($C_{27}H_{36}NO_4^-$), 420.2541 (1.4, $C_{27}H_{34}NO_3^-$, 0.7), 410.2697 (27.6, $C_{26}H_{36}NO_3^-$, 1.0), 369.1935 (1.3, $C_{22}H_{27}NO_4^{-\cdot}$, 2.8), 353.2120 (**a**, 2.7, $C_{23}H_{29}O_3^-$, 0.7), 312.1239 (**b**, 5.4, $C_{18}H_{18}NO_4^-$, 0.7), 301.1317 (35.2, $C_{17}H_{19}NO_4^-$, 0.9), 286.1083 (**100.0**, $C_{16}H_{16}NO_4^-$, 0.6), 272.0927 (31.8, $C_{15}H_{14}NO_4^{-\cdot}$, 0.5), 247.0850 (29.8, $C_{13}H_{13}NO_4^{-\cdot}$, 0.1), 244.0979 (**c**, 2.4, $C_{14}H_{14}NO_3^-$, 0.1), 230.0821 (**d**, 2.0, $C_{13}H_{12}NO_3^-$, 0.7), 178.0511 (**e**, 1.0, $C_9H_8NO_3^-$, 0.7)
41	13.55	472.2855	MS		472.2855 ($C_{31}H_{38}NO_3^-$, 0.5)
			MS^2 [**472**]	45	472 ($C_{31}H_{38}NO_3^-$), 454.2740 (17.0, $C_{31}H_{36}NO_2^-$, 2.6), 444.2903 (6.4, $C_{30}H_{38}NO_2^-$, 1.2), 403.2148 (7.7, $C_{26}H_{29}NO_2^{-\cdot}$, 1.3), 381.2306 (**100.0**, $C_{24}H_{31}NO_3^-$, 0.8), 353.2116 (**a**, 44.2, $C_{23}H_{29}O_3^-$, 1.7), 335.1526 (40.2, $C_{21}H_{21}NO_3^{-\cdot}$, 0.4), 312.1605 (**b**, 52.9, $C_{19}H_{22}NO_3^-$, 0.1), 281.1057 (13.4, $C_{17}H_{15}NO_3^-$, 0.1), 244.0980 (**c**, 19.5, $C_{14}H_{14}NO_3^-$, 0.3), 230.0824 (**d**, 11.3, $C_{13}H_{12}NO_3^-$, 0.4), 190.0511 (6.3, $C_{10}H_8NO_3^-$, 1.0)
42	12.55	500.3015	MS		500.3015 ($C_{29}H_{42}NO_6^-$, 0.4)
			MS^2 [**500**]	45	500 ($C_{29}H_{42}NO_6^-$), 424.2854 (100.0, $C_{27}H_{38}NO_3^-$, 0.7)
			MS^3 [500 → **424**]	45	424 ($C_{27}H_{38}NO_3^-$), 406.2741 (29.2, $C_{27}H_{36}NO_2^-$, 2.6), 396.2899 (35.6, $C_{26}H_{38}NO_2^-$, 2.4), 381.2300 (32.2, $C_{24}H_{31}NO_3^{-\cdot}$, 2.5), 368.2221 (79.8, $C_{23}H_{30}NO_3^-$, 2.7), 367.2142 (15.9, $C_{23}H_{29}NO_3^{-\cdot}$, 3.0), 353.2114 (**a**, 55.6, $C_{23}H_{29}O_3^-$, 2.3), 340.1908 (31.9, $C_{21}H_{26}NO_3^-$, 3.0), 312.1598 (**b**, 65.6, $C_{19}H_{22}NO_3^-$, 2.3), 300.1599 (27.7, $C_{18}H_{22}NO_3^-$, 2.2), 298.1442 (32.6, $C_{18}H_{20}NO_3^-$, 2.4), 287.1521 (**100.0**, $C_{17}H_{21}NO_3^{-\cdot}$, 2.2), 286.1442 (44.3, $C_{17}H_{20}NO_3^-$, 2.2), 272.1287 (87.5, $C_{16}H_{18}NO_3^-$, 2.0), 244.0974 (**c**, 51.3, $C_{14}H_{14}NO_3^{-\cdot}$, 1.9), 233.1053 (61.1, $C_{13}H_{15}NO_3^-$, 1.9), 230.0818 (**d**, 45.7, $C_{13}H_{12}NO_3^-$, 1.9), 218.0818 (45.7, $C_{12}H_{12}NO_3^-$, 2.2), 202.0507 (7.9, $C_{11}H_8NO_3^{-\cdot}$, 1.5), 190.0506 (10.3, $C_{10}H_8NO_3^-$, 1.7), 178.0507 (**e**, 29.0, $C_9H_8NO_3^{-\cdot}$, 1.6)
43	14.02	514.3179	MS		514.3179 ($C_{30}H_{44}NO_6^-$, 1.0)
			MS^2 [**514**]	45	514 ($C_{30}H_{44}NO_6^-$), 438.3014 (100.0, $C_{28}H_{40}NO_3^-$, 0.1)
			MS^3 [514 → **438**]	45	438 ($C_{28}H_{40}NO_3^-$), 420.2898 (51.0, $C_{28}H_{38}NO_2^-$, 2.3), 410.3056 (32.7, $C_{27}H_{40}NO_2^-$, 2.0), 369.2304 (28.0, $C_{23}H_{31}NO_3^{-\cdot}$, 1.5), 353.2115 (**a**, **100.0**, $C_{23}H_{29}O_3^-$, 2.1), 312.1600 (**b**, 58.6, $C_{19}H_{22}NO_3^{-\cdot}$, 1.7), 301.1678 (88.8, $C_{18}H_{23}NO_3^{-\cdot}$, 1.9), 272.1288 (9.2, $C_{16}H_{18}NO_3^-$, 1.6), 247.1209 (48.7, $C_{14}H_{17}NO_3^{-\cdot}$, 1.8), 244.0975 (**c**, 42.4, $C_{14}H_{14}NO_3^-$, 1.6), 230.0819 (**d**, 42.8, $C_{13}H_{12}NO_3^-$, 1.4), 178.0508 (**e**, 17.5, $C_9H_8NO_3^-$, 1.0)

Table S2. Continued

44	13.55	548.3015	MS		548.3015 ($C_{33}H_{42}NO_6^-$, 0.5)
			MS^2 [**548**]	45	548 ($C_{33}H_{42}NO_6^-$), 472.2854 (100.0, $C_{31}H_{38}NO_3^-$, 0.7)
			MS^3 [548 → **472**]	45	472 ($C_{31}H_{38}NO_3^-$), 454.2742 (21.6, $C_{31}H_{36}NO_2^-$, 2.1), 444.2900 (6.47, $C_{30}H_{38}NO_2^-$, 1.7), 403.2145 (7.7, $C_{26}H_{29}NO_2^{\cdot-}$, 2.0), 381.2302 (**100.0**, $C_{24}H_{31}NO_3^-$, 1.9), 353.2115 (**a**, 47.8, $C_{23}H_{29}O_3^-$, 1.9), 335.1521 (38.8, $C_{21}H_{21}NO_3^{\cdot-}$, 1.8), 312.1600 (**b**, 50.0, $C_{19}H_{22}NO_3^-$, 1.6), 281.1053 (11.9, $C_{17}H_{15}NO_3^-$, 1.4), 244.0976 (**c**, 19.2, $C_{14}H_{14}NO_3^{\cdot-}$, 1.3), 230.0820 (**d**, 8.9, $C_{13}H_{12}NO_3^-$, 1.2), 190.0508 (**e**, 6.1, $C_{10}H_8NO_3^-$, 0.7)

Table S3. Antibacterial activities (relative growth inhibition [%] of *Bacillus subtilis*) of *Albatrellus* extract from fresh fruiting bodies.

Fungal species	Extraction	Inhibition [%] (c = 1 μg/mL)	Inhibition [%] (c = 5 μg/mL)	Inhibition [%] (c = 10 μg/mL)	Inhibition [%] c = 50 μg/mL
A. citrinus	EE	11.4 (±5.8)	66.9 (±6.9)	73.7 (±2.4)	97.2 (±5.5)
	MeOH	35.1 (±11.1)	45.8 (±13.9)	65.2 (±9.9)	87.7 (±4.7)
	Ac/HCl	30.3 (±21.6)	50.8 (±16.1)	58.0 (±10.3)	89.2 (±6.0)
A. ovinus 1	EE	15.9 (±6.4)	70.0 (±5.0)	72.5 (±5.2)	90.8 (±6.1)
	MeOH	44.2 (±6.1)	50.4 (±10.3)	61.6 (±7.9)	82.5 (±2.3)
	Ac/HCl	42.6 (±12.4)	66.2 (±7.1)	68.7 (±7.8)	84.9 (±8.3)
A. ovinus 2	EE	9.7 (±6.6)	57.4 (±15.7)	72.2 (±4.8)	87.4 (±5.2)
	MeOH	32.8 (±8.6)	36.7 (±5.3)	39.5 (±5.3)	75.6 (±4.1)
	Ac/HCl	27.8 (±3.8)	41.7 (±9.1)	66.7 (±3.0)	82.5 (±4.6)
A. subrubescens 1	EE	10.6 (±5.7)	39.0 (±16.0)	77.2 (±5.3)	95.9 (±6.5)
	MeOH	28.9 (±12.9)	28.4 (±13.9)	39.1 (±4.4)	59.6 (±9.2)
	Ac/HCl	26.1 (±11.0)	38.9 (±11.1)	59.8 (±6.7)	86.1 (±8.2)
A. subrubescens 2	EE	10.4 (±7.2)	62.6 (±13.5)	77.4 (±9.2)	100.3 (±8.8)
	MeOH	42.7 (±5.8)	41.5 (±8.8)	46.4 (±16.2)	66.8 (±12.4)
	Ac/HCl	44.0 (±10.9)	55.0 (±15.5)	61.3 (±14.6)	78.0 (±8.9)
A. subrubescens 3	EE	8.2 (±5.1)	56.1 (±6.5)	69.9 (±7.3)	103.8 (±7.0)
	MeOH	22.7 (±7.2)	32.2 (±5.5)	36.6 (±5.4)	77.0 (±5.8)
	Ac/HCl	9.1 (±8.9)	24.0 (±8.9)	63.9 (±8.9)	97.4 (±5.4)

Table S4. Antibacterial activities (relative growth inhibition [%] of *Bacillus subtilis*) of *Albatrellus* extracts from dried fruiting bodies.

Fungal species	Extraction	Inhibition [%] (c = 1 µg/mL)	Inhibition [%] (c = 5 µg/mL)	Inhibition [%] (c = 10 µg/mL)	Inhibition [%] c = 50 µg/mL
A. cristatus 1	EE	18.2 (±8.5)	23.2 (±9.5)	36.6 (±7.5)	80.0 (±5.7)
	MeOH	35.9 (±7.8)	35.4 (±6.5)	36.5 (±7.6)	58.5 (±14.2)
	Ac/HCl	24.2 (±9.0)	33.9 (±8.6)	37.4 (±6.6)	62.9 (±9.2)
A. cristatus 2	EE	27.1 (±3.9)	44.3 (±8.0)	54.5 (±10.1)	88.9 (±12.8)
	MeOH	26.2 (±20.1)	46.5 (±20.1)	54.2 (±20.9)	70.8 (±11.4)
	Ac/HCl	39.6 (±9.8)	46.6 (±10.9)	53.1 (±16.1)	63.6 (±18.4)
A. hirtus 1	EE	20.8 (±6.0)	36.7 (±1.6)	52.7 (±11.0)	77.1 (±3.9)
	MeOH	29.7 (±6.4)	31.0 (±6.0)	31.6 (±7.3)	66.8 (±3.2)
	Ac/HCl	31.5 (±7.6)	42.7 (±7.3)	59.8 (±10.3)	66.5 (±6.4)
A. hirtus 2	EE	-5.7 (±10.3)	16.3 (±8.9)	33.3 (±13.2)	74.6 (±7.3)
	MeOH	21.9 (±12.4)	23.3 (±7.0)	30.4 (±5.8)	66.2 (±9.4)
	Ac/HCl	17.7 (±11.1)	44.6 (±9.0)	64.5 (±4.7)	83.0 (±3.2)
A. ovinus 3	EE	2.6 (±4.7)	27.5 (±10.2)	39.2 (±9.7)	95.6 (±6.9)
	MeOH	26.3 (±9.5)	26.0 (±13.2)	42.2 (±11.7)	59.1 (±6.8)
	Ac/HCl	25.8 (±8.7)	40.0 (±10.4)	48.3 (±9.9)	78.7 (±12.1)
A. ovinus 4	EE	45.3 (±15.2)	50.5 (±5.5)	58.9 (±3.3)	85.5 (±6.0)
	MeOH	24.1 (±9.8)	35.0 (±16.6)	38.9 (±13.9)	54.4 (±12.2)
	Ac/HCl	48.8 (±13.9)	37.3 (±11.1)	39.9 (±11.9)	50.2 (±6.3)
A. ovinus 5	EE	14.6 (±10.5)	33.6 (±7.3)	56 (±12.4)	82.0 (±7.9)
	MeOH	37.5 (±12.1)	43.6 (±18.0)	46.9 (±6.4)	76.6 (±6.8)
	Ac/HCl	37.0 (±10.7)	42.1 (±1.7)	56.3 (±7.2)	82.8 (±9.0)
A. ovinus 6	EE	20.8 (±9.4)	36.7 (±11.1)	55.5 (±9.3)	89.5 (±8.8)
	MeOH	32.0 (±8.3)	44.2 (±17.0)	46.2 (±10.2)	90.4 (±7.6)
	Ac/HCl	29.6 (±15.1)	37.0 (±6.7)	51.8 (±7.1)	93.6 (±6.5)
A. subrubescens 4	EE	21.7 (±14.8)	42.1 (±18.0)	51.3 (±13.9)	80.4 (±13.9)
	MeOH	6.6 (±11.3)	19.3 (±8.9)	33.1 (±6.3)	39.7 (±7.9)
	Ac/HCl	23.9 (±10.4)	33.0 (±8.6)	39.3 (±8.2)	64.6 (±10.5)
A. subrubescens 5	EE	0.5 (±6.9)	15.1 (±8.3)	30.1 (±8.5)	77.0 (±13.4)
	MeOH	26.1 (±5.4)	29.7 (±9.1)	30.7 (±6.0)	56.2 (±2.6)
	Ac/HCl	15.9 (±12.5)	21.5 (±6.8)	35.7 (±6.7)	59.5 (±9.4)
A. subrubescens (cf)	EE	7.6 (±7.2)	27.5 (±6.3)	34.5 (±8.1)	78.7 (±8.0)
	MeOH	36.8 (±13.)0	33.7 (±8.9)	34.4 (±8.3)	37.2 (±3.1)
	Ac/HCl	21.9 (±15.)3	32.4 (±13.8)	41.3 (±10.2)	57.4 (±12.0)
A. ssp. 1	EE	48.4 (±5.2)	69.4 (±6.2)	77.6 (±5.2)	100.1 (±4.6)
	MeOH	31.9 (±18.7)	61.6 (±4.6)	67.5 (±3.8)	82.7 (±3.5)
	Ac/HCl	49.4 (±8.3)	65.8 (±11.1)	68.5 (±7.4)	84.0 (±8.3)
A. ssp. 2	EE	3.4 (±10.0)	59.2 (±9.1)	71.7 (±7.1)	88.5 (±9.4)
	MeOH	6.0 (±12.1)	31.8 (±13.8)	61.8 (±9.6)	77.7 (±8.5)
	Ac/HCl	0.2 (±18.0)	63.3 (±4.1)	68.4 (±10.2)	86.1 (±6.5)

Table S5. Antibacterial activities (relative growth inhibition [%] of *Bacillus subtilis*) of *A. syringae* extract from mycelial culture.

Fungal species	Extraction	Inhibition [%] (c = 1 µg/mL)	Inhibition [%] (c = 5 µg/mL)	Inhibition [%] (c = 10 µg/mL)	Inhibition [%] c = 50 µg/mL)
A. syringae	EE	22.6 (±7.2)	34.2 (±7.0)	43.6 (±1.8)	86.4 (±4.4)
	MeOH	13.9 (±4.2)	25.7 (±1.1)	29.7 (±4.4)	43.1 (±3.8)
	LLEE	34.1 (±6.2)	44.6 (±6.6)	50.3 (±6.6)	70.8 (±15.3)
	LLW	26.2 (±6.3)	19.8 (±8.3)	26.0 (±13.2)	40.4 (±11.6)

Table S6. Antibacterial activities (bacterial luminescence [%] of *Aliivibrio fischeri* after 1 h and 24 h treatment) of *Albatrellus* extracts from fresh fruiting bodies.

Fungal species	Extraction	Luminescence [%] after 1 h (c = 50 µg/mL)	Luminescence [%] after 24 h (c = 50 µg/mL)
A. citrinus	EE	62.2 (±3.7)	> 100
	MeOH	57.1 (±2.8)	> 100
	Ac/HCl	58.5 (±1.1)	99.5 (±20.5)
A. ovinus 1	EE	66.6 (±14.8)	> 100
	MeOH	62.6 (±3.2)	> 100
	Ac/HCl	62.7 (±2.5)	70.7 (±3.7)
A. ovinus 2	EE	52.8 (±1.5)	78.2 (±6.8)
	MeOH	71.6 (±2.2)	> 100
	Ac/HCl	61.8 (±2.2)	49.0 (±4.4)
A. subrubescens 1	EE	61.1 (±5.3)	90.3 (±6.9)
	MeOH	79.0 (±2.3)	> 100
	Ac/HCl	74.2 (±2.3)	> 100
A. subrubescens 2	EE	54.7 (±1.4)	> 100
	MeOH	75.4 (±3.8)	> 100
	Ac/HCl	89.5 (±1.3)	> 100
A. subrubescens 3	EE	44.2 (±13.1)	> 100
	MeOH	55.4 (±9.3)	> 100
	Ac/HCl	52.5 (±13.3)	83.3 (±5.8)

Table S7. Antibacterial activities (bacterial luminescence [%] of *Aliivibrio fischeri* after 1 h and 24 h treatment) of *Albatrellus* extracts from dried fruiting bodies.

Fungal species	Extraction	Luminescence [%] after 1 h (c = 50 µg/mL)	Luminescence [%] after 24 h (c = 50 µg/mL)
A. cristatus 1	EE	97.8 (±4.2)	> 100
	MeOH	97.7 (±4.2)	> 100
	Ac/HCl	> 100	> 100
A. cristatus 2	EE	71.5 (±1.3)	> 100
	MeOH	76.8 (±2.0)	95.8 (±24.0)
	Ac/HCl	98.5 (±2.9)	85.1 (±32.1)
A. hirtus 1	EE	86.3 (±1.5)	39.4 (±3.6)
	MeOH	89.8 (±2.2)	45.5 (±6.5)
	Ac/HCl	90.4 (±1.6)	42.7 (±2.0)
A. hirtus 2	EE	88.7 (±3.6)	37.8 (±7.1)
	MeOH	> 100	80.7 (±2.0)
	Ac/HCl	n.t.	n.t.
A. ovinus 3	EE	57.9 (±1.7)	54.4 (±10.2)
	MeOH	64.2 (±1.6)	86.3 (±24.7)
	Ac/HCl	62.8 (±2.8)	52.4 (±5.3)
A. ovinus 4	EE	52.3 (±2.9)	30.8 (±3.1)
	MeOH	n.t.	n.t.
	Ac/HCl	71.9 (±2.7)	78.4 (±13.5)
A. ovinus 5	EE	63.7 (±1.6)	56.5 (±5.5)
	MeOH	68.0 (±6.0)	> 100
	Ac/HCl	74.7 (±3.2)	> 100
A. ovinus 6	EE	71.7 (±5.0)	> 100
	MeOH	78.3 (±5.5)	> 100
	Ac/HCl	77.4 (±4.5)	> 100
A. subrubescens 4	EE	82.0 (±3.1)	> 100
	MeOH	78.0 (±1.7)	> 100
	Ac/HCl	98.2 (±4.8)	> 100
A. subrubescens 5	EE	58.6 (±3.4)	49.6 (±6.6)
	MeOH	58.8 (±2.8)	82.7 (±12.4)
	Ac/HCl	64.2 (±2.7)	71.7 (±13.6)
A. subrubescens (cf)	EE	61.0 (±1.7)	42.4 (±4.5)
	MeOH	76.3 (±1.0)	> 100
	Ac/HCl	70.1 (±1.8)	> 100
A. ssp. 1	EE	34.3 (±0.4)	50.2 (±2.1)
	MeOH	48.0 (±1.4)	95.5 (±18.1)
	Ac/HCl	41.7 (±1.6)	> 100
A. ssp. 2	EE	38.3 (±0.8)	55.9 (±6.0)
	MeOH	57.7 (±1.9)	> 100
	Ac/HCl	65.7 (±1.4)	88.1 (±14.2)

n.t. = not tested

Table S8. Hit list of the top-13 peaks based on positive ion ESI-FTICR-MS data correlated with the antibacterial bioactivity profiles against *B. subtilis* of the *Albatrellus* extracts ($c_{extract}$ = 10 µg/mL).

Rank	Spearman correlation coefficient	$[M+Na/K/H]^+$ (*m/z*)	elemental composition	DBE	Error [ppm]	possible compound
1	0.68	383.1986	$C_{22}H_{32}O_3K^+$	6.5	0.8	Hydroxyneogrifolin (**9**)
2	0.51	367.2245	$C_{22}H_{32}O_3Na^+$	6.5	0.4	Hydroxyneogrifolin (**9**)
3	0.50	739.4553				
4	0.48	368.2280	$C_{22}{}^{13}C_1H_{32}O_2Na^+$			Isotope peak of *m/z* 367.2245
5	0.47	398.2385	$C_{23}{}^{13}C_1H_{34}O_4Na^+$			Isotope peak of *m/z* 397.2354
6	0.40	384.2022				
7	0.40	740.4595				Isotope peak of *m/z* 739.4553
8	0.40	367.2040				
9	0.40	395.2196	$C_{22}H_{32}O_4Na^+$	7.5	0.8	scutigeral (**3**)/grifolic acid (**13**)
10	0.39	290.0860				
11	0.39	319.1054				
12	0.39	351.2296	$C_{22}H_{32}O_2Na^+$	6.5	0.4	Grifolin(**1**)/Neogrifolin (**2**)
13	0.39	397.2354	$C_{23}H_{34}O_4Na^+$	6.5	1.2	

Table S9. Hit list of the top-10 peaks based on positive ion ESI-FTICR-MS data correlated with the antibacterial bioactivity profiles against *B. subtilis* of the *Albatrellus* extracts ($c_{extract}$ = 50 µg/mL).

Rank	Spearman correlation coefficient	$[M+Na/K/H]^+$ (*m/z*)	elemental composition	DBE	Error [ppm]	possible compound
1	0.68	367.2245	$C_{22}H_{32}O_3Na^+$	6.5	0.4	Hydroxyneogrifolin (**9**)
2	0.60	368.2280	$C_{22}{}^{13}C_1H_{32}O_2Na^+$			Isotope peak of *m/z* 367.2245
3	0.59	383.1986	$C_{22}H_{32}O_3K^+$	6.5	0.8	Hydroxyneogrifolin (**9**)
4	0.59	395.2196	$C_{22}H_{32}O_4Na^+$	7.5	0.8	Scutigeral (**3**)/Grifolic acid (**13**)
5	0.58	351.2296	$C_{22}H_{32}O_2Na^+$	6.5	0.4	Grifolin(**1**)/Neogrifolin (**2**)
6	0.54	396.2228	$C_{22}{}^{13}C_1H_{32}O_4Na^+$			Isotope peak of *m/z* 395.2196
7	0.49	365.2090				
8	0.46	739.4553				
9	0.45	401.2301				
10	0.43	384.2022	$C_{22}{}^{13}C_1H_{32}O_2K^+$			Isotope peak of *m/z* 383.1986

Table S10. Cell proliferation inhibitory effects of PC3 and HT29 [%] of *Albatrellus* extract from fresh fruiting bodies.

Fungal species	Extraction	PC3 Inhibition [%] (c = 50 µg/mL)	HT29 Inhibition [%] c = 50 µg/mL
A. citrinus	EE	69.2 (±2.1)	54.8 (±1.7)
	MeOH*	-18.3 (±8.5)	-20.3 (±7.3)
	Ac/HCl	7.8 (±13.4)	8.1 (±6.8)
A. ovinus 1	EE	74.7 (±12.9)	23.2 (±15.0)
	MeOH*	54.2 (±3.7)	20.3 (±5.6)
	Ac/HCl	62.5 (±20.6)	32.2 (±15.9)
A. ovinus 2	EE	60.9 (±16.1)	29.4 (±27.4)
	MeOH*	28.7 (±7.8)	2.0 (±8.7)
	Ac/HCl	65.2 (±14.1)	38.6 (±15.3)
A. subrubescens 1	EE	36.9 (±5.6)	-11.4 (±15.0)
	MeOH*	-15.6 (±6.7)	-19.0 (±4.2)
	Ac/HCl	23.2 (±11.8)	-2.1 (±6.1)
A. subrubescens 2	EE	29.0 (±17.2)	-3.5 (±24.8)
	MeOH*	-33.9 (±5.4)	-44.0 (±1.8)
	Ac/HCl	-1.6 (±14.7)	-5.1 (±4.1)
A. subrubescens 3	EE	26.3 (±3.1)	-0.4 (±7.3)
	MeOH*	2.5 (±2.5)	-6.9 (±6.2)
	Ac/HCl	44.3 (±9.6)	42.8 (±4.8)

* tested concentration may deviate because of poor solubility in DMSO

Table S11. Cell proliferation inhibitory effects of PC3 and HT29 [%] of *Albatrellus* extracts from dried fruiting bodies.

Fungal species	Extraction	PC3 Inhibition [%] (c = 50 µg/mL)	HT29 Inhibition [%] c = 50 µg/mL
A. cristatus 1	EE	8.4 (±19.1)	-7.1 (±8.6)
	MeOH*	-74.0 (±7.6)	-83.1 (±2.9)
	Ac/HCl	10.7 (±11.1)	-10.8 (±4.5)
A. cristatus 2	EE	-6.3 (±6.6)	-15.4 (±9.9)
	MeOH*	4.9 (±1.6)	-1.9 (±5.1)
	Ac/HCl	13.0 (±9.7)	-20.7 (±7.3)
A. hirtus 1	EE	67.2 (±10.9)	70.2 (±5.1)
	MeOH*	-3.9 (±5.1)	45.3 (±1.8)
	Ac/HCl	37.1 (±3.7)	72.3 (±3.2)
A. hirtus 2	EE	65.2 (±14.3)	68.9 (±2.8)
	MeOH*	6.9 (±3.4)	25.5 (±0.3)
	Ac/HCl	34.6 (±4.9)	65.4 (±8.0)
A. ovinus 3	EE	9.1 (±4.8)	-16.1 (±8.4)
	MeOH*	0.4 (±4.1)	-14.2 (±7.6)
	Ac/HCl	16.2 (±4.2)	-15.3 (±3.8)
A. ovinus 4	EE	27.7 (±7.0)	-23.8 (±9.6)
	MeOH*	-2.7 (±4.2)	-4.2 (±6.6)
	Ac/HCl	14.7 (±17.0)	-8.7 (±8.9)
A. ovinus 5	EE	28.8 (±17.5)	4.9 (±19.5)
	MeOH*	9.2 (±0.3)	0.2 (±2.1)
	Ac/HCl	10.1 (±9.6)	-6.2 (±6.9)
A. ovinus 6	EE	31.6 (±14.2)	1.1 (±6.7)
	MeOH*	3.7 (±8.5)	-8.1 (±5.7)
	Ac/HCl	12.8 (±16.5)	-8.9 (±13.5)
A. subrubescens 4	EE	10.3 (±4.1)	-17.4 (±9.9)
	MeOH*	-13.9 (±4.3)	-4.7 (±12.8)
	Ac/HCl	15.6 (±4.2)	-26.0 (±17.8)
A. subrubescens 5	EE	8.9 (±6.1)	-8.1 (±25.5)
	MeOH*	22.7 (±3.8)	-0.8 (±6.6)
	Ac/HCl	5.1 (±8.3)	-7.5 (±8.0)
A. subrubescens (cf)	EE	16.2 (±5.8)	0.6 (±13.0)
	MeOH*	-14.5 (±7.1)	27.4 (±3.1)
	Ac/HCl	16.7 (±5.4)	-4.9 (±9.2)
A. ssp. 1	EE	10.4 (±5.6)	13.7 (±5.7)
	MeOH*	-5.8 (±9.1)	0.9 (±4.8)
	Ac/HCl	-6.0 (±5.1)	-7.4 (±4.6)
A. ssp. 2	EE	50.5 (±13.0)	51.8 (±6.7)
	MeOH*	4.8 (±4.5)	-11.5 (±5.1)
	Ac/HCl	-9.7 (±13.0)	-16.7 (±4.8)

* tested concentration may deviate because of poor solubility in DMSO

Table S12. Cell proliferation inhibitory effects of PC3 and HT29 [%] of *A. syringae* extract from mycelial culture.

Fungal species	Extraction	PC3	HT29
		Inhibition [%] (c = 50 µg/mL)	Inhibition [%] c = 50 µg/mL
A. syringae	EE	8.1 (±7.8)	23.4 (±5.8)
	MeOH*	-6.0 (±5.0)	-9.1 (±8.0)
	LLEE	28.5 (±8.6)	36.5 (±4.4)
	LLW	12.4 (±3.4)	9.4 (±7.1)

* tested concentration may deviate because of poor solubility in DMSO

11.2.6 Determination of the antibacterial potential against *Bacillus subtilis* of *Suillus* spp. (Basidiomycetes).

Ramona Heinke, Pia Schöne, Norbert Arnold, Jürgen Schmidt, Ludger Wessjohann
Manuscript in preparation

An overview of specimens used in the different studies is given in the supporting information in Table S1. Selected strains [*S. acerbus* KSH328 (Sac); *S. bovinus* KSH228 (Sb3), KSH229 (Sb4), KSH313 (Sb5), KSH324 (Sb6), KSH325 (Sb7); *S. collinitus* KSH232 (Sc4); *S. cothurnatus* KSH330 (Sco); *S. granulatus* KSH234 (Sg3), KSH235 (Sg4), KSH236 (Sg5); *S. intermedius* KSH241 (Sin); *S. punctipes* KSH249 (Spu2), KSH250 (Spu3); *S. salmonicolor* KSH251 (Ssa); *S. tridentinus* KSH253 (St3), KSH254 (St4), KSH255 (St5); *S. variegatus* KSH256 (Sv3), KSH257 (Sv4), KSH258 (Sv5), KSH259 (Sv6)] from the culture collection of the Institute of Plant Biochemistry (Halle, Germany) were also investigated. The antibacterial properties against *Bacillus subtilis* of crude extracts from several *Suillus* species were analyzed and summarized in Tables S2-S4. The hit lists of peaks exhibiting a positive correlation of the bioactivity against *B. subtilis* ($c_{extract}$ = 100 µg/mL) with the negative ion ESI-FTICR-MS data are given in Tables S5 and S6.

Table S1. Collection number and origin of the investigated *Suillus* species

Fungal species	Collection	Location	Date	Collected and determined	Extract No.
S. americanus (Peck) Snell	23 (ly)	USA (Wachusett Mountains/MA)	09/21/85	Exk. Steglich	Sam
S. bovinus (L.) Kuntze	75/97 (ly)	Pupplinger Au, Bavaria, Germany	10/06/97	Arnold	Sb1
S. bovinus (L.) Kuntze	K-I/11 (ly)	Tomburg, North Rhine-Westphalia, Germany	09/22/85		Sb2
S. bovinus (L.) Kuntze	29/10 (fr)	Halle, Saxony-Anhalt, Germany	09/20/10	Arnold	Sb8
S. bovinus (L.) Kuntze	31/10 (fr)	Halle, Saxony-Anhalt, Germany	09/26/10	Franke	Sb9
S. bovinus (L.) Kuntze	65/11 (fr)	Pupplinger Au, Bavaria, Germany	10/22/11	Arnold	Sb10
S. collinitus (Fr.) Kuntze	K-X/43 (ly)	Karlstadt	10/16/90		Sc1
S. cf. *collinitus* (Fr.) Kuntze	K-V/23 (ly)	Karlstadt	10/15/89		Sc2
S. collinitus (Fr.) Kuntze	K-I/24 (dr)	Götenich	10/08/88	Oertel	Sc3
S. collinitus (Fr.) Kuntze	54/11 (fr)	Bad Bibra NSG	10/20/11	Arnold	Sc5
S. granulatus (L.) Kuntze	220/96 (ly)	near Rammersberg, Bavaria, Germany	10/28/96	Arnold	Sg1
S. granulatus (L.) Kuntze	46/95 (ly)	near Bonn, North Rhine-Westphalia, Germany	09/12/95	Arnold	Sg2
S. grevillei (Klotzsch) Singer	378/94 (ly)	Leutasch	09/18/92	Beyer	Sgr1
S. grevillei (Klotzsch) Singer	K-V/24 (ly)	Kottenforst	07/29/88		Sgr2
S. grevillei (Klotzsch) Singer	1/10 (fr)	Auerberg	08/31/10	Arnold	Sgr3
S. luteus (L.) Roussel	K-V/19 (ly)	Kottenforst	09/24/87		Sl1
S. luteus (L.) Roussel	204/96 (ly)	Abensberg	10/10/96	Arnold	Sl2
S. luteus (L.) Roussel	30/10 (fr)	Halle, Saxony-Anhalt, Germany	09/20/10	Arnold	Sl3
S. pictus (Peck) A. H. Sm. & Thiers	382/94 (ly)	USA (Wachusett Mountains/MA)	00/00/94	Exk. Steglich	Spi
S. punctipes (Peck) Singer	78/2001 (ly)	Myles Standish State Forest	10/14/01	Arnold/Besl	Spu1
S. spec.	K-V/44 (ly)	Nassereith	09/00/89		Sssp
S. tridentinus (Bres.) Singer	R555/88 (ly)	near Regensburg, Bavaria, Germany	10/12/88		St1
S. tridentinus (Bres.) Singer	40/95 (ly)	near Nassereith, Tyrol, Austria	09/12/95	Mühlbauer/Steglich	St2
S. variegatus (Fr.) Fr.	382/94 (ly)	Gattern, Tyrol, Austria	09/18/92	Beyer	Sv1
S. variegatus Britzelm.	69/96 (ly)	near Regensburg, Bavaria, Germany	09/19/96	Mühlbauer	Sv2
S. variegatus Britzelm.	36/11 (fr)	near Regensburg, Bavaria, Germany	09/26/11	Arnold	Sv7
S. viscidus (L.) Roussel	16/97 (ly)	Triptis	07/22/97	Arnold	Svi1
S. viscidus (L.) Roussel	K-V/16 (ly)	Gr. Kahlenberg	10/12/82		Svi2
S. viscidus (L.) Roussel	8/11 (fr)	Pilzausstellung Munich	09/19/11		Svi3
S. viscidus (L.) Roussel	68/11 (fr)	Oberbernbacher Wood	10/22/11		Svi4

dr = air dried; fr = fresh; fz = frozen; ly = freeze-dried collection

Table S2. Antibacterial activities (relative growth inhibition [%] of *Bacillus subtilis*) of *Suillus* extracts from dried fruiting bodies.

Extract No.	Inhibition [%] (c = 1 µg/mL)	Inhibition [%] (c = 10 µg/mL)	Inhibition [%] (c = 100 µg/mL)
Sam	12.8 (±8.6)	29.6 (±9.3)	72.4 (±15.0)
	18.3 (±7.3)	37.8 (±8.4)	70.5 (±15.4)
Sb1	9.4 (±10.0)	26.6 (±14.2)	68.2 (±28.8)
	25.0 (±15.6)	32.2 (±15.8)	76.6 (±21.3)
Sb2	22.2 (±14.4)	36.5 (±16.0)	70.5 (±25.6)
	15.0 (±10.8)	33.8 (±11.9)	70.0 (±21.9)
Sc1	10.5 (±6.1)	36.9 (±3.6)	87.3 (±8.7)
	15.8 (±8.4)	41.5 (±10.5)	88.7 (±10.9)
Sc2	20.0 (±9.3)	35.9 (±11.9)	88.2 (±8.1)
	16.2 (±7.4)	37.0 (±11.8)	87.5 (±6.7)
Sc3	9.1 (±10.4)	47.0 (±9.8)	87.9 (±4.6)
	25.6 (±9.8)	49.4 (±9.6)	91.3 (±5.7)
Sg1	23.9 (±8.8)	43.8 (±8.3)	94.6 (±5.6)
	23.7 (±12.0)	62.4 (±12.1)	90.2 (±4.6)
Sg2	27.7 (±7.2)	30.4 (±9.2)	69.7 (±16.9)
	13.3 (±7.8)	36.9 (±7.5)	83.6 (±9.7)
Sgr1	16.9 (±5.9)	67.3 (±2.6)	83.5 (±6.5)
	23.3 (±6.2)	64.1 (±15.5)	88.4 (±6.9)
Sgr2	25.4 (±6.8)	73.9 (±6.1)	92.7 (±7.0)
	24.7 (±5.7)	75.0 (±7.6)	88.3 (±7.2)
Sl1	23.4 (±9.6)	46.9 (±7.1)	91.3 (±4.9)
	23.8 (±7.7)	47.5 (±12.2)	89.1 (±5.1)
Sl2	13.0 (±6.3)	75.2 (±4.5)	98.1 (±2.8)
	10.4 (±7.4)	78.0 (±6.4)	88.6 (±6.2)
Sp1	21.3 (±8.0)	34.8 (±9.3)	80.6 (±15.8)
	23.7 (±5.4)	44.0 (±10.7)	75.1 (±15.7)
Spu1	6.2 (±4.9)	63.3 (±7.8)	90.3 (±5.7)
	9.7 (±9.9)	57.8 (±8.3)	88.1 (±5.9)
Sssp	21.6 (±11.2)	53.4 (±11.1)	94.2 (±6.7)
	19.2 (±8.7)	54.4 (±6.4)	92.6 (±6.0)
St1	19.0 (±6.6)	33.0 (±12.6)	88.5 (±22.4)
	31.1 (±11.7)	45.2 (±5.5)	92.2 (±19.4)
St2	5.2 (±8.5)	26.5 (±9.4)	89 (±6.9)
	31.4 (±5.3)	32.5 (±7.6)	86.2 (±6.9)
Sv1	28.4 (±13.2)	39.4 (±7.0)	85.9 (±4.0)
	12.0 (±3.8)	34.0 (±6.5)	80.4 (±9.3)
Sv2	17.4 (±8.5)	24.4 (±11.2)	76 (±4.8)
	1.0 (±8.9)	18.5 (±6.0)	75.5 (±9.4)
Svi1	13.6 (±7.1)	30.8 (±10.0)	77.3 (±14.9)
	21.7 (±3.3)	41.4 (±10.6)	73.9 (±15.7)
Svi2	24.8 (±3.9)	51.3 (±12.7)	74.4 (±13.2)
	23.8 (±5.2)	56.5 (±14.8)	72.6 (±16.6)

Table S3.   Antibacterial activities (relative growth inhibition [%] and of *Bacillus subtilis*) of *Suillus* extracts from mycelial cultures.

Extract No.	Inhibition [%] (c = 1 µg/mL)	Inhibition [%] (c = 10 µg/mL)	Inhibition [%] (c = 100 µg/mL)
Sac	15.7 (±6.9)	19.3 (±7.3)	34.5 (±10.5)
	19.3 (±9.6)	27.1 (±8.1)	67.7 (±17.1)
Sb3	7.3 (±10.5)	14.8 (±15.2)	80.6 (±5.7)
	17.2 (±10.4)	19.9 (±12.9)	90.6 (±16.5)
Sb4	1.2 (±8.1)	14.4 (±9.0)	37.5 (±7.9)
	21.6 (±8.4)	20.9 (±7.4)	52.4 (±9.6)
Sb5	13.7 (±6.7)	18.4 (±5.3)	21.9 (±9.2)
	3.7 (±7.7)	16.1 (±8.8)	46.2 (±9.1)
Sb6	22.9 (±11.8)	34.1 (±10.4)	43.7 (±6.9)
	9.2 (±7.3)	22.1 (±8.1)	50.2 (±14.5)
Sb7	22.3 (±11.8)	24.7 (±11.8)	61.0 (±8.3)
	4.8 (±8.4)	10.2 (±8.0)	41.1 (±12.9)
Sc4	16.1 (±8.5)	20.3 (±13.0)	113.4 (±12.1)
	5.6 (±8.3)	22.8 (±12.8)	112.6 (±11.4)
Sco	7.5 (±4.8)	17.0 (±6.9)	56.4 (±9.6)
	16.3 (±7.1)	23.2 (±5.5)	90.0 (±4.2)
Sg3	21.4 (±15.0)	35.7 (±8.5)	32.0 (±10.3)
	12.5 (±7.7)	34.4 (±8.6)	66.2 (±9.3)
Sg4	35.4 (±14.6)	32.9 (±13.9)	89.3 (±17.9)
	-5.5 (±3.3)	4.1 (±6.1)	51.0 (±15.1)
Sg5	6.6 (±7.6)	10.9 (±3.3)	47.3 (±11.4)
	17.5 (±9.8)	8.9 (±5.9)	32.2 (±11.0)
Sin	15.2 (±4.1)	21.2 (±8.2)	79.8 (±13.4)
	11.6 (±6.7)	35.1 (±6.3)	97.8 (±4.5)
Spu2	1.0 (±5.6)	13.9 (±9.7)	88.6 (±11.6)
	15.4 (±9.0)	19.3 (±9.8)	94.2 (±8.5)
Spu3	12.0 (±8.6)	16.6 (±6.8)	44.3 (±12.1)
	15.9 (±9.0)	21.6 (±8.5)	56.9 (±12.6)
Ssa	6.1 (±5.4)	15.5 (±6.8)	50.7 (±13.3)
	17.5 (±6.0)	20.9 (±10.6)	74.7 (±4.2)
St3	12.9 (±8.5)	36.6 (±11.5)	88.6 (±10.2)
	27.3 (±14.5)	35.1 (±14.2)	78.3 (±5.6)
St4	34.9 (±11.0)	42.0 (±5.5)	71.8 (±6.7)
	21.5 (±9.2)	48.6 (±14.7)	82.4 (±9.9)
Sv3	18.8 (±7.1)	25.5 (±8.2)	39.2 (±14.5)
	16.5 (±10.5)	11.8 (±6.9)	15.1 (±7.9)
Sv4	6.9 (±16.0)	12.8 (±6.9)	30.7 (±7.2)
	25.4 (±10.9)	21.2 (±9.6)	38.3 (±7.0)
Sv5	36.4 (±13.6)	61.1 (±10.0)	95.4 (±10.4)
	6.5 (±4.5)	54.1 (±7.8)	100.6 (±14.7)
Sv6	11.7 (±4.9)	18.4 (±7.4)	21.5 (±12.1)
	11.3 (±19.2)	16.2 (±15.3)	23.1 (±10.1)

Table S4. Antibacterial activities (relative growth inhibition [%] of *Bacillus subtilis*) of *Suillus* extracts from fresh fruiting bodies.

Extract No.	Inhibition [%] (c = 1 µg/mL)	Inhibition [%] (c = 10 µg/mL)	Inhibition [%] (c = 100 µg/mL)
Sb8	19.4 (±8.7)	32.3 (±8.7)	108.9 (±8.5)
Sb9	3.8 (±6.8)	6.5 (±6.0)	81.8 (±13.8)
Sb10	8.3 (±8.8)	14.7 (±6.2)	53.9 (±4.6)
	20.3 (±7.7)	22.2 (±7.4)	54.9 (±7.4)
Sc5	6.2 (±3.7)	6.5 (±0.9)	28.4 (±7.3)
	12.5 (±6.5)	12.1 (±5.5)	38.7 (±7.5)
Sgr3	24.5 (±9.6)	28.4 (±7.5)	54.2 (±11.5)
Sl3	30.6 (±7.1)	33.2 (±5.2)	87.4 (±5.6)
Sv7	9.9 (±8.7)	19.6 (±10.5)	49.4 (±12.5)
Svi3	9.3 (±1.3)	22.0 (±6.1)	91.8 (±10.8)
Svi4	6.0 (±6.9)	28.0 (±5.3)	100.8 (±2.7)
	16.6 (±8.9)	37.7 (±4.5)	99.1 (±9.4)

Table S5. Selected peaks from the hit list based on negative ion ESI-FTICR-MS data correlated with the antibacterial bioactivity profiles against *B. subtilis* of the *Suillus* species extracts (Sb1, Sb2, Sg1, Sg2, St1, St2, Sv1 and Sv2, $c_{extract}$ = 100 µg/mL).

Rank	Spearman correlation coefficient	[M-H]$^-$ (*m/z*)	elemental composition	DBE	Error [ppm]	possible compound
22	0.49	409.2384	$C_{26}H_{33}O_4^-$	10.5	0.1	tridentoquinone
23	0.49	425.2335	$C_{26}H_{33}O_5^-$	10.5	0.4	hydroxylated tridentoquinone

Table S6. Hit list of the top-10 ranked peaks based on negative ion ESI-FTICR-MS data correlated with the antibacterial bioactivity profiles against *B. subtilis* of the *Suillus bovinus* extracts (Sb1-Sb10, $c_{extract}$ = 100 µg/mL).

Rank	Spearman correlation coefficient	[M-H]$^-$ (*m/z*)	elemental composition	DBE	Error [ppm]	possible compound
1	0.43	381.3376	$C_{24}H_{45}O_3^-$	2.5	0.5	not determind
2	0.41	333.2438	$C_{21}H_{33}O_3^-$	5.5	0.8	
3	0.41	293.2122	$C_{18}H_{29}O_3^-$	4.5	0.1	9-oxo-ODE
4	0.40	329.2334	$C_{18}H_{33}O_5^-$	2.5	0.2	9,10,13-11(*E*)-THOD
5	0.39	277.2173	$C_{18}H_{29}O_3^-$	4.5	0.01	octadecatrienoic acid

11.3   Declaration on the author contributions to the publications on which this thesis is based

The present cumulative dissertation based on the following scientific publications:

Chapter 2:   Heinke, R., Franke, K., Michels, K., Wessjohann, L., N.A. Awadh Ali, Schmidt, J. (2012), Analysis of furanocoumarins from Yemenite *Dorstenia* species by liquid chromatography/electrospray tandem mass spectrometry. *J. Mass Spectrom.* **47**, 7-22.

I isolated furanocoumarins from *Dorstenia foetida*, performed the sample preparation of all used furanocoumarins, measured all samples on the ion trap system, established the fragmentation rules, and wrote the manuscript draft. N.A. Awadh Ali collected the plant material of *Dorstenia foetida* and determined the species. The other analyzed furanocoumarins were isolated from *D. gigas* by K. Franke. K. Michels gave me an introduction in the ion trap system and in the procedures of mass spectrometry. L. Wessjohann designed and supervised the project and edited the manuscript. J. Schmidt participated in the design of the project and in the writing of the manuscript, performed the ESI-FTICR-MS measurements, and provided helpful discussions.

Chapter 3:   Heinke, R., Arnold, N., Wessjohann, L., Schmidt, J. (2013) Negative ion electrospray tandem mass spectrometry of prenylated fungal metabolites and their derivatives. *Anal. Bioanal. Chem.* **405**, 177-189.

I performed the sample preparation of all used prenylated benzoquinones and phenols, measured all samples on both the ion trap and the LTQ Orbitrap system, established the fragmentation rules, and wrote the manuscript. N. Arnold was responsible for the procurement of the authentic compounds investigated and of fungal organisms. L. Wessjohann designed and supervised the project and edited the manuscript. J. Schmidt participated in the design of the project and in the writing of the manuscript, performed the ESI-FTICR-MS measurements, and provided helpful discussions.

Chapter 4:   <u>Heinke, R.</u>, Schöne, P., Arnold, N., Wessjohann, L., Schmidt, J. (2014) Metabolite profiling and fingerprinting of *Suillus* species (Basidiomycetes) by electrospray mass spectrometry. *Eur. J. Mass Spectrom.* **20**, 85-97.

I designed the project, supervised the extraction and sample preparation, measurements of the samples on the ion trap system and first principal component analyses (PCA) and characterization of the samples. I performed the multivariate data analyses using the chemometrics software SIMCA® (SIMCA-P+ 12.0.1, Umetrics) and interpreted the results of the PCA, HCA and OPLS-DA. P. Schöne prepared the extracts, measured the samples and performed the first PCAs and characterization of the samples as part of her bachelor's thesis. N. Arnold provided the analyzed fungal organisms and provided helpful discussions. L. Wessjohann supervised the project and edited the manuscript. J. Schmidt participated in the design of the project and in the writing and editing of the manuscript, performed the ESI-FTICR-MS measurements, and provided helpful discussions.

Chapter 5:   Michels, K.,   Haid, M.,   Gohr, A.,   Heinke, R.,   Schmidt, J.,   Arnold, N., Wessjohann, L. Reverse Metabolomics – a correlation approach for the direct identification of active compounds in complex mixtures. **unpublished**.

I performed the extraction and sample preparation of the analyzed *Albatrellus* species, measured the metabolite profils of crude extracts from *Albatrellus* species on the ion trap and determined the antibacterial bioactivity, identified the potential bioactive compound using mass spectral data, and had a great contribution writing the manuscript. K. Michels, M. Haid and A. Gohr performed the proof of concept experiments and performed the 'reverse metabolomics' approach and the activity correlation analysis (AcorA) and they participated in the writing of the manuscript. K. Michels measured the *Hygrophorus* extract on the ion trap and determined the antibacterial activity of those extracts, whereas M. Haid measured the *Hygrophorus* extract using ESI-FTICR-MS. A. Gohr performed the bioinformatics part, the comparison of AcorA with PCA and QPAR, wrote the theory part and the part of the comparison studies. J. Schmidt participated in the writing of the manuscript, performed the ESI-FTICR-MS measurements of the *Albatrellus* extracts, and provided helpful discussions. N. Arnold provided the analyzed fungal organisms. L. Wessjohann designed the experiments and supervised the project and the experimental setup for the proof of concept. He participated in writing and editing the manuscript.

Chapter 6: <u>Heinke, R.</u>, Stark, S., Laub, A., Ehrlich, A., Arnold, N., Schmidt, J., Wessjohann, L. New antibacterial active metabolites of *Albatrellus* species (Basidiomycetes) identified by activity correlation analysis. **unpublished**.

I performed the extraction and sample preparation of the analyzed *Albatrellus* species and determined the antibacterial bioactivity against *Bacillus subtilis*, identified the potential bioactive compound using mass spectral data, and had a great contribution writing the manuscript. S. Stark performed the *Aliivibrio fischeri* assay and A. Ehrlich the cell proliferation assay. A. Laub did the UHPLC-ESI-MS^n measurements of the metabolites of interest of crude extracts from *Albatrellus* species on the Orbitrap system. J. Schmidt participated in the writing of the manuscript, performed the ESI-FTICR-MS measurements of the *Albatrellus* extracts, and provided helpful discussions. N. Arnold provided the analyzed fungal organisms. L. Wessjohann designed and supervised the project and edited the manuscript.

Acknowledgment

An dieser Stelle möchte ich meinen besonderen Dank Prof. Dr. Ludger Wessjohann aussprechen, für die Betreuung und die Möglichkeit, meine Dissertation am Leibniz-Institut für Pflanzenbiochemie (IPB) Halle anfertigen zu können. Des Weiteren bedanke ich mich bei ihm für die Möglichkeit bei der Ausgestaltung der Arbeit mitzuwirken, für das selbständige wissenschaftliche Arbeiten und für das mir gegenüber gebrachte Vertrauen. Für die mögliche Übernahme eines Zweitgutachtens danke ich Prof. Dr. Uwe Karst vielmals.

Besonderer Dank gilt Dr. Jürgen Schmidt, der mir bei allen fachlichen Fragen zur Seite stand, für die Diskussionen über Ergebnisse und Probleme, als auch der hervorragenden Zusammenarbeit beim Verfassen der Publikationen, sowie für die Zeit und Gespräche die wir führten. Ebenfalls danke ich Dr. Norbert Arnold und Dr. Katrin Franke für die Pilzexkursionen, die Unterstützung beim Sammeln der Pilzfruchtkörper, beim Lösen fachlicher Probleme sowie der Unterstützung und Betreuung. Weiterhin danke ich Christine Kuhnt für die Unterstützung bei technischen und massenspektrometrischen Fragen und Martina Lerbs für die ESI-MS-Messungen. Für die Durchführung der Biotests danke ich Sebastian Stark und Anja Ehrlich.

Mein herzlicher Dank gilt Pia Schöne, die im Rahmen Ihrer Bachelorarbeit und als wissenschaftliche Mitarbeiterin mit viel Einsatz und Sorgfalt an einem Teil der hier vorgestellten Ergebnisse mitgewirkt hat und für die aus der Zusammenarbeit entstandenen Freundschaft. Bei Annegret Laub möchte ich mich ebenfalls herzlich für die Unterstützung vor allem in den letzten Wochen am Institut, sowie für die Messungen an der Orbitrap bedanken. Stephanie Krause-Hielscher und Annika Denkert danke ich für die schöne Zeit im Technikum und angenehme, freundliche Arbeitsatmosphäre. Weiterer Dank gilt den Mitarbeiter der Abteilung Natur- und Wirkstoffchemie, u.a. Susann Riemer-Köhler, Anne-Katrin Bauer, Jeanette Keim, Katharina Michels, Robert Berger, Dr. Danilo Meyer, Dr. Martin Dippe, Prof. Dr. Bernhard Westermann und allen Doktoranden aus D103 und C116 für die freundliche Gesellschaft, super Gespräche, Grillabende und weiter nette Abende. Ich möchte mich weiterhin bei allen bedanken, die mich bei meiner Arbeit unterstützt haben.

Für die finanzielle Unterstützung durch die Studienstiftung des deutschen Volkes in Form eines Promotionsstipendiums möchte ich mich ebenfalls besonders bedanken sowie für die Möglichkeiten, im Rahmen der Doktoraden Foren anregende Gespräche und Diskussionen zu führen und für die Teilnahme an einem Spanisch-Sprachkurs. Der Deutschen Gesellschaft für Massenspektrometrie danke ich für ein Reisestipendium, welches mir die Teilnahme an der 19th International Mass Spectrometry Conference (IMSC) in Kyoto (Japan) ermöglichte.

Zuletzt gilt meinen Eltern besonderer Dank für die große Unterstützung während des gesamten Pharmaziestudiums sowie der Promotionszeit und dass sie mir stets den Rückhalt boten. Auch meinem Bruder möchte ich danken, der immer für mich da ist.

Publication list

Publications in peer-reviewed journals

Heinke, R., Schöne, P., Arnold, N., Schmidt, J., Wessjohann, L. "Determination of the antibacterial potential against *Bacillus subtilis* of *Suillus* spp. (Basidiomycetes)." **Manuscript in preparation**.

Heinke, R., Stark, S., Laub, A., Ehrlich, A., Arnold, N., Schmidt, J., Wessjohann, L. "New antibacterial active metabolites of Albatrellus species (Basidiomycetes) identified by activity correlation analysis." **unpublished**.

Michels, K., Haid, M, Gohr, A., Heinke, R., Schmidt, J., Arnold, N., Wessjohann, L. "Reverse metabolomics – a correlation approach for the direct identification of active compounds in complex mixture." **unpublished**.

Michels, K., Heinke, R., Schöne, P., Kuipers, O. P., Arnold, N., & Wessjohann, L. A. (2015). „A fluorescence-based bioassay for antibacterials and its application in screening natural product extracts." J. Antibiot., doi: 10.1038/ja.2015.71

Brauer, M. C., Neves Filho, R. A., Westermann, B., Heinke, R., & Wessjohann, L. A. (2015). „Synthesis of antibacterial 1, 3-diyne-linked peptoids from an Ugi-4CR/Glaser coupling approach." Beilstein J. Org. Chem., 11, 25-30.

Mueller, H., Heinze, M., Heinke, R., Schmidt, J., Roos, W. (2014) "Self-regulation of phytoalexin production: a non-biosynthetic enzyme controls alkaloid biosynthesis in cultured cells of *Eschscholzia californica*." Plant Cell Tiss. Org., **119**, 661-676.

Farag, M.A., Mohsen, M., Heinke, R., Wessjohann, L.A. (2014) "Metabolomic fingerprints of 21 date palm fruit varieties from Egypt using UPLC/PDA/ESI-qTOF-MS and GC-MS analyzed by chemometrics." *Food Res. Int.* **64**, 218-226.

Heinke, R., Schöne, P., Arnold, N., Wessjohann, L., Schmidt, J. (2014) "Metabolite profiling and fingerprinting of *Suillus* species (Basidiomycetes by electrospray mass spectrometry." *Eur. J. Mass Spectrom.* **20**, 85-97.

Westermann, B., Dörner, S., Brauch, S., Schaks, A., Heinke, R., Stark, S., van Delft, F.L., van Berkel, S.S. (2013) "CuAAC-mediated diversification of aminoglycoside–arginine conjugate mimics by non-reducing di- and trisaccharides." *Carbohydrate Research* **371**, 61-67.

Heinke, R., Arnold, N., Wessjohann, L., Schmidt, J. (2013) "Negative ion electrospray tandem mass spectrometry of prenylated fungal metabolites and their derivatives." *Anal. Bioanal. Chem.* **405**, 177-189.

Heinke, R., Franke, K., Michels, K., Wessjohann, L., Awadh Ali, N.A., Schmidt, J. (2012), "Analysis of furanocoumarins from Yemenite *Dorstenia* species by liquid chromatography/electrospray tandem mass spectrometry." *J. Mass Spectrom.* **47**, 7-22.

Heinke, R., Franke, K., Porzel, A., Wessjohann, L.A., Awadh Ali, N.A., Schmidt, J. (2011) "Furanocoumarins from *Dorstenia foetida.*" *Phytochemistry* **72**, 927-932.

Lectures

Heinke, R., Electrospray mass spectrometry of fungal metabolites. 46. Doktorandenworkshop. Naturstoffe: Chemie, Biologie und Ökologie, 11. October 2013, Bayreuth.

Heinke, R., Arnold, N., Wessjohann, L., Schmidt, J., Mass spectrometry-based metabolite profiling of crude fungal extracts. 46. Jahrestagung der Deutschen Gesellschaft für Massenspektrometrie (DGMS), 10. - 13. March 2013, Berlin.

Heinke, R., Höhere Pilze – Eine Quelle für neue bioaktive Naturstoffe!?, Doktorandenforum Natur und Gesellschaft (Studienstiftung des deutschen Volkes), 31. May - 03. June 2012, Bad Homburg.

Heinke, R., Arnold, N., Wessjohann, L., Schmidt, J., Negative ion tandem mass spectrometry of prenylated fungal metabolites and their derivatives. Joint Conference of Polish Mass Spectrometry Society and German Mass Spectrometry Society (DGMS), 04. - 07. March 2012, Poznań, Polen.

Heinke, R., Franke, K., Porzel, A., Ali, N.A.A., Wessjohann, L.A., Schmidt, J., Furanocoumarins from *Dorstenia foetida.* 7th Plant Science Student Conference (PSSC), 14. - 17. June 2011 Halle/Saale.

Heinke, R., Massenspektrometrie und "Reverse Metabolomics" von prenylierten Naturstoffen und deren Derivaten. „Doktorandenforum Natur" (Studienstiftung des deutschen Volkes), 02. - 05. June 2011, Berlin.

Poster presentations

Heinke, R., Arnold, N., Wessjohann, L.A., Schmidt, J. Negative ion tandem mass spectrometry of prenylated fungal metabolites and their derivates. 19th International Mass Spectrometry Conference (IMSC), 15. - 21. September 2012, Kyoto, Japan.

Heinke, R., Franke, K., Awadh Ali, N.A., Wessjohann, L.A., Schmidt, J., Liquid chromatography-electrospray tandem mass spectrometry-based metabolite profiling of furanocoumarins from Yemenite *Dorstenia* species. Trends in Metabolomics – Analytics and Application (DECHEMA), 19. - 20. May 2011, Frankfurt/Main.

Heinke, R., Arnold, N., Wessjohann, L., Schmidt, J., Negative ion tandem mass spectrometry of prenylated fungal metabolites. 44. Jahrestagung der Deutschen Gesellschaft für Massenspektrometrie (DGMS), 27. Februar - 02. March 2011, Dortmund.

Heinke, R., Franke, K., Porzel, A., Awadh Ali, N.A., Schmidt, J., Wessjohann, L.A., Analysis of prenylated furanocoumarins from Yemenite *Dorstenia* species. 23. Irseer Naturstofftage (DECHEMA), 23. - 25. Februar 2011, Irsee.

Heinke, R., Franke, K., Michels, K., Wessjohann, L., Arnold, N., Schmidt, J., Structural investigations of furanocoumarins by positive ion electrospray tandem mass spectrometry. 43. Jahrestagung der Deutschen Gesellschaft für Massenspektrometrie (DGMS), 07. - 11. March 2010 Halle/Saale.

Curriculum vitae

Personal data

Name:	Ramona Heinke
Date/place of birth:	24. April 1985 in Potsdam
Nationality:	German
Address:	Fürstenweg 10
	A-6020 Innsbruck

School education

1997 – 2004	Hermann-von-Helmholtz-Gymnasium, Potsdam
	Degree: general qualification for university entrance

Academic studies

11/2009	license to practice pharmacy
07/2009	Diploma, Dipl. Pharmacist (Dipl.-Pharm.)
05/2009 – 10/2009	Pharmacist at practical training, Kröllwitz-Apotheke Halle/Saale
11/2008 – 04/2009	Diploma, Martin-Luther-University Halle-Wittenberg in cooperation with the Leibniz Institute of Plant Biochemistry Halle/Saale
	Topic: "Phytochemische Untersuchungen von Furanocumarinen aus jemenitischen *Dorstenia*-Arten"
10/2004 – 10/2008	Studies of pharmacy, Martin-Luther-University Halle-Wittenberg

Work experiences

Since 06/2014	Scientist, Bionorica Research GmbH
12/2009 – 12/2010	Pharmacist, Kröllwitz-Apotheke Halle/Saale
11/2009 – 03/2010	Research assistant, Agrochemical Institute Piesteritz e.V. (AIP) AN-Institute of the Martin-Luther-University Halle-Wittenberg

Dissertation

Since 04/2010	Dissertation, Leibniz Institute of Plant biochemistry Halle, Martin-Luther-University Halle-Wittenberg (Faculty of Chemistry)
07/2010 – 05/2013	Dissertation supported by a grant of the 'Studienstiftung des deutschen Volkes'

Eidesstattliche Erklärung

Hiermit erkläre ich an Eides statt, dass ich die vorliegende Dissertation selbstständig und ohne unzulässige Hilfe Dritter angefertigt habe. Es wurden keine anderen als die von mir angegebenen Hilfsmittel und Quellen verwendet. Die aus anderen Quellen direkt oder indirekt übernommenen Daten wurden unter Angabe der Literatur gekennzeichnet.

Die Dissertation wurde ausschließlich der Naturwissenschaftlichen Fakultät II der Martin-Luther-Universität Halle-Wittenberg vorgelegt und bisher an keiner anderen Hochschule oder Universität zur Erlangung des Doktorgrades eingereicht.

_____   _____
         Datum   (Ramona Heinke)